NTNU
Norwegian University of
Science and Technology

Analysis of frequency stability: How wind power and HVDC connections affect the future power system

Håkon Hellebust

Master of Energy and Environmental Engineering
Submission date: June 2018
Supervisor: Kjetil Uhlen, IEL

Norwegian University of Science and Technology
Department of Electric Power Engineering

Preface

This master thesis was carried out during spring 2018 at the Department of Electric Power Engineering, NTNU.

I wish to thank my supervisor, Professor Kjetil Uhlen, for his guidance and supervision. It was always interesting and helpful when he shared his comprehensive knowledge. I would also like to express my gratitude to Abel Assegid Taffese for his assistance. He possesses extraordinary problem-solving skills.

A massive thanks to my family for their never-ending support through all my education.

Lastly, I would like to thank my girlfriend for reminding me that it is more to life than writing this thesis.

Håkon Hellebust

Trondheim, June 2018

Abstract

Many modern power systems are facing massive changes. Two of the main development trends are more interconnections between neighboring power systems and significant growth in installed capacity of wind power and other decoupled production. These technologies might affect the levels of inertia in the power system, and thus possibly reduce the frequency stability. To always have satisfactory system stability is vital for a successful operation of the power grid, now and in the future. The recent development of in the fields of controllers and power electronics enable HVDC links and wind turbines to contribute to the frequency stability.

This thesis aimed to illuminate the implications on frequency stability from the development trends of more wind power and HVDC connections in power system. Would it lead to less system inertia? Would the system become more or less stable in the future? What can be done to maintain satisfactory system stability? An extensive literature study was conducted, with the main findings presented in this report. A set of frequency response indicators were introduced to facilitate examination of the frequency responses to disturbances. Simulations were conducted to examine the contribution from HVDC and wind power both without measures to improve the frequency response and with additional controllers providing synthetic inertia. The primary emphasis has been on the Nordic system which was the base for the simulation model. Simulations have also been conducted in a smaller and more transparent model.

Four main scenarios have been investigated: Situations with very high and low inertia in the present system (2017) and the future (2030). Five disconnection events and one short-circuiting have been studied for all the scenarios. The events along with the scenarios have been extremes, meaning that they are representing the grid under extraordinary conditions. For the future scenarios, additional controllers have in turn been enabled for wind power production and HVDC connectors to explore their possible contribution the frequency support.

The major parts of the simulations were conducted in an extensive Nordic simulation model. The results indicated that the future grid would experience far less inertia during operation hours where the inertia levels already a low. Most frequency response indicators suggested that the frequency response was deteriorated in the future grid when no measures of mitigation had been implemented. At some hours, the disturbances induced more than 30% higher frequency deviations in the future grid. The expanding technologies of wind power and HVDC connections are replacing conventional generation, reducing system inertia and other favorable properties associated with such production. During scenarios with very high load (winter at peak hours), the results showed that system inertia would

remain at a stable high level. Two conceptual controllers were developed to allow the HVDC connections and wind turbines to provide synthetic inertia to the grid. This proved to improve the frequency response significantly. These results suggest that the expanding technologies can successfully offer frequency support to stabilize the power grid.

Voltages and power flows have been briefly examined to explore the most critical operating conditions. Significant voltage dips and power flow changes, both with oscillations, were detected. Some voltages were dipping more than 10% of nominal value. However, the oscillations died quickly and the system remained stable for all disturbances in all scenarios.

Several sources of error could have affected the validity of the results. The controllers developed were conceptual, and may not induce a response similar to complex and optimized controller developed by professionals. Modeling the future is also associated with considerable uncertainties, as the input for the future never can be known precisely. However, the results are strengthened by simulating in two models (one complex and one simple), and by corresponding to existing research and expectations.

The topic of interest is complicated, and further studies to illuminate how wind power and HVDC connections affect the power system is necessary. Some of the most interesting future studies may include improving the controllers, testing and tuning the model to a real-world system, and examining the effects on the HVDC and wind components when they are providing synthetic inertia.

Sammendrag

Mange moderne kraftsystemer står overfor store endringer i tiden som kommer. To av de viktigste utviklingstrekkene for det nordiske kraftsystemet er økt fornybar produksjon og flere HVDC-kabler til andre kraftsystem. Den økte utbredelsen av disse teknologiene kan redusere mengden treghetsmoment (engelsk: inertia) i systemet og dermed føre til dårligere stabilitet i kraftsystemet. Å holde mengden treghetsmoment på et tilfredsstillende nivå til enhver tid er en av de viktigste forutsetningene for å holde kraftsystemet stabilt. Utviklingen i kraftelektronikk og kontrollsystemer åpner for muligheten til at vindkraft og HVDC-kabler likevel kan bidra til å øke stabiliteten.

Denne oppgaven belyser hvordan frekvensstabiliteten påvirkes når stadig mer vindkraft og flere HVDC-tilkoblinger blir tilknyttet kraftsystemet. Vil dette føre til mindre treghetsmoment? Vil systemet bli mer eller mindre utsatt for forstyrrelser i fremtiden? Hva kan gjøres for å opprettholde tilfredsstillende systemstabilitet?

En omfattende litteraturstudie har blitt utført og de viktigste funnene blir presentert i denne rapporten. En rekke indikatorer ble brukt for å undersøke frekvensresponsen til ulike forstyrrelser i "nåtidens" og "framtidens" kraftnett. Simuleringer ble utført i en liten og en stor simuleringsmodell for å undersøke hvordan HVDC- kabler og vindkraft påvirker systemets frekvensrespons. Dette ble først gjennomført uten noen ekstra tiltak for å øke stabiliteten i systemet, og deretter med kontrollere som tilrettela for "kunstig treghetsmoment" (engelsk: synthetic inertia) fra HVDC og vindkraft. Oppgaven er relevant for alle kraftsystem som står overfor de nevnte endringer, men vil være særlig relevant for det nordiske kraftsystemet siden data fra dette systemet har blitt brukt som utgangspunkt for simuleringene og i oppgaven generelt.

Fire hovedscenarioer har blitt undersøkt: Situasjoner med svært høy og lav treghetsmoment i dagens system (2017) og fremtidig system (2030). Fem avbruddshendelser og en kortslutning har blitt studert for alle scenariene. Både hendelsene og scenariene representerte ekstreme tilfeller. Hendelsene omfattet svikt i generatorer, kraftlinjer og en HVDC-kabel som alle hadde svært høye laster. For fremtidsscenarioene har kontrollsystemer for vindkraftproduksjon og HVDC-system blitt testet hver for seg for å undersøke muligheten disse har til å bidra til frekvensstabiliteten i kraftnettet.

Mesteparten av simuleringene ble gjennomført i en omfattende simuleringsmodell av det nordiske kraftsystemet. Resultatene indikerte at kraftsystemet i fremtiden vil ha vesentlig lavere treghetsmoment i situasjoner hvor det allerede er lite treghetsmoment (lavlasttimer på sommeren). Altså vil situasjoner som allerede er kritiske for stabiliteten i systemet bli enda mer kritisk. Dette ble blant annet observert ved at de fleste frekvensresponsindika-

torer ble tydelig forverret for de gjeldene scenarioene fra 2017 til 2030 – så lenge ingen stabiliserende tiltak ble gjennomført. For eksempel førte noen av forstyrrelsene til mer enn 30% høyere frekvensavvik i kraftnettet anno 2030 enn i 2017. Dette resultatet kommer i stor grad av at den ekspanderende teknologien for vindkraft og HVDC-kabler erstatter konvensjonelle generatorer som i dag bidrar med treghetsmoment. Scenarioene med svært høy last (topplasttimer på vinteren) viste seg å ha omtrent like mye treghetsmoment i 2030 som i 2017.

To kontrollsystem ble utviklet for at HVDC-tilkoblingene og vindturbinene skulle ha mulighet til å bidra med kunstig treghetsmoment i framtiden. På den måten ønsker man at HVDC-kabler og vindkraft kan bidra positivt til stabiliteten i kraftsystemet. Omfattende simuleringer tydet på at frekvensresponsen ble betydelig forbedret.

Spenninger og lastflyt i systemet som følge av forstyrrelsene har også blitt undersøkt for å avdekke mulige kritiske konsekvenser i nettet. Store spenningsfall og hurtige lastflytendringer ble observert (begge med store svingninger). For enkelte noder i nettet ble det observert spenningsfall på mer enn 10%. Til tross for dette forble systemet stabilt for alle simuleringene.

Flere feilkilder kan ha påvirket resultatene. Kontrollsystemene som ble utviklet var grunnleggende og konseptuelle, og bør utforskes videre før man kan konkludere sikkert om bidragene fra disse. Grunnet begrensinger i simuleringsprogrammet ble kun en type vindturbiner modellert, og all vindkraft konsentrert på seks ulike noder i det nordiske kraftsystemet. En modell av framtiden er generelt forbundet med store usikkerheter, da framtidig produksjon, forbruk, installert kapasitet, osv. er basert på estimater. Resultatene styrkes imidlertid av at simuleringene ble gjennomført i to modeller (en enkel og en omfattende), og fordi de svarte til eksisterende forskning og forventninger.

Oppgaven belyser en svært omfattende problemstilling og videre studier av hvordan vindkraft og HVDC-tilkoblinger påvirker kraftsystemet er nødvendig. Interessante videre studier vil omfatte forbedring av kontrollerne, samt testing og kalibrering av modellen mot et virkelig system. I tillegg må det undersøkes mer i dybden hvordan de enkelte HVDC- og vindkomponentene oppfører seg når de bidrar med med kunstig treghetsmoment.

Abbreviations

AC	Alternating current
AGC	Automativ generation control
AVR	Automatic Voltage Regulator
DC	Direct current
DFIG	Doubly Fed Induction Generator
ESS	Energy Storage Systems
FCR	Frequency Containment Reserves
FRC	Fully Rated Converter
FRR	Frequency Regulating Reserves
HVDC	High voltage direct current
NVE	Norwegian Water Resources and Energy Directorate
p.u.	per unit
PWM	Pulse Width Modulation
ROCOF	Rate of change of frequency
RR	Replacement Reserves
SCIG	Squirrel-Cage Induction Generator
TSO	Transmission System Operator
VSC	Voltage source converter

Contents

List of Tables **XI**

List of Figures **XII**

1 Introduction **1**

1.1 Background and motivation 1

1.2 Problem statement 1

1.2.1 Elaboration and specification 2

1.2.2 Limitations 3

1.3 Approach 4

1.4 Outline 4

2 Frequency stability - Theory and context **5**

2.1 Power imbalances 5

2.2 System frequency 6

2.2.1 The Nordic frequency area 6

2.3 Frequency stability and control 7

2.3.1 The dynamics of frequency response 7

2.3.2 Frequency response indicators 9

2.3.3 Reserves 11

2.4 Inertia 13

2.4.1 Theoretical background 13

2.4.2 Swing equation 15

2.4.3 Current development and future concerns 16

2.4.4 Measures of mitigation 18

2.4.5 Synthetic inertia 18

2.4.6 Inertia in the Nordic system 20

2.5 Variable energy sources 21

2.5.1 Wind power 22

2.5.2 Wind power in the Nordics 23

2.6 HVDC systems . . . 23
2.6.1 Nordic HVDC connections . . . 24

3 Customized control systems **26**
3.1 Background . . . 26
3.2 HVDC controller . . . 27
3.3 Wind power controller . . . 30

4 Approach to analysis **32**
4.1 Simulation tool: DIgSILENT PowerFactory . . . 32
4.1.1 Relevant model components . . . 32
4.2 Small test network (STN) . . . 35
4.2.1 Development and characteristics . . . 36
4.2.2 Scenarios . . . 38
4.2.3 Results and discussion . . . 39
4.2.4 Conclusion . . . 41
4.3 Large scale model (N44) . . . 42
4.3.1 Modifications . . . 43
4.3.2 Development of the scenarios . . . 46
4.3.3 Simulation events . . . 48
4.3.4 Measurement points . . . 49
4.3.5 Assumptions . . . 50

5 Results **52**
5.1 Inertia calculation . . . 52
5.2 Frequency bias calculation . . . 52
5.3 Disconnections of generators and HVDC line . . . 53
5.4 Short-circuiting critical lines . . . 58
5.5 Disconnection of critical lines . . . 60

6 Discussion **62**
6.1 Discussion of results . . . 62

6.1.1 System inertia . . . 62
6.1.2 Controllers . . . 63
6.1.3 Frequency response indicators . . . 64
6.1.4 Voltage response . . . 67
6.1.5 Load flow response . . . 69
6.1.6 Small test network . . . 70
6.1.7 Hypotheses . . . 70
6.1.8 Implications of assumptions . . . 71
6.2 Sources of error . . . 74
6.3 Validity of the results . . . 74

7 Conclusion **76**
7.1 Summary and concluding remarks . . . 76
7.2 Recommendations for further work . . . 78

References **80**

A Glossary **83**

B Frequency control action overview **85**

C Modern wind turbines **86**

D Block diagram - PowerFactory PWM Current Controller **89**

E PowerFactory line diagrams **90**
E.1 Main grid . . . 90
E.2 HVDC connections sub-grid . . . 90
E.3 Wind power sub-grid . . . 91

F Scenario data **92**
F.1 Scenario 1 . . . 92
F.2 Scenario 2 . . . 94
F.3 Scenario 3 . . . 97

F.4 Scenario 4 99

G Component data **102**

G.1 Governor - HYGOV 102

G.2 AVR - SEXS 103

H Simulation results **104**

H.1 Delta - Frequency responses 104

H.2 Epsilon - Frequency responses 104

H.3 Zeta - Frequency responses 105

H.4 Zeta - Reactive response in Finland 105

H.5 Eta - Frequency responses 107

I Swing equation and inertial response - An example **109**

J Spreadsheets - Inertia calculation **110**

K Spreadsheets - Frequency bias calculation **112**

L Lead compensator **114**

List of Tables

1 Nordic wind power capacity 23
2 Nordic HVDC interconnections[1][4][13]. 25
3 Component data for the STN 37
4 STN results - Frequency quality indicators 39
5 STN results - Frequency bias 41
6 Data for wind power generators in the N44 model 45
7 Data for simulation events 48
8 Load flows on critical lines prior to event Gamma and Eta 49
9 Results - Inertia (calculations) 52
10 Results - Frequency bias factor (calculations) 52
11 Results - Beta: Frequency response indicators 54
12 Results - Beta, scenario 3 (no controllers): Power flows 55
13 Results - Zeta: Frequency response indicators 56
14 Results - Zeta, scenario 3 (no controllers): Power flows 57
15 Results - Eta, scenario 3 (no controllers): Voltages 58
16 Results - Eta, scenario 3 (no controllers): Power flows 59
17 Results - Gamma: Frequency drops 60
18 Results - Gamma, scenario 2: Power flows 61
19 Results - Zeta, scenario 3 (no controllers): Reactive power flows 106
20 Results - Eta: Frequency drops 108

List of Figures

1 General frequency response for a sudden disconnection of a generator 7
2 Frequency response indicators 9
3 Conceptual response of reserves due to system disturbances 11
4 The effect of system inertia on frequency response 16
5 Danish and Swedish wind power production[19] 22
6 Nordic HVDC connections 24
7 Block diagram - General closed-loop feedback system 26
8 Block diagram - Frame for the HVDC control system 27
9 Block diagram - HVDC controller 27
10 Frequency response for different PWM controller settings 29
11 Power output response for different PWM controller settings 29
12 Block diagram - Wind power controller 30
13 Frequency response for different wind controller settings 31
14 Power output response for different wind controller settings 31
15 Wind generation connected to node Blafalli 33
16 HVDC link connected to node Malmö 34
17 Single line diagram - Small test network 36
18 Frequency responses for different STN scenarios 39
19 Original model configuration for HVDC link (passive) 45
20 Simplified model configuration for HVDC link (passive) 45
21 Results - Scenario 1: Frequency responses 53
22 Results - Beta, summer scenarios: Frequency responses 54
23 Results - Beta, winter scenarios: Frequency responses 54
24 Results - Beta, scenario 3 (no controllers): Voltage responses 55
25 Results - Beta, scenario 3 (no controllers): Power flows 55
26 Results - Zeta, summer scenarios: Frequency responses 56
27 Results - Zeta, scenario 3 (no controllers): Voltage responses 57
28 Results - Zeta, scenario 3 (no controllers): Power flows 57

29 Results - Eta, scenario 3 (no controllers): Voltage responses 58
30 Results - Eta, scenario 3 (no controllers): Power flows 58
31 Results - Gamma, summer scenarios: Frequency responses 60
32 Results - Gamma, summer scenarios: Frequency responses (zoomed) 60
33 Results - Gamma, winter scenarios: Frequency responses 60
34 Results - Gamma, winter scenarios: Frequency responses (zoomed) 60
35 Results - Gamma, scenario 2: Voltage responses 61
36 Results - Gamma, scenario 2: Power flows 61
37 Frequency controlled actions in the Nordics[24] 85
38 Wind turbine generator system - Type 1 86
39 Wind turbine generator system - Type 2 86
40 Wind turbine generator system - Type 3 86
41 Wind turbine generator system - Type 4 86
42 PWM current controller[32] 89
43 Single line diagram - N44 Main grid 90
44 Single line diagram - N44 subgrid: HVDC 90
45 Single line diagram - N44 subgrid: Wind power 91
46 Data - Scenario 1, part 1 92
47 Data - Scenario 1, part 2 93
48 Data - Scenario 2, part 1 94
49 Data - Scenario 2, part 2 95
50 Data - Scenario 2, part 3 96
51 Data - Scenario 3, part 1 97
52 Data - Scenario 3, part 2 98
53 Data - Scenario 4, part 1 99
54 Data - Scenario 4, part 2 100
55 Data - Scenario 4, part 3 101
56 Data - Governor HYGOV 102
57 Data - AVR SEXS 103
58 Results - Delta, summer scenarios: Frequency responses 104

59 Results - Delta, winter scenarios: Frequency responses 104
60 Results - Epsilon, summer scenarios: Frequency responses 104
61 Results - Epsilon, winter scenarios: Frequency responses 104
62 Results - Zeta, summer scenarios: Frequency responses 105
63 Results - Zeta, winter scenarios: Frequency responses 105
64 Reactive power flows from Sweden to Finland (event Zeta) 105
65 Response for a generator at node Helsinki (event Zeta) 105
66 Results - Eta, summer scenarios: Frequency responses 107
67 Results - Eta, summer scenarios (zoomed): Frequency responses 107
68 Results - Eta, winter scenarios: Frequency responses 107
69 Inertia calculations, part 1 110
70 Inertia calculations, part 2 111
71 Frequency bias calculations, part 1 112
72 Frequency bias calculations, part 2 113
73 Block diagram - Lead compensator 114
74 General bode plots for the lead compensator 115

1 Introduction

1.1 Background and motivation

The Nordic power system is facing significant changes. New HVDC cables are strengthening the connection to the continent. Renewable solutions such as solar and wind power are multiplying while some nuclear plants and coal power plants are shut down[1]. New technologies, especially in the fields of power electronics and controllers, have the potential to change the operation of the power system on both small and large scale.

A well functioning electrical power system is the core of the modern society. The power system needs to be in equilibrium to provide satisfactory system services. Thus, maintaining the balance between generation and consumption is one of the most fundamental challenges. The system frequency changes when there is an imbalance. If the frequency deviates significantly from the nominal value, it may cause load-shedding and other adverse consequences in the grid.

Rotating masses that are directly connected to the grid is one of the most vital system properties considering the initial frequency response. It is known as system inertia. HVDC connections and most generation from wind, solar and other renewables (excluding stored hydro) do not inherently contribute to the regulation of system frequency, as they have no rotating masses synchronously connected to the grid. At the same time, new technologies that utilize power electronics allow more industrial loads to be decoupled from the grid[13]. Decoupling of generation and load reduces system inertia. A system with low levels of inertia is vulnerable to power imbalances, as the frequency response degrades. In cases with large shares of decoupled components, additional frequency control may be necessary to maintain satisfactory power system stability.

Until the last years, the percentage of decoupled production in the Nordics was relatively low, and the capacity of the HVDC connections modest. This has allowed the new technologies to be implemented without being too concerned about their effect on inertia and system stability. After the millennium, the proportion of variable speed generation has increased rapidly and new requirements for future production are expected to ensure system stability.

1.2 Problem statement

The main objective of this master thesis is to study how increased HVDC capacity and wind power generation affect the frequency stability of the power system in the future.

The thesis also aims to investigate how the new technologies can be used to contribute to system inertia, and how this may affect the dynamic frequency response. Will HVDC and wind power production reduce system inertia and thereby create more challenging operation situations? Can they contribute to regulation of the system to maintain or even improve the frequency stability?

The hypothesis is that new technologies without synchronous coupling to the grid will reduce system inertia if they are not equipped with suitable controllers. Secondly, the hypothesis is that reduced system inertia will deteriorate the frequency response following a power imbalance.

In addition to frequency responses, power flows and system voltages will be briefly examined to detect possible critical implications.

1.2.1 Elaboration and specification

Throughout this thesis, the author aims to explore and elaborate the dynamic response of the power system, emphasizing the challenges that wind power generation and HVDC connections may introduce. The main focus will be on the initial system reaction. Several scenarios will be investigated to understand how the new technologies will affect the system and how they can be implemented without compromising the stability of the grid. A simulation software, DIgSILENT PowerFactory, will be the primary tool for achieving this.

A simulation model of the Nordic grid will be used for the investigations. All data that are utilized in the model reflects this real system, giving the results more strength and validity. This makes the thesis highly relevant for the Nordic grid, but also for other power systems that face many of the same challenges.

General specifications of the objective include the following: By "future", the thesis will be considering the next decade, with simulations targeting 2030. "New technologies" are in general concerning upcoming technologies that are coupled to the grid via power electronics. This includes wind power, solar power, HVDC links, etc. However, as this report mainly investigates wind power and HVDC, these will be the primary target when the expression is used. When discussing whether the new technologies will be able to contribute (positively) to system stability, it is mainly referred to the different control mechanisms enabled by power electronics that may be used to modify the power output to provide inertial frequency support.

The PowerFactory simulations model used in this thesis is well suited for dynamic fre-

quency studies. However, as it is an aggregated model, it is not ideal for studying voltages. As the power flows are only visible for larger areas, studying these will mainly provide information about cross-border flows and flows between the larges zones. These are some of the reasons why this thesis primarily will focus on frequency studies.

1.2.2 Limitations

- All studies that are conducted by the author, except for the literature study, will be related to the computer simulations for a simplified model of the Nordic frequency area. No tests on real components or grids have been conducted.
- Optimizing advanced controllers are not within the scope of this thesis. Two basic controllers were created to investigate if such solutions would enhance system frequency response, and to explore their potential.
- As only a few operating scenarios are explored, they represent only a fraction of the possible situations that may occur in the real grid. The scenarios chosen are out of the ordinary situations were system inertia is very low or very high. However, the results may also provide relevant information about less extreme situations.
- There are several actions that can be taken to enhance system stability in the future grid when levels of natural inertia are low. Numerous solutions will be mentioned, but only one measure will be thoroughly explored (synthetic inertia).
- All simulations are performed from stable initial conditions at 50 Hz. Thus, disturbances that are initiated at other operation conditions are not investigated.
- An existing simulation model of the Nordic grid has been used as a base for the simulations conducted. This model, called N44, is a compact version of the real Nordic grid. Several components are missing, including all Danish nodes. Thus, no results for Denmark or other absent nodes and components will be provided. Iceland is also excluded from "the Nordics" as their electrical power system has no connection to the other Nordic countries.
- The main interest is the frequency responses of the system. Only a brief investigation is given voltages and power flows for the most critical situations.
- The main emphasis will be given the system as a whole and not individual components.
- The thesis does not consider economic aspects.

1.3 Approach

The following approach was carried out to investigate the problem statement: A comprehensive literature study was conducted. Then, the computer simulation program DIgSILENT PowerFactory was used to test different scenarios concerning system frequency response. First, a smaller test system was created to develop and test different events, configurations, and scenarios. Then, a comprehensive model of the Nordic power system was studied and modified to suit the investigation of the relevant problems for this thesis. Simulations including several disturbances were performed to examine the dynamic responses of the system. Further modifications were made to the model to make it represent a future grid with additional wind power and HVDC connections. Another set of simulations was then carried out. At last, controllers were created and added to the wind generation and some of the HVDC connections for the future scenarios. This was done to investigate how the given technologies could contribute to the inertial response to enhance system stability. After the simulations were completed, an extensive discussion was carried out to illuminate the effects of the developing trends for wind power and HVDC connections, both with and without additional control measures.

A considerable amount of time was used to master the simulation program. Countless hours and effort have been invested to achieve the necessary in-depth knowledge and skills required to perform the operations that lie behind the simulation results.

Most figures have either been designed by the author or are diagrams retrieved from developed or modified models in the simulation program PowerFactory. The figures that are extracted from other sources are clearly marked with references.

1.4 Outline

The thesis is organized as follows: Chapter 2 contains a review of the literature study. It gives insight into the theoretical background necessary to understand and discuss the studies that have been performed. Chapter 3 presents the controllers created for the HVDC interconnections and wind turbines. Chapter 4 gives a thorough explanation of the simulations, including approach, modifications, system description, etc. The chapter includes both the small test network and the more substantial Nordic model. The results for the Nordic grid simulations are presented in chapter 5. In chapter 6, the results are discussed thoroughly to explore the findings and the implications they may represent. The validity of results is also considered. Chapter 7 includes concluding remarks and suggestions for further work.

2 Frequency stability - Theory and context

Power system stability can be explained as the system ability to reclaim equilibrium after a disturbance. It is commonly divided into three main parts: Rotor angle stability, frequency stability, and voltage stability[21]. This thesis investigates mainly the frequency stability after large disturbances in the system.

An approach to the theoretical foundation and background is made in this chapter. Theory and context will be presented for frequency dynamics and power imbalances. The frequency response after disturbances will be thoroughly explained. The concept of inertia will be presented, along with its significant implications. The last part of this chapter provides an introduction to actors of particular interest; wind power generation and HVDC connections. This is partly based on the project report prior to this thesis[14].

2.1 Power imbalances

The "normal state" of a power system is the operating condition where power production meets consumption, the reserve requirements are fulfilled, and the frequency, voltage and energy transmissions are within normal limits[3]. However, imbalances arise continuously, and they promote changes in different parameters, such as the system frequency. Often, the very first sign of disturbances or faults in the grid is frequency deviating from the nominal frequency. If power imbalances are not appropriately handled, they may damage equipment and lead to blackouts.

There are numerous potential reasons for imbalances in the power system, ranging from weather changes, unanticipated load changes, power system component faults, etc. Not to mention that the total load changes continuously while most of the production is scheduled on an hour-to-hour or a fifteen-minute basis. Independent of the cause, reserves are activated to mitigate the imbalances. Reserves are enabled for both up and down regulation. For most faults, a well-functioning power system will activate reserves to restore the frequency and to limit adverse consequences. To minimize the need for reserves, which can both be expensive and scarce, and the risks of harmful effects in general, it is reasonable to keep the imbalances at a low level.

In power systems like the Nordic one, the energy production and consumption is estimated ahead of time. Power imbalances happen continuously, as it is impossible to predict consumption, variable production (wind, PV, etc.), exchanges, losses, faults, etc. with 100% accuracy. Thus, (small) imbalances are not a sign of a malfunctioning system per se. Reducing the deviations to the point where they are negligible, would be a significant

technical challenge and not the most socio-economic solution. A system must therefore be able to handle some imbalances without causing any significant problems.

2.2 System frequency

Considering an electrical system, the frequency is the rate of oscillation for the alternating current (AC). Under normal operation, most large power systems have a nominal frequency of 50 Hz or 60 Hz. During normal operation, the frequencies at all locations in a synchronous area are of approximately the same. All directly connected rotating masses, such as generators, have the same frequency as the system.

To ensure a satisfactory power system performance, the system frequency must stay close to nominal value. Even small deviations should be kept to a minimum, as they may induce damaging vibrations in the synchronous generators, etc. More substantial deviations may damage equipment or lead to load shedding. In the worst case, this can lead to fault cascades and blackouts in the power system[39]. In a robust power system, the frequency is not overly sensitive to power imbalances. Several factors decide the system frequency development during a fault or disturbance event. The initial frequency response is mainly dependent on the disturbance magnitude, the inertia in the system and controlled frequency responses[10]. After the initial reaction, several reserves may be activated to contain and restore frequency to its nominal value.

2.2.1 The Nordic frequency area

The Nordic power system is a large interconnected synchronous frequency area that includes Norway, Finland, Sweden and eastern Denmark. As the electrical boundary to other systems is clear, it is recognized as *one* system. The nominal frequency in the Nordic synchronous area is 50.00 Hz. One of the primary goals for the system operators is to maintain frequency at this level at all times, as all electrical components connected to the Nordic grid are made for this frequency[8]. The *normal state of the frequency* in the Nordic grid is when the frequency varies between 49.90 and 50.10 Hz[4]. When the frequency deviates from nominal values, measures of mitigation are performed to restore it. A graphical overview of frequency controlled actions in the Nordics are presented in appendix B.

The Nordic power system consists of 11 bidding zones. They are distributed in Norway, Sweden, Finland and eastern Denmark (DK2). Western Denmark (DK1) is *not* a part of the Nordic synchronous area. Being interconnected in one frequency area strengthens the security of supply and encourage socio-economic solutions across bidding-zones and

borders. However, it does also mean that a distortion or fault in one part of the system will affect the rest of the system. Nord Pool is facilitating the majority of the Nordic power trading[26].

2.3 Frequency stability and control

2.3.1 The dynamics of frequency response

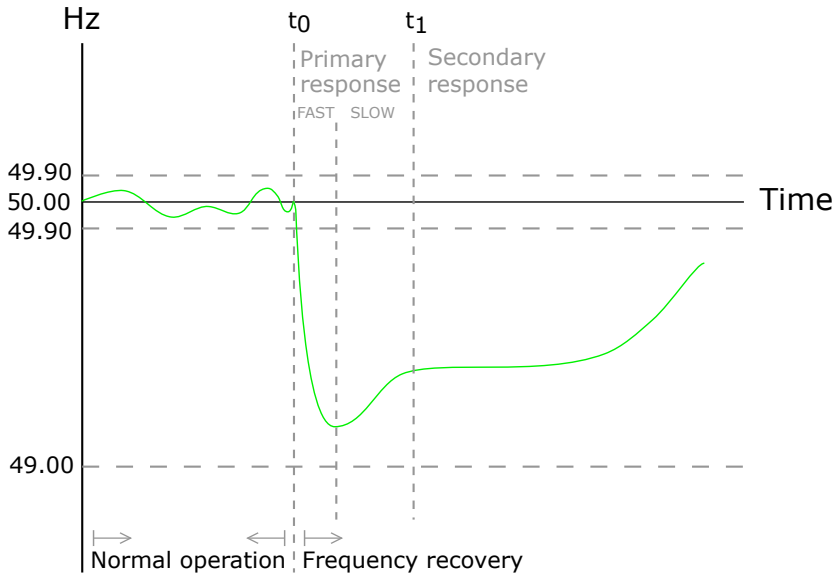

Figure 1: General frequency response for a sudden disconnection of a generator

The general frequency response to a disturbance initiated by a loss of a generator is shown in figure 1. Until t_0 the system is in a normal state, with a frequency close to its nominal value. At t_0, a large disturbance occurs. The response seen in the figure is relevant for sudden imbalances where the consumption becomes higher than the production. This includes sudden disconnections of production units, unexpected connections of new loads or step-up load increases. The four stages of a generic frequency response are described below.

Stage 1 - Rotor swings

When an imbalance occurs in the grid, the rotational speed and the power output of the generators are affected. Generators that possess unique properties react slightly differently from one another. When rotors respond differently, their frequency will oscillate around the system frequency. This is described as rotor swings. All machines will behave a slightly different concerning speed and load angle, depending on their inertia and grid topology. Machines with low inertia will get more significant rotor swings than devices with high

inertia. The generators that are close to the imbalance will in general experience larger swings than production units far away[21]. The machines will swing against each other for a few seconds, and converge as the oscillations dampen due to losses, and power system stabilizers (PSS), etc[34]. Stage 1 lasts for the first few seconds after a disturbance.

Stage 2 - Frequency drop
Stage 2 - the frequency drop - is initiated just after the generators start to swing. The rotors in the system begin to change their speed due to the power imbalance, causing the system frequency to fall. This frequency drop can last for several seconds[21]. If a generator is lost, the remaining generators will decelerate, providing additional energy to the system. If a load is lost, the generators will speed up to absorb some of the surplus energy. In contrast to stage 1, the dynamics of stage 2 does not depend on the electrical distance from the disturbance, as the frequency is a global system parameter. The magnitude of the disturbance and the system inertia have traditionally been the properties that affect the frequency drop[21]. However, new technologies, enabled by power electronics, may facilitate a stabilizing contribution when suitable controllers are implemented.

Stage 3 - Primary control
The third stage lasts for several seconds and is decided by how the production and consumption are affected by the frequency change. Primary control is exercised by the turbine governing systems[21]. The primary controls are purely proportional, providing power support proportional to the frequency deviation Δf. The activation is done locally[38].

The generators source of mechanical power is the prime mover. Depending on the energy source, the prime mover may be a steam, gas, hydro or wind turbine, etc. All prime movers react by decreasing rotational speed as the load is increased, or vice versa. This is originally a non-linear relation, but governor mechanisms usually contribute to making the relationship linear. When a governor is present on a prime mover, it is adjusted to provide drooping characteristics[5].

Stage 4 - Secondary control
Even if a generator has a governing system, it may not be able to return to the nominal frequency by itself after a disturbance. The set-points of generation characteristic, such as P_{ref}, must be changed[21]. The secondary controller consists of both a proportional and an integral part. This stage lasts for several seconds to a minute.

In an interconnected power system, such as the Nordic grid, a centralized control system is used to solve the re-scheduling of the generators optimally. To restore the frequency, maintain power flows between interconnected areas and manage the power allocation among the production units, the central automatic generation control (AGC) (see appendix A) is activated[21]. AGC is implemented to allow all sub-systems to have their own regulator.

2.3.2 Frequency response indicators

There is a range of indicators that can be used for measuring and comparing frequency responses. Several indicators that are identified by the Nordic TSOs[13] are explained below and shown in figure 2. Some of these have been used in this thesis to examine the frequency responses.

When the frequency response based on the results are explained or discussed in general terms in this thesis, it is always referred to the frequency response indicators.

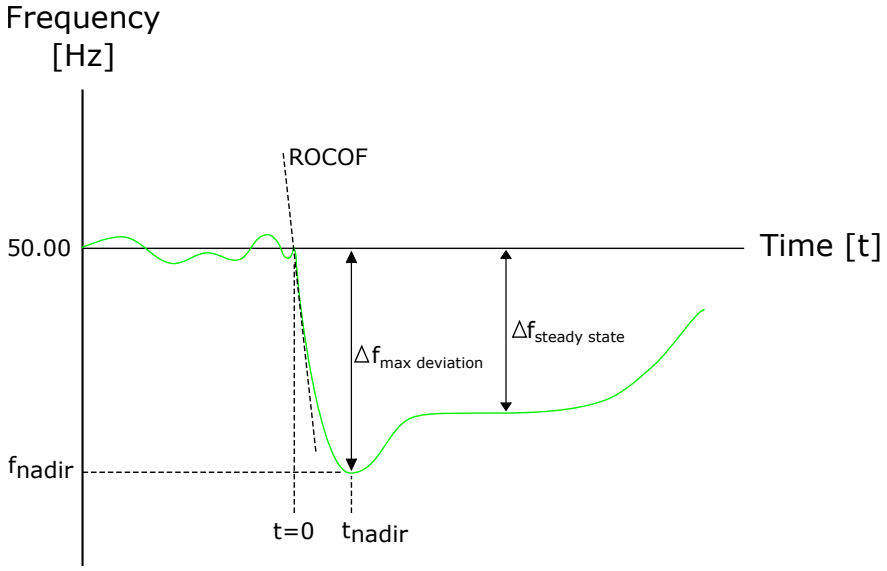

Figure 2: Frequency response indicators

Minimum (maximum) instantaneous frequency
The lowest or highest frequency during a disturbance. When investigating frequency drops, the lowest point on the frequency-time graphs are named nadir.

Time to minimum (maximum) instantaneous frequency
The time after the event was initiated where the frequency minimum/maximum is found. For real systems, there might be challenging to decide when an event begins. However, that is not a problem in this thesis as the times where the events occur are explicitly defined.

Maximum frequency deviation
A measure of the total frequency change, as the frequency prior to the disturbance event seldom is exactly 50.00 Hz in a real system. However, this indicator is not relevant for the simulations conducted as all events are defined to happen from an initial value of f = 50.00 Hz.

Steady state frequency deviation
The absolute value of the deviation from the initial frequency value to the frequency after a disturbance has been stabilized (often measured $90 - 150s$ after event occurrence)[13].

Rate of Change of Frequency (ROCOF)
One of the negative consequences of reduced system inertia is the increased rate of change of frequency. Equation 2.1 is derived from the swing equation (see section 2.4.2), and shows how ROCOF is proportional to the power imbalance ΔP and inversely proportional to the system inertia.

$$RoCoF = \frac{df}{dt} = \frac{\Delta P \cdot f_n}{2 \cdot H_{system}} \, [Hz/s] \tag{2.1}$$

where H_{system} is the inertia constant, f is the system frequency and f_n is the nominal frequency of the given system.

Equation 2.1 shows how increased inertia reduces the ROCOF, giving the system more time to activate appropriate reserves. The ROCOF may be observed graphically in figure 2.

Frequency bias factor
A robust power system is not overly sensitive to disturbances. The frequency bias factor, λ_R, is a measure on how much the steady state frequency changes, $\Delta f_{steady\,state}$, as a result of a change in active power, ΔP. It also indicates the amount of generated power that must be provided or reduced to restore the frequency, given a frequency change of Δf. When a disturbance results in permanent frequency change due to loss of load or generation, the frequency bias factor λ_R can be estimated by the following equation.

$$\lambda_R = \frac{\Delta P}{\Delta f_{steady\,state}} \, [MW/Hz] \tag{2.2}$$

If a linear relationship between the turbine mechanical power and the valve position is assumed, the following relation holds[21]:

$$\frac{\Delta f_{steady\,state}}{f_n} = -\rho \cdot \frac{\Delta P_m}{P_n} \tag{2.3}$$

where ρ is the droop of the machine. The droop of a machine is the percentage speed change required to move the valves from entirely open to closed[21]. Combining equation 2.2 and 2.3, gives the total frequency bias for a system consisting of N machines as:

$$\lambda_R = \sum_{i=1}^{N} \frac{P_{n,i}}{\rho_i \cdot f_n} \, [MW/Hz] \tag{2.4}$$

where $P_{n,i}$ is the rated power for generator i, ρ_i is the rated power for generator i and f_n is the nominal frequency.

Loads also tend to be frequency dependent. If the relationship is assumed to be linear, an equation for the relationship between change in load and change in frequency can be developed. It would have the same form as equation 2.3.

Other response indicators

The main work on dynamic responses in this report concerns frequency. However, a brief investigation of voltage and load flow responses for critical events have been conducted. This was done to explore a broader range of possible implications the disturbances might have. For voltages and load flow, the nadirs, steady-state deviations and magnitude of oscillations have been the primary indicators of interest.

2.3.3 Reserves

When an imbalance occurs, reserves must be activated up or down to achieve a new equilibrium. Different power system might have different conventions for reserves and the use of them. In the Nordic grid, there are three main categories of frequency reserves to maintain satisfactory operation of the power system. These are primary reserves, secondary reserves and the tertiary reserves.

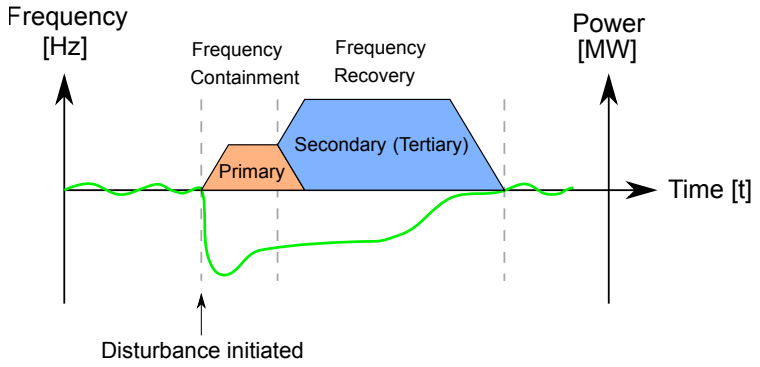

Figure 3: Conceptual response of reserves due to system disturbances

Figure 3 shows conceptually how the different reserves may be activated to support a power system after a disturbance. First, the primary reserves are activated to stabilize the frequency. These reserves can be fast (inertial response) and slow (governor response).

Then, secondary reserves are activated to restore the frequency to its nominal value. They are gradually replacing the primary reserves. If necessary, tertiary reserves are also enabled to help recover frequency and to replace secondary reserves.

Primary reserves

Just after a power imbalance, all generators that are equipped with a governor or speed controller will modify their power output set-point to provide power reserves[39]. This is known as activation of the primary reserves, or the Frequency Containment Reserves (FCR)[24]. Primary reserves are automatically activated within seconds of an imbalance and should be fully activated within 30 seconds. The reserves may be operating for several minutes. The objective of the primary reserves are to stabilize system frequency by restoring power balance[34][39].

In the Nordics, FCR is divided into frequency controlled normal operation reserve (FCR-N), frequency controlled disturbance reserve (FCR-D) and voltage controlled disturbance reserve. (The latter reserve is often used as system protection and is automatically triggered by network voltages. It is not further relevant for this thesis.) The FCR-N are regulating the frequency within 49.9 – 50.1 Hz, while FCR-D is providing power reserves for frequency deviations in the range of 49.9 – 49.5 Hz[3]. FCR-N is distributed between the different sub-systems in the Nordic synchronous area. Each sub-system provides a certain amount of reserves to allow operating in island mode in extreme situations[24]. In the Nordic Grid Code (2007) it is stated that there should be a volume and composition of FCR-D sufficient to withstand dimensioned faults in a way that the system frequency never drops below 49.50 Hz[8]. Automatic load shedding may be used as FCR-D. The reserves must be able to operate until other reserves (e.g., fast active disturbance reserves) are activated. As for the FCR-N, each sub-system needs to provide a certain amount of reserves[24].

Not all types of generation are suitable for sustained frequency response. In the Nordics, hydro governors are the main contributor to the primary response due to their favorable governor dynamics.

Secondary reserves

Secondary reserves or automatic Frequency Restoration Reserves (aFRR) is automatically activated to restore the frequency back to the nominal value and any tie-line power exchanges back to the given set-points. It also relieves the primary reserves[38]. Secondary reserves are provided by units in the area where the imbalance occurred and may respond as quickly as 30 seconds after an imbalance has occurred[3]. It is possible for industrial customers to provide aFRR to the system, although most of the reserves are associated with power generation. A system with secondary reserves are only a recent practice in the Nordics, as it was introduced in 2013 (test period commenced in 2012)[8].

Tertiary reserves

Tertiary reserves are also known as manually activated frequency restoration reserves (mFRR). They are activated by the TSOs in the Nordic system (in Norway: STATNETT) and are used to bring the system back to normal operating condition[38]. Tertiary frequency control modifies the set-points of power generation and loads, facilitating the provision of tertiary reserves[39]. This controlling mechanism resets the reference values of generating units based on optimal flow calculations. In this way, a socio-economic solution is enforced. The tertiary control is the slowest control mechanism, with an activation time of 15 minutes.

Tertiary reserves are used for frequency control, to solve bottlenecks and to restore the primary and secondary reserves and power transmissions to applicable limits after a disturbance event. mFFR may also be used for counter trading and to cover forecasting errors. It is the local parameters (loads, generation, transmission capacity, bottlenecks, etc.) of the system that decides the amount of reserves that are necessary[3].

To enable normal operation after a disturbance, it is necessary to have tertiary reserves distributed among all sub-systems in the grid. Tertiary reserves are traded in a common Nordic market (and can be supplied by both production units and consumers[8].

Reactive reserves

When the situation calls for it, reactive reserves may be activated either automatically or manually. The reserves must be allocated to ensure satisfactory system operation at dimensioning faults. This must be reflected in size, regulation capability and geographical location[3].

2.4 Inertia

2.4.1 Theoretical background

The word *inertia* can be described as the opposing forces on a physical body to change its motion. In an electrical power system, inertia is related to the rotating masses that are directly connected to the grid and their ability to counteract frequency changes. As it is desirable to maintain frequency around a nominal value, inertia is regarded as an advantageous property in the power grid.

For a cylindrical body (like a rotor in a generator) rotating around its central axis, the moment of inertia J is

$$J = \frac{1}{2} \cdot m \cdot r^2 \, [kg \cdot m^2] \tag{2.5}$$

where m is the mass and r is the radius of the cylinder. It can be observed from equation 2.5 how a heavy machine will have a more significant moment of inertia than a light one. The inertia constant, H, are related to the moment of inertia as follows:

$$H = \frac{J \cdot \omega_0^2}{2 \cdot S} \, [s] \tag{2.6}$$

where ω_0 is the nominal angular frequency and S is the rated apparent power of the machine. The inertia constant, H, is a quantified value related to the kinetic energy of a rotor. It tells how many seconds a generator needs at synchronous speed and rated power to provide the same amount of electrical energy as the stored kinetic energy of the rotor[21].

The total inertia constant for a power system, H_{system}, can be calculated using equation 2.7, below. The equation applies for a system with N units, and is based on the weighted sum of the inertia constants for each individual machine:

$$H_{system} = \frac{\sum_{i=1}^{N} (H_i \cdot S_{n\,i})}{\sum S_{n\,i}} \, [s] \tag{2.7}$$

where $S_{n\,i}$ is the rated apparent power of a machine i.

The kinetic energy E_k for a rotating body is related to the moment of inertia by

$$E_k = \frac{1}{2} \cdot J \cdot \omega^2 \, [J] \tag{2.8}$$

where ω is the angular velocity of the rotating body.

The total system inertia may also be calculated in kinetic energy [GWs], which is more convenient than seconds as for the inertia constant[12]. As this is common practice, the kinetic energy approach will be used for the calculations in this thesis. The total kinetic energy stored in the rotating masses $E_{k\,system}$ can be calculated by

$$E_{k\,system} = H_{system} \cdot S_{n\,system} = \sum_{i=1}^{N} (H_i \cdot S_{n\,i}) \tag{2.9}$$

2.4.2 Swing equation

The contribution from a synchronous connected machine to the system stability can be explored by investigating equation 2.10: *The swing equation* (damping neglected, and frequency/angular speed assumed close to nominal value):

$$2H\frac{d\omega}{dt} = P_m - P_e\,[p.u.] \tag{2.10}$$

where H is the inertia constant, t is time, P_m is mechanical power supplied by the generator, P_e is electrical power demand and ω is the rotational speed. The frequency is proportional to the rotational speed:

$$\omega = 2 \cdot \pi \cdot f\,[rad/s] \tag{2.11}$$

Frequency is a global parameter, being the same throughout the system. As the system frequency is related to the speed of the connected generators, equation 2.10 shows how the system frequency behaves when there is an imbalance between power input and output. One observes how a system with high inertia gets a smaller frequency reaction than a low inertia system.

Substituting equation 2.6 and 2.8 into equation 2.10 gives another form of the swing equation, where the change of kinetic energy as a response to an imbalance is described:

$$\frac{d}{dt}(\frac{1}{2}J\omega^2) = \frac{d}{dt}E_k = P_m - P_e\,[p.u.] \tag{2.12}$$

The equation above (2.12) shows how an imbalance in the system ($P_m - P_e \neq 0$) will lead to a change in kinetic energy stored in the generator(s) in the power system.

The mechanical power P_m changes very slowly compared to the electrical power P_e, due to the relatively slow governor response[12]. Thus, one can assume that the mechanical power is approximately constant initially after a disturbance ($\Delta P_{m\,i} = 0$). By rearranging equation 2.10 under these conditions one can observe how the rate of change of frequency (ROCOF) is limited by inertia only, right after the occurrence of an imbalance.

$$ROCOF = \frac{df}{dt} = \frac{d\omega_e}{dt} = \frac{-1}{2 \cdot H} \cdot \Delta P_e\,[p.u.] \tag{2.13}$$

Equation 2.13 gives the inherent inertia response of a synchronous machine that is directly connected to the grid. The equation shows how ROCOF is inversely proportional to the

inertia constant, and proportional to the change of electrical power ΔP_e. The negative sign indicates that the power reaction will be of opposite sign to the frequency change, and thus oppose the disturbance. This confirms the practical knowledge saying that larger inertia *reduces* the amplitude of frequency deviations. The maximum frequency deviation is indirectly reduced when ROCOF is reduced, as reserves get more time to be activated. See appendix I for a more thorough explanation of how the swing equation describes the initial frequency response.

The contribution of inertia on the initial frequency response can be seen on the figure below (figure 4). A system with three synchronously connected conventional generators does have a better frequency response than the systems with one or two generators. This is mainly seen on the frequencies deviating less from nominal value and on the reduced ROCOF. The time of nadir is almost unchanged.

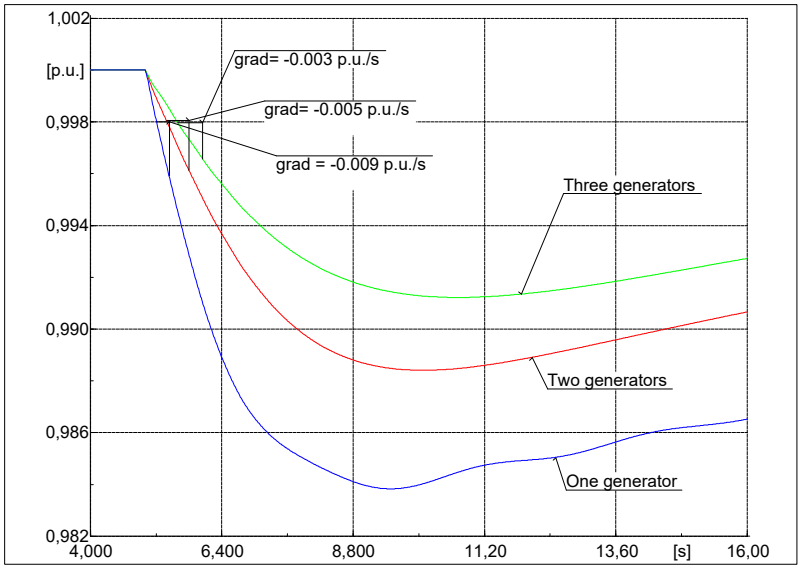

Figure 4: The effect of system inertia on frequency response

2.4.3 Current development and future concerns

It is the accumulated contribution from loads and generators that provide sufficient inertia to the system to facilitate stable operation. Most of the inertia in the electrical power system today is situated in the large rotating masses in synchronous generators. These can be found in hydro, thermal, nuclear power plants, etc. Loads may also contribute to the inertia in a system, e.g. when large industrial motors are directly coupled to the grid, much in the same way as generators. If a power system has critically low inertia, measures of mitigation must be taken to prevent stability issues from rising.

One of the main concerns for the power system in the near future, and the motivation for this thesis, is the comprehensive changes that the Nordic grid faces where the level of system inertia is expected to fall. Reasons for this include[13]:

- The share of distributed generation and renewable production that is not synchronously connected to the grid is expected to rise.
- Some nuclear and thermal generators are decommissioning.
- More interconnectors from the Nordic grid to the continent.
- More loads are expected to be connected through power electronics[34].

Power electronics are becoming increasingly important in the complex and advanced power systems of the 21st century. They lead to a reduction in system inertia as they electrically decouple generation and loads from the grid. (Visual examples of coupled and decoupled wind power generation systems are given in appendix C.) Recent trends in installed production capacity show an increase of wind and solar power at the same time as some thermal and nuclear power plants are shutting down. In modern power production from renewable sources, including wind and solar power, there are often no rotating masses directly coupled to the grid. As these types of generation do not inherently contribute to system inertia, system inertia is reduced when they replace conventional production.

The initial ROCOF depends on system inertia (equation 2.10. Low inertia in the system leads to a faster change of frequency. The capability of the system to withstand frequency changes deteriorates when the system inertia decreases. The power system mechanisms and codes that today are successfully operating to maintain system stability may not be sufficient in the power system of tomorrow. Faults that originally represented a small risk of causing problems may become critical due to the new and faster rate of change of frequency. Also, the original means of frequency containment reserves might not be sufficient for the new situation. If disturbances happen in situations with insufficient inertia, the frequency drop may be too rapid for the reserves to react sufficiently. Then, the frequency can reach values where load-shedding are initiated, even though there are reserves in the system. As frequency dynamics are behaving quicker in low inertia systems than areas with high inertia, inertia differences can also lead to large transient frequencies and oscillations in multi-area power systems like the Nordic. If the power transients after a disturbance are amplified, it might violate the line constraints, ultimately triggering protective equipment like relays. Disconnecting the line might stress the system further, and may in worst case start a cascade of incidents that lead to damaging circumstances or blackouts. However, meshed system designs will be more resilient to disturbances concerning frequency dynamics[38].

2.4.4 Measures of mitigation

The Norwegian TSO, STATNETT, acknowledge that maintaining sufficient level of inertia in the Nordic grid is one of the main challenges for the years to come[4]. This is vital to ensure system stability and operational security. In the reports [4] and [12], several actions to enhance system stability by increasing or maintaining system inertia are suggested. Some of these are listed below:

- Minimum requirements of inertia in the system. This means that some generators can be asked to run even when it is not considered the most economically optimal solution. Some incentive or support must be given to the affected producers.
- Limiting the power output of the largest units (both HVDC links and generators) to reduce the largest possible disturbance to a satisfactory level.
- Providing synthetic inertia or similar to the system. This concept will be described further in section 2.4.5.
- Adding synchronous condensers or other rotating masses to the grid.
- Including more of the fastest reserves (FCR), or increasing the reaction speed of other reserves to counteract the momentary frequency change.
- Letting more generators run at a lower average output, instead of only having a few generators at high output. This will increase system inertia.
- Provide some economic scheme that gives incentives to contribute to inertial support, especially during critical hours.
- Quickly providing additional power by emergency power injection (EPC) or disconnection of large loads such as pumps for pump-storage hydropower plants.

2.4.5 Synthetic inertia

As a response to a disturbance, the synchronously connected generators in the grid will change their mechanical torque (and thus the power) proportional to the rate of change of frequency (ROCOF). Synthetic inertia is a contribution of electrical torque proportional to ROCOF from power sources that do not inherently have an inertial response. This is often enabled by suitable controllers. Thus, synthetic inertia is not inertia per se, but a controlled response that imitates the favorable reaction of connected rotating masses. To be able to supply synthetic inertia, there must be some stored energy behind the power electronics in the power supply. Examples include batteries and rotating masses in wind

turbines, or any other power system that are coupled via DC connections[10]. Adding measures of frequency support to HVDC is possible by e.g. ESS or additional control systems allowing synthetic inertia. Synthetic inertia solutions were not implemented in the Nordic grid by 2017[13]. More information on wind power and synthetic inertia are presented in the following paragraph.

Wind power and inertial response

The turbines usually produce maximum power at the given wind speed, allowing few adjustments to provide power support. The absence of reserve opportunities is a drawback for wind power integration, especially in areas where wind power represents a significant share of the total power production. However, recent development in power electronics and wind turbine technology facilitates new and improved control options. There are two main approaches for wind turbines providing synthetic inertia, in addition to solutions offered by Energy storage systems (ESS): Releasing hidden inertia and releasing reserve capacity in pitch[7][30]. To release hidden inertia, the kinetic energy stored in the rotating masses are utilized by changing the rotational speed. In this way, energy can be provided or absorbed from the grid. Wind turbines operate typically at maximum power output. In these situations, there are no reserves available. However, one can decide to run the turbines at less than optimal speeds, and then use pitch control to exploit this to provide an inertial response.

A drawback with frequency support from wind power is that synthetic inertia from wind turbines may only be provided for a short period of time. The turbines would stall if too much kinetic energy were extracted[18]. This could lead to cascades of stalling, and worsen the situation considerably. It should also be noted that wind turbines only have stored energy when they are operational (blades rotating). As the turbine changes its kinetic energy to provide inertial support to the system, there must be a phase of recovery afterward to bring the turbine back to the original operational state.

As synthetic inertia is not dependent on a physical entity in the same way as inertia is directly dependent on the rotating mass, the virtual moment of inertia does not need to represent the actual amount of energy that is stored in the system. Thus, it is possible for synthetic inertia to provide even *better* stability services than conventional generators. This is because the setpoints of the virtual response can be set quite freely, being able to release energy much faster than a conventional system[34].

Several technical solutions that allow wind turbines to provide inertial response have been developed over the last decade, as the rapid increase of installed wind turbines makes it necessary to find solutions to enhance system stability. Two providers with such solutions are General Electric (WindINERTIA™)[23] and ENERCON (ENERCON Inertia Emulation)[16].

2.4.6 Inertia in the Nordic system

There are no requirements on system inertia in the Nordics today. However, sufficient levels of inertia are required to reach power system targets such as not allowing a dimensioning incident to induce frequencies near 49.00 Hz, to assure that no measures of load shedding are necessary[4].

The present power generation of Norway, Sweden and Finland are characterized by thermal, hydro and nuclear plants[13]. Most of these contribute substantially to system inertia. Denmark on the other hand, have a significant share of wind power capacity, providing less inertia. Having critically low system inertia usually is not a problem during normal operation in the Nordic grid as there is a significant share of large, directly connected power plants that provide large amounts of inertia.

The development of more variable energy sources, together with some reduction of nuclear and thermal plants, indicates that the Nordic system inertia might be reduced in the years to come. At the same time, HVDC connections to other frequency areas are increasing. This does not favor system frequency stability, as it may allow situations with very little system inertia to appear more frequently and potentially with even less inertia than today. New power plants and HVDC interconnectors also tend to have massive capacity, which may increase the risk for more significant and more frequent disturbances. The TSOs estimate that the Nordic system will have less inertia than required 1-19% of the time in 2025 (depending on the climate year)[4].

Different operational situations have different amounts of system inertia. Worst case scenarios or other extremes should be considered. Extreme system inertia situations may be identified based on the contribution from activated generators:

- **Scenario with high inertia:** This situation may occur on a cold winter day during peak hours, leading to sky-high consumption. Most conventional generators need to be operational, especially if power import is modest or variable production is low. This would result in very high system inertia.
- **Scenario with low inertia:** This situation occurs typically at summer nights when the total system load is low. Few conventional generators are operating. The inertia situation can be further deteriorated by having significant wind power production or high import due to low continental energy prices. This would lead to more conventional production being temporarily shut down. The system inertia will be very low. Summer nights are also identified by the Norwegian TSO, STATNETT, as some of the most critical operating hours concerning inertia[4].

The two extremes above will be further investigated during simulations to explore the impact of inertia in the Nordic grid and to study different actions that can be made to improve system stability.

2.5 Variable energy sources

Some renewable power plants, like wind and solar plants, get their energy from what is classified as variable energy sources or intermittent energy sources. These energy sources are expected to have a considerable increase in installed capacity during the next decades[1]. Being a *variable* energy source means that the source, and therefore the production, can not be easily controlled to meet the demand, as they are heavily dependent on current conditions like the weather. A wind turbine produces energy when the wind is blowing and not necessarily when there is a high demand. The power production is complicated to predict and may fluctuate rapidly. In contrast, *dispatchable generation* can store their power source. This group includes, among others, hydropower plants with magazines and thermal plants. These are straightforward to predict and control, and the production can be adjusted when demand calls for it. Power generation that is quick and easily adjustable is ideal for covering system imbalances.

The term "modern wind turbines" usually refers to the variable speed operation and turbines being electrically decoupled from the grid. Most modern variable energy sources are connected to the grid via power electronics, such as converters. This is shown in appendix C, where line diagrams of four types of wind turbines are displayed. This decoupling is the reason why modern wind turbines do not inherently contribute to the system inertia, even though they have rotating masses. As system inertia increases system stability, high shares of renewable energy sources contribute negatively to system stability by making it more vulnerable to disturbances. It may be necessary to implement means of mitigation in the future power system to assure sufficient system stability if levels of "natural" inertia are low. Such measures are presented in section 2.4.4.

Another challenge with variable energy sources is that spinning reserves and inertia in the system may fluctuate. This is because dispatchable generation must cover the gap between power demand and variable energy production. Thus, the inertia in the system might change from high to low, and back again, within hours. When the system inertia is challenging to predict, the operation of the power system becomes more complicated. It becomes increasingly difficult for the system operators to assure a satisfactory system state and doing so in a cost-efficient manner.

As it is vital for system operation to maintain power equilibrium, there must always be an adequate amount of power reserves available. Today, it is mainly the easily control-

lable dispatchable generation that provides these reserves. When traditional power plants are temporarily or permanently shut down due to the new variable power production, it reduces accessible system reserves. Thus, variable power sources as of today are both causing more imbalances and reducing the availability of reserves needed to respond to them. Also, variable energy sources makes the use of reserves less predictable and more fluctuating [7][39]. These critical issues must be solved for the future power system to operate satisfactorily.

2.5.1 Wind power

As wind power accounts for the vast majority of variable energy production in the Nordics, it is the only variable power source that was modeled in this thesis.

Wind turbines can generate vast amounts of electric energy by utilizing the energy in the moving air. The power that can be extracted from the wind by a wind turbine is given by

$$P_{mech} = \frac{1}{2} \cdot C_p(\lambda, \omega) \cdot \rho \cdot A \cdot v_w^3 \, [W] \tag{2.14}$$

where ρ is the air density, A is the area swept by the blades, v_w is the wind speed and C_p is a performance coefficient. The performance coefficient is dependent on both the tip speed ratio λ and the blade pitch angle β. According to Betz's limit, a wind turbine can at most extract $\frac{16}{27}$ (about 59.3%) of the kinetic energy in the wind[21].

One of the main characteristic features of wind power production is the significant variations of production, both when considering short and long time scale[15]. This is the main reason why the power output from wind turbines is hard to predict. An example of the fluctuations in power output can be shown in figure 5, where the aggregated wind power production for Sweden and Denmark are shown.

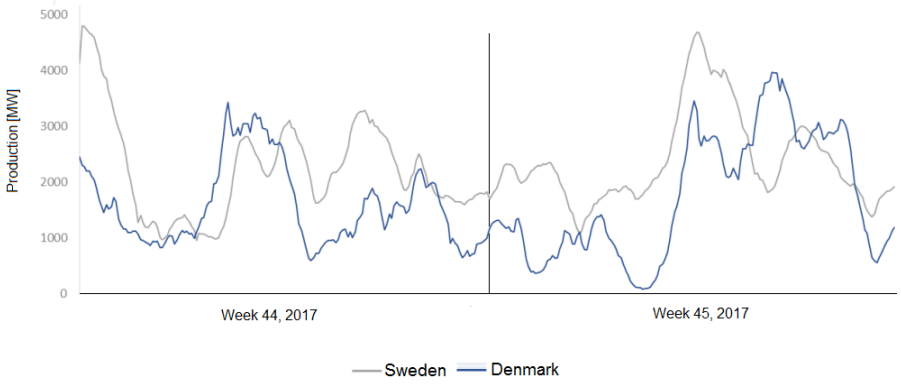

Figure 5: Danish and Swedish wind power production[19]

There are four main types of wind turbines in the present wind power industry[30]. These are presented in appendix C. For the simulations conducted in this thesis, only type 4 has been implemented in the model as it is expected to account for the majority of future installed wind power capacity.

2.5.2 Wind power in the Nordics

The Nordic countries have significant wind power resources[11], and Norway has one of the highest potentials for wind power in Europe due to its long and windy coastline[9]. Installed wind power capacity has increased over the last decades, both in the Nordics and most other European countries[42]. There are several reasons for this; Fighting climate change, nuclear power plants and coal power plants are shutting down, increased electricity demand, etc. The need for more energy production in the Nordics is further strengthened by the investments in increased transmission capacity to the continent [20].

In the table below, the installed wind power capacities in the Nordic countries by the end of 2016 are listed. The expected capacities by 2030 are estimations based on comprehensive analysis of the power market by the Norwegian regulators, NVE. They have estimated that the Nordic wind power capacity will be doubled from 2017 to 2030, giving a total wind power production of around 80 TWh[2] (corresponding to installed capacity of approximately 26-30000 MW). It is anticipated that this increase is shared by the Nordic countries as shown in table 1, below.

	Actual capacity 2016 [MW][42]	Estimated capacity 2030 [MW]
Norway	838	6200
Sweden	6494	9400
Finland	1539	3000
Denmark	5230	9500

Table 1: Nordic wind power capacity

2.6 HVDC systems

An HVDC system is an electrical power system that transfers energy at high voltage and direct current, as an alternative to an alternating current (AC) system. At the connections to the AC systems, there are HVDC converter stations. In back-to-back systems, the HVDC system consists only of one HVDC converter station. In such case, the station is equipped with a DC connection between the two HVDC converter units[35]. HVDC

is often used to transfer energy over long distances, as long-distance AC transmission is associated with high losses. HVDC transmission also allows uncomplicated coupling between areas that are not synchronous or regions with different frequencies.

Recent development in technology has introduced Voltage Source Converter (VSC) HVDC systems. These have become popular because of their separate control of active and reactive power, high quality voltage wave forms and because they are suitable for connecting variable speed generation (such as wind power) to the grid[43]. The simple power control is convenient when it is desired to enable the HVDC connection to contribute frequency stability. This is why HVDC with VSC solutions are used for the simulations conducted in this thesis where the (active) HVDC connections are contributing to the inertial response. A challenge with HVDC technologies providing fast responses is that the modified power flow will affect the other end of the cable. Practical solutions for this have not been investigated in this report.

2.6.1 Nordic HVDC connections

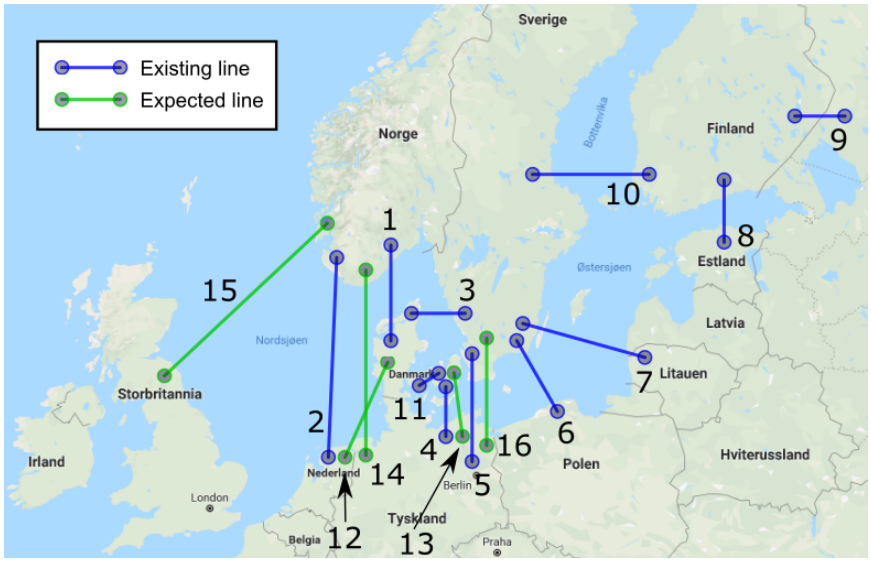

Figure 6: Nordic HVDC connections

The Nordic power system has several HVDC connections to other power grids today. As seen in figure 6, the Nordic grid has interconnections to the Netherlands, Germany, Denmark (DK1), Poland, Lithuania, Estonia and Russia. The total HVDC capacity from the Nordic frequency area is about 8500 MW[4] (2018), see table 2. By 2026, it is anticipated to have increased to 12000 MW. The relevant interconnection were implemented in N44.

HVDC cables are under construction from Norway to United Kingdom (North Sea Link), from Norway to Germany (Nord Link), and from Denmark (DK2) to Germany (Kriegers Flak). Several other projects are being considered, although these are not under construction yet. The projects that are connecting Western Denmark to other markets, such as Viking Link (Denmark to the United Kingdom) and Cobra (Denmark to the Netherlands) are not a part of the Nordic frequency area.

	Project name	Connection	Capacity	Commissioning
1	Skagerrak 1-4	NO-DK1	1632 MW	In operation
2	NorNed	NO-NL	700 MW	In operation
3	Konti-Skan 1-2	SE-DK1	680/740 MW	In operation
4	Kontek	DK2-DE	600 MW	In operation
5	Baltic Cable	SE-DE	600 MW	In operation
6	SwePol Link	SE-PL	600 MW	In operation
7	NordBalt	SE-LT	700 MW	In operation
8	Estlink 1-2	FI-EE	1000 MW	In operation
9	Vyborg Link	FI-RU	1400 MW	In operation
10	Fenno-Skan 1-2	SE-FI	1200 MW	In operation
11	Great Belt Power Link (Storebælt HVDC)	DK1-DK2	600 MW	In operation
12	Cobra	DK1-NL	700 MW	2019
13	Kriegers Flak	DK2-DE	400 MW	2019
14	Nord Link	NO-DE	1400 MW	2020
15	North Sea Link	NO-UK	1400 MW	2021
16	Hansa PowerBridge	SE-DE	700 MW	2025/2026

Table 2: Nordic HVDC interconnections[1][4][13].

Table 2 is mainly based on the STATNETT report "Challenges and opportunities" (2016)[4]. The country codes are as follows; NO = Norway, SE = Sweden, DK = Denmark, FI = Finland, LT = Lithuania, NL = the Netherlands, DE = Germany, EE = Estonia, UK = United Kingdom and RU = Russia.

3 Customized control systems

In this chapter, a presentation will be given of the two controllers that were developed for the wind power production and HVDC model in the simulation program PowerFactory. It will be explained how they may affect a power system, with examples from the "Small test network" (STN). It is assumed that the reader possesses basic knowledge on the field.

The two controllers will be referred to as the "HVDC controller" and the "wind power controller" in this chapter and the rest of the thesis.

3.1 Background

In the future, there will be an increasing number of hours where a large portion of the energy consumption in the Nordics is covered by HVDC import, wind power or other solutions without natural inertial response. Thus, to ensure satisfactory system operation, it may be necessary to implement controllers to allow wind power and HVDC to contribute positively to the system stability. This has been the motivation for creating the additional controllers in this thesis. The parenting strategy for the controllers was to provide inertial support to the system by controlling a power response based on measurements of the system frequency. The contribution should preferably be similar, or better, than the frequency support from the conventional technologies.

According to Dorf and Bishop (2011)[6], a control system is several components that are connected in such a way that the desired system response is obtained. This is based on the fundamental theory of a cause-effect relationship in linear system theory. A simple system with a closed-loop feedback system is presented below, figure 7. It shows a basic configuration that has been used as inspiration for the development of the controllers in this thesis.

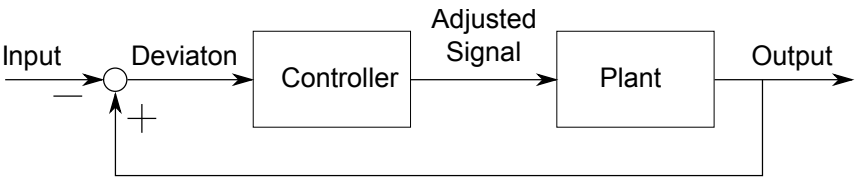

Figure 7: Block diagram - General closed-loop feedback system

3.2 HVDC controller

The main goal for this controller was to allow the modeled HVDC connection to contribute to the inertial response. The HVDC connection in this thesis was modeled as a voltage source behind a Phase Width Modulation (PWM) Voltage Source Converter (VSC) converter. The converter was by default equipped with an internal current controller in PowerFactory. The block diagram of the current controller are found in appendix D, for comprehensive information see [32]. In short, the current controller used the converter voltage (associated with the modulation ratio) to keep the current close to the reference value. By adjusting the input signal id_{ref} to the current controller, one could indirectly control P_{out} as the voltage at the node remains close to constant. This allowed the HVDC model to provide an inertial contribution to stabilize the system frequency. Thus, the controller was implemented on the PWM converter with the strategy of utilizing the existing design to provide inertial support to the system.

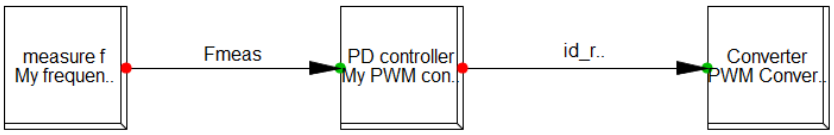

Figure 8: Block diagram - Frame for the HVDC control system

Figure 8 shows the frame for the HVDC controller that has been developed. In short, the three boxes have the following properties (from left to right); the first box measured the frequency at the AC bus and then sent this signal to the controller. The second box, the controller, are further explained in the next paragraph, but the essence is that it used the measured frequency (input) to calculate a suitable id_{ref} (output) which was sent to the last box in the frame. The last box is merely a representation of the PWM converter, meaning that it receives the signal that is transmitted from the second box. The converter adjusted the power flow based on this signal.

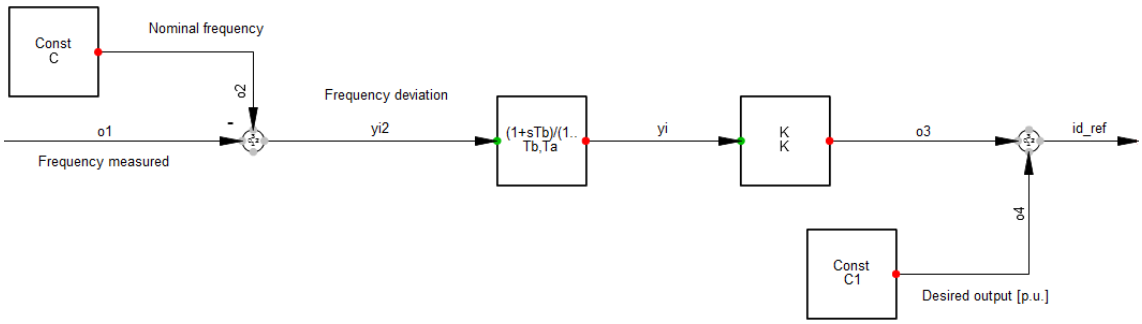

Figure 9: Block diagram - HVDC controller

Figure 9 shows the controller configuration. The input $o1$ is the measured frequency at the connected AC bus. At the first summation point, this value was subtracted from the signal $o2$. As $o2 = C = f_{nominal}$, the sum $yi2 = o2 - o1$ represented the frequency deviation.

The second box, $\frac{1+s \cdot Tb}{1+s \cdot Ta}$ (where $Tb > Ta$), is a lead compensator. It gave a derivative contribution to signals with frequency between $\frac{1}{Tb}$ and $\frac{1}{Ta}$ rad/s. A well tuned lead compensator can improve system stability significantly. Dissecting it, $\frac{1+s \cdot Tb}{1}$ gives a high gain for high frequencies, much like a derivative block. However, the second part, $\frac{1}{1+s \cdot Ta}$, reduces the gain at high frequency. In total, the lead compensator gives a high gain at high frequencies, but not as high a D controller. For the same reason, a lead compensator provides less noise than a D controller. See appendix L for more information on the lead compensator.

The next box contains a proportional term, meaning that the signal yi was multiplied by a constant K, giving signal $o3$. The last part of the controller added the signal $o3$ and a new constant $o4 = C1$. $C1$ was a permanent offset, giving the desired value for P_{out} given stable operation.

The unknowns in the HVDC controller were C, C1, K, Ta and Tb. C was the nominal frequency (50.00 Hz). C1 represented (indirectly) the desired power output (per unit). This varied between scenarios and cases, but was for the STN set to 0.6 (p.u.). Ta and Tb were decided based on the trial and error method and discussions with the supervisor. They are chosen to be $Tb = 2$ and $Ta = 0.2$, which satisfy the criteria of a lead compensator: $Tb > Ta$. The gain K has been explored by trial and error in order to find a stable solution with a reasonable inertial contribution from the HVDC links. $K = 0.3$ has been used for the main simulations. This gain allowed a momentary active power contribution from the HVDC links of around 15% of nominal values, at the same time as the system remained stable after all events.

Example

Examples are convenient to illustrate the controller performance. A step-up load disturbance in the STN network was used for this example. The rating of the PWM converter was 25 MW, and the desired output at stable operation was 15 MW. Thus $C1$ equals 0.6 [p.u], as $0.6 \cdot 25MW = 15MW$.

During stable operation at nominal frequency, $f_{meas} = 50.00$. As $C = f_{nominal} = 50.00$, the sum $yi2$ becomes zero. When the input to the P and lead compensator boxes are 0, the output also becomes 0. At the last summation point, the calculation becomes $o3 + o4 = 0 + 0.6 = 0.6$. Thus, the output signal becomes 0.6 p.u. and the power output becomes 15 MW, as desired.

If a disturbance happens, e.g. a step-up load increase or a loss of a generator, the frequency falls. The measured frequency becomes less than nominal frequency. This deviation, $yi2 > 0$, becomes modified through the lead compensator and proportional term and at the end added to the permanent offset. The sum $o3 + o4$ will now become larger than the value during normal operation, $id_{ref} = o3 + o4 > o4$. Thus, the power output from the modeled HVDC will become 15 MW *plus* some extra power support to counteract the negative frequency change. This shows that the HVDC has been given the ability to contribute to the inertial response to frequency changes. Several simulations have been conducted in the STN to confirm if the controllers work as planned.

Figure 10 and 11 gives the system frequency response and power outputs from the HVDC model for the given disturbance. One can observe the effect of the customized controller. When $k = 0$, being equivalent to no controller, it can be seen from figure 9 that the contribution from the controller due to frequency deviations is zero. Thus, the green lines depict the system response without the controller. One may observe that the frequency response improves when k increases. The frequency drop seems to be reduced, and the nadir is rising. Figure 11 shows how this is possible. The power output rises quickly as a response to the disturbance to reduce the total imbalance.

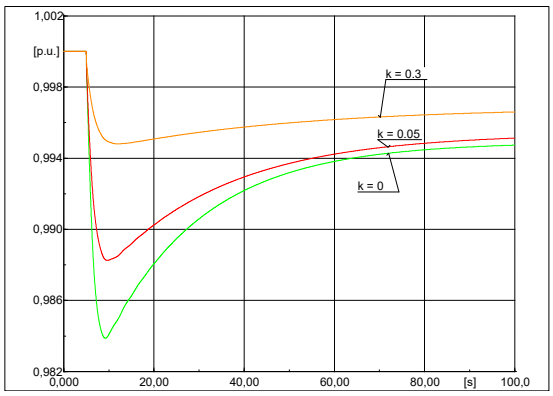

Figure 10: Frequency response for different PWM controller settings

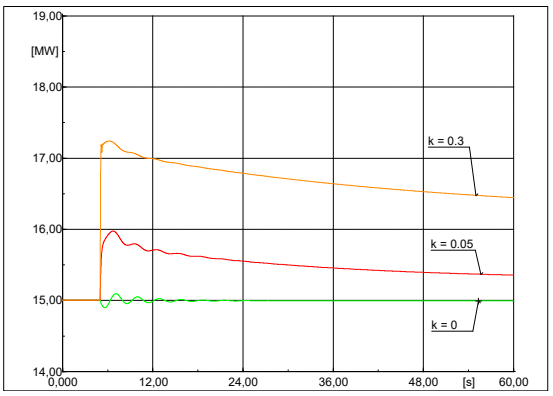

Figure 11: Power output response for different PWM controller settings

The controller was designed to allow HVDC to provide an inertial response. The steady-state contribution was not a concern. Thus, the permanent frequency deviation may not be accurate when the controllers are activated. As the main scope was to investigate the inertial response when the controllers were enabled, this was not regarded a problem. However, it has been suggested in section 7.2 Recommendations for further work that developing and exploring the responses from more comprehensive controllers with corrected long-term responses would be interesting.

3.3 Wind power controller

The FRC wind power template in PowerFactory was already equipped with a controller system. For practical reasons, it was decided to modify the existing controller rather than to replace it or to add a second controller. In this section, the attention will be given the self-made modification to the existing controller and not to the existing control system from the PowerFactory library. See [33] for more details on the PowerFactory template for the wind turbine. The goal for the additional controller (loop) that was implemented by the author was to allow wind turbines to contribute to the inertial response.

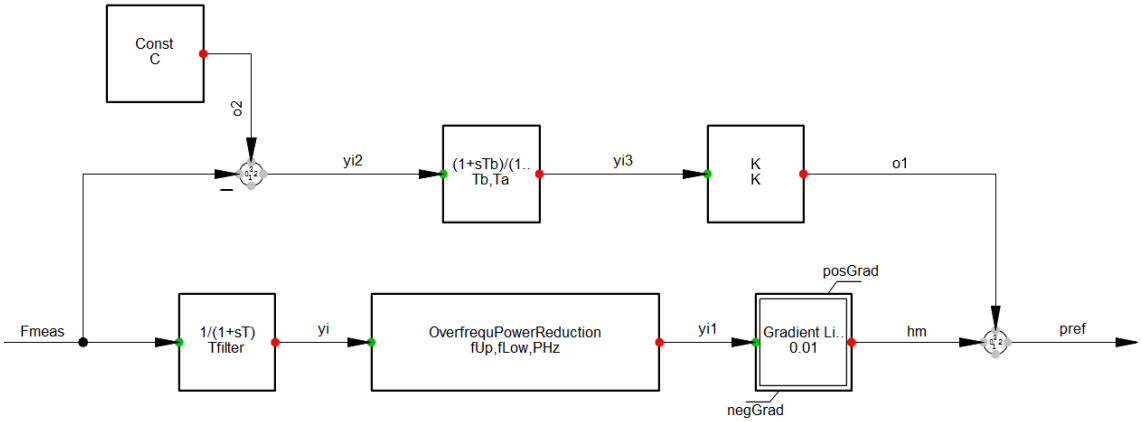

Figure 12: Block diagram - Wind power controller

Figure 12 shows two branches. The lower one is a part of the existing FRC controller given in the PowerFactory template library. The upper branch was developed for the simulations conducted. This additional branch will now be explained: The output for the whole block system shown in the figure is $pref$, a power reference used to control the power output of the wind turbine. By increasing it, the power output from the turbine(s) would increase, and vice versa. The goal of the additional control loop was thus to modify the $pref$ value according to the system frequency, to allow the wind turbine to provide an inertial response during disturbances.

The first summation point subtracted the measured frequency (Fmeas) from a constant C. As the constant was the nominal frequency, the output $yi2$ represent the frequency deviation from the desired frequency. In the same way as for HVDC controller, the deviation was modified by a lead compensator and a proportional block. At last, the signal ($o1$), was added to the original signal provided by the existing system, leading to the output $pref$. The unknowns in the wind controller was C, K, Ta and Tb. C was the nominal frequency (50 Hz). Ta and Tb were set to $Tb = 2$ and $Ta = 0.2$, decided by trial and error and by supervisor guidance. The existing synthetic inertia wind controller, GE

WindINERTIA™, can momentarily increase the power output 5-10% of rated power to support the system for large under frequency events[23]. The gain K has been chosen by trial and error to allow the wind turbines in the simulation models to provide frequency support in the same range for the simulations conducted in this thesis. $K = 0.3$ was used for the main simulations, if nothing else is stated.

Investigating the wind controller; If the measured frequency was 50 Hz, the signal to the lead compensator would become zero - meaning no change from desired steady-state power output from the wind turbine. The frequency would rise if there were a loss of load in the system. Then $yi2 < 0$, eventually leading to reduced power output. In this way, the controller allows the wind turbine to contribute to the inertial response.

Simulations have been conducted in the STN to confirm the effect of the wind turbine controller. The frequency and power response is displayed below.

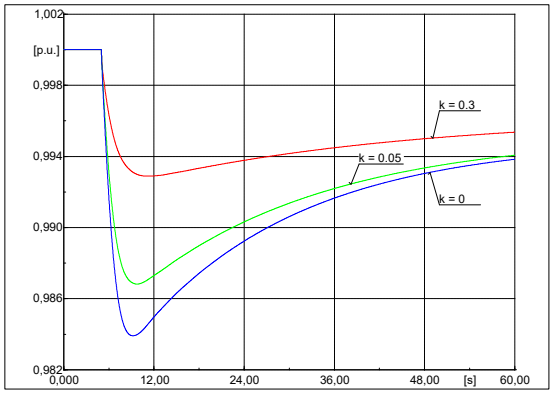

Figure 13: Frequency response for different wind controller settings

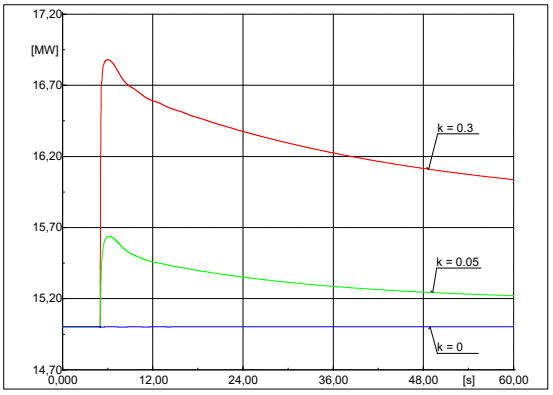

Figure 14: Power output response for different wind controller settings

The frequency response from a wind power plant with the controller was quite similar to the HVDC system in the previous section. When $k = 0$, equivalent to having no controller, no extra power was provided during the disturbance and the frequency response was disadvantageous. As the contribution from the controller was increased, k raised, and one can observe a reduction of the frequency drop. Based on the figures 13 and 14, the controller was working as expected.

Like the HVDC controller, the wind controller was not designed for a permanent response. There is a limit to how much power a wind turbine can provide for synthetic inertia as extracting additional power would reduce the rotor speed. Thus, wind power may not exert lasting power support (assuming that it was initially running at maximum power output). The permanent frequency deviation will not be studied when the wind controllers are activated.

4 Approach to analysis

This chapter gives an extensive insight into the simulations conducted. First, a short presentation of the simulation program and some of the essential network components are provided. Then, the Small testing network (STN) is thoroughly explained. It was used to create and test main components, events and scenarios on a smaller scale, both to gain knowledge on the general mechanisms and to obtain references for the simulations conducted on the main simulation model (N44). At last, N44 is presented and explained. This includes information about the approach, general data, scenario and specifics, and more.

To fully appreciate this chapter, some experience with PowerFactory (or similar simulation tool) is necessary.

4.1 Simulation tool: DIgSILENT PowerFactory

The software DIgSILENT PowerFactory is a comprehensive calculation and simulation tool that may be used for a wide range of electrical power system analysis. PowerFactory version 7 was the very first power system analysis software in the world that had an integrated graphical single-line interface[28].

The program is dedicated to analyzing electrical power systems and controls to facilitate an optimization process of planning and operation of such systems. PowerFactory is an engineering toolbox that may be used to conduct load flow, harmonic, modal or stability analysis, or short-circuit calculations as well as protection coordination[28]. The user interface includes an interactive single-line diagram with drawing functions, extensive editing capabilities as well as a wide range of calculation features[29]. This makes PowerFactory well suited for analyzing systems consisting of a variety of generating units, loads, protection equipment, line, transformers, etc. The single line feature, along with a range of other relevant functions, has been most helpful to understand and develop simulation systems suitable for this thesis.

4.1.1 Relevant model components

A power grid is a complex system where many different components are vital for satisfactory operation. In this thesis, the components that are of special interest are related to the HVDC links and the wind power plants. Most other components are standard or already implemented in the simulation model N44. The most relevant components will

now be briefly explained. For further insight into any PowerFactory component or the program itself, the reader is encouraged to read the DIgSILENT PowerFactory 2018 User Manual[29]. Components that are explained will have their PowerFactory model name stated in parenthesis.

Wind turbines

All wind power generation in the grid models is represented as a number of 2.5 MW Fully rated converters (FRC) systems (type 4, appendix C) connected through transformers. An aggregated generator (ElmGenstat) and converter (ElmTr2) are given as one template in PowerFactory, named "DIgSILENT FullyRatedConv WTG 2.5MW 50Hz". After implementing the template and connecting it to the appropriate bus in the grid, the converter was modified to a voltage and power capacity suiting the system and scenario. The number of WTGs at each wind farm was chosen to make the total capacity equal to what is expected in the future (see table 6). Type 4 wind turbines do not inherently contribute to the dynamic response of the system, but this can be facilitated by implementing suitable controllers (see section 3). Controllers were implemented on all wind turbines in the N44 model, although not always activated. It is stated clearly for the different scenarios and events whether the controllers are enabled or not.

An example of a wind farm connected to the N44 model in PowerFactory is displayed below.

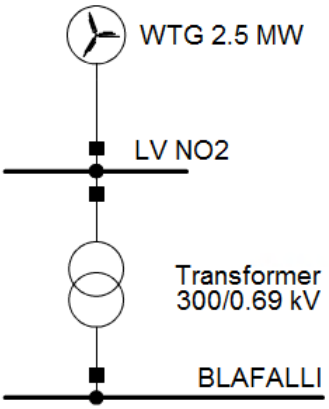

Figure 15: Wind generation connected to node Blafalli

HVDC links (passive)

The HVDC connections in the existing N44 have been modeled as negative loads. This is a convenient and simple way to model HVDC, but does not allow any additional control systems to be implemented. This model of the HVDC link was named "passive" as it was not able to provide frequency support.

The passive HVDC links do not require any extra nodes in PowerFactory, in contrast to

the active HVDC connected (requires one additional node for each HVDC link). As the total number of nodes in PowerFactory were limited (due to license restrictions), only a few of the existing N44 HVDC connections were replaced by active HVDC links. Examples of passive HVDC links in the PowerFactory model can be found in figure 19 and 20.

HVDC links (active)

The negative loads (passive HVDC connections) had to be replaced to explore how HVDC links could contribute to the system dynamics. This was the reason why "active" HVDC connections were implemented to the system.

The active HVDC links were modeled as constant DC voltage sources behind PWM converters. An example of a HVDC connection in the N44 model is displayed in figure 16. The voltage source was a DC voltage source (ElmDcu) with one terminal. Nominal voltage was set to twice the AC voltage at the connection bus. Apart from this, no standard settings were changed. A PWM converter with one DC connection (ELmVscmono) was used for the HVDC model. Rated voltages and power were adjusted to the connected buses. The integrated current controller was enabled.

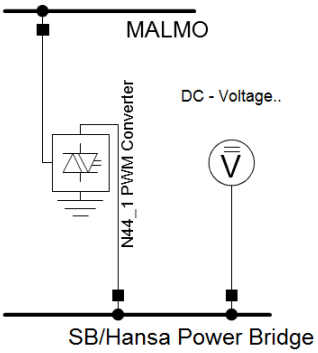

Figure 16: HVDC link connected to node Malmö

Conventional generator

A synchronous generator (ElmSym) was used to represent conventional production. This could later be compared to different HVDC and wind power solutions in the grids representing the future. The generators have been equipped with an automatic voltage regulator (AVR) ("SEXS", global PowerFactory library) and a governor ("HYGOV", global PowerFactory library) (see appendix G).

Dependent loads

A large power system, as the Nordic frequency areas, consists of both simple and complex loads. Some loads draw almost constant power, while some loads are more dependent on voltage or frequency. Dependent loads have some self-regulation that is advantageous for system stability.

There are several ways to model dependent loads. It has been decided to use the polynomial model (also called ZIP model) for simulations in this thesis. The ZIP model assumes one of these features for all loads[21]:

- **Constant power demand (P)** - Convenient for load flow calculations, but are not suited for other analysis - especially where large voltage variations are present.
- **Constant current demand (I)** - Allows load demand to have a linear relationship to the voltage, and gives a better representation of power demand for a mix of load devices.
- **Constant impedance (Z)** - Load demand is proportional to the voltage squared. Gives a good representation for some loads (for example some lighting loads), but are not suited for modeling of stiff loads.

By using the ZIP model, the benefits from all these separate models are used in combination by the use of the following formulas for active load P and reactive load Q:

$$\begin{aligned} P &= P_0 \cdot (aP \cdot (\frac{U}{U_0})^2 + bP \cdot (\frac{U}{U_0}) + cP)) \\ Q &= Q_0 \cdot (aQ \cdot (\frac{U}{U_0})^2 + bQ \cdot (\frac{U}{U_0}) + cQ)) \end{aligned} \tag{4.1}$$

where U_0, P_0 and Q_0 are initial operating condition values. The coefficients aP, bP, cP, aQ, bQ and cQ gives the share of loads that are modeled as constant power demand, constant current demand or constant impedance. It was decided to use $aP = 0$, $bP = 0.4$, $cP = 0.6$, $aQ = 0$, $bQ = 0$ and $cQ = 1$ following a discussion with the supervisor. Thus, modelling 40% of the active load as constant current demand and 60% as constant impedance. All reactive loads are modelled as constant impedances. This was expected to give a fair representation of the actual loads.

The ZIP model was implemented in PowerFactory by using complex loads (TypLodind). See the PowerFactory user manual on loads[31] for in-depth information on loads in the simulation program.

4.2 Small test network (STN)

A small network with relevant components from N44 was created in PowerFactory. The motivation was to develop and test new components and scenarios in a less complicated environment. Small component contributions could be hard to detect in the comprehensive

N44 model where numerous elements affect each other and the final results. Thus, creating the STN would simplify the simulation approach, reduce work hours and better illustrate the main trends of the different scenarios. The goal was that one could use the results and knowledge obtained throughout the work on the small test network when developing, running and discussing the simulations of the sizeable N44 system.

4.2.1 Development and characteristics

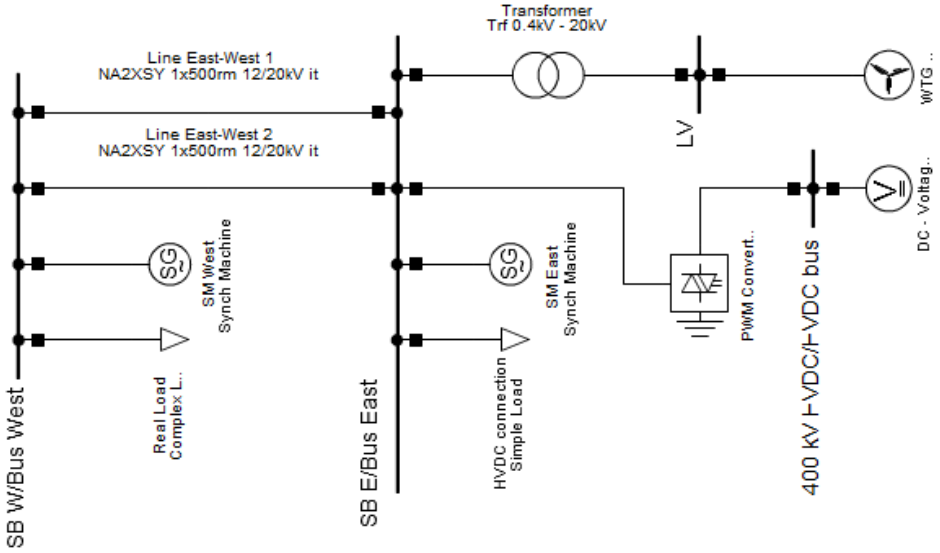

Figure 17: Single line diagram - Small test network

The final STN design can be seen in figure 17. To keep the model design simple, it was chosen to include as few components as possible and to have only two main buses. These buses were named "East" and "West". Two power lines were connected to ensure sufficient transfer capacity between the nodes. A load and a synchronous machine were attached to node West. The load was chosen to be a complex load (see section 4.1.1) representing the consumption of the entire system. The machine at node West was set to be the reference machine for the system and was equipped with a local voltage controller. The generator was adjusted to cover half of the total consumption and to be modeled as a hydropower generator.

Four different elements were attached to node East. These would in term be activated to cover the second half of the load. This system design made it simple and efficient to study the different dynamic responses. The four elements were "Wind power", "HVDC connection (active)", "HVDC connection (passive)" and a synchronous generator. The synchronous generator represented conventional generation and shared all properties with

the generator at node West, except for not being a reference machine. The three other components are described in section 4.1.1. PowerFactory allows a wide range of component specifics to be adjusted. However, most existing component values were kept unchanged as it was not within the scope of work to evaluate and improve standard settings. Relevant data for the components are found in table 3.

Governors (PowerFactory global type: HYGOV) and automatic voltage regulation (PowerFactory global type: SEXS) were implemented to the synchronous generators. Standard settings were used, except for the following at the HYGOV: Temporary droop r = 0.4 and permanent droop R = 0.06. These values are within the typical ranges for these settings and given these values as they were the same as the droop settings used in the N44 model. See appendix G for all governor and AVR data.

For each simulation, only two components were feeding power to the grid at the same time: The generator at node West and *one* of the elements at node East. The single load at node West was the only consumer of power (except system losses). The power transfer was distributed on the two lines.

The system frequency was set to standard 50.00 Hz and the system voltage to 20 kV. A load event was created to make a disturbance in the system. The event was a step-up load event at t = 5 s, where the active power consumption at the load was increased by 10%. Having a sudden step increase in load induces a quite similar reaction as if a generation unit suddenly reduced its output by the same amount.

Component name(s)	Type (PowerFactory code)	Generation	Rating
Load at node West	Load (TypLodind)	-30 MW	-
SM West/East	Synchronous Machine (ElmSym)	15 MW	35 MVA
HVDC link (passive)	Load (ElmLod)	15 MW	-
HVDC link (active)	PWM Converter (ElmVscmono)	20 MW	400 kV_{DC}/20 kV_{AC}, 25 MVA
	DC Voltage source (ElmDcu)	400 kV	-
Wind power	FRC WT (ElmGenstat)	15 MW	25 MVA
	Transformer (ElmTr2)	-	0.4/20 kV, 25 MVA
Line East-West 1/2	Line (ElmLne)	-	20 kV, 0,605 kA
Bus West/East	Bus (ElmTerm)	-	20 kV
Bus Wind	Bus (ElmTerm)	-	0.4 kV
Bus HVDC	Bus (ElmTerm)	-	400 kV_{DC}

Table 3: Component data for the STN

4.2.2 Scenarios

The following scenarios were investigated:

- A - Base scenario: Two traditional generating units contributing 15 MW each to cover the total consumption. This illustrates a high inertia situation where mainly conventional generators are running.
- B - Wind scenario, without additional control: 15 MW of wind generation replaces the traditional production unit at bus East. No measures of controlling the wind power to contribute to inertial response were taken. This situation is similar to a future scenario of a real grid with significant amounts of wind power, but where the turbines are not providing frequency support.
- C - Wind scenario, with additional control: Like scenario B, but with an extra control loop (see section 4.1.1) to facilitate inertial frequency support. This scenario is relevant for a future grid where wind power contributes to inertial response.
- D - HVDC scenario, without additional control: 15 MW comes from an HVDC connection which replaces the traditional production unit at bus East. The DC connection is modeled as a negative load and has therefore no measures to contribute to the inertial response. Scenario D possess similarities to a future grid with significant HVDC interconnections, but where HVDC does not provide frequency support.
- E - HVDC scenario, with additional control: 15 MW comes from an HVDC connection, replacing the traditional production unit. A PD control loop (see section 4.1.1) was added to the PWM converter to allow initial frequency support. This case may illustrate the future situation with HVDC controllers.

4.2.3 Results and discussion

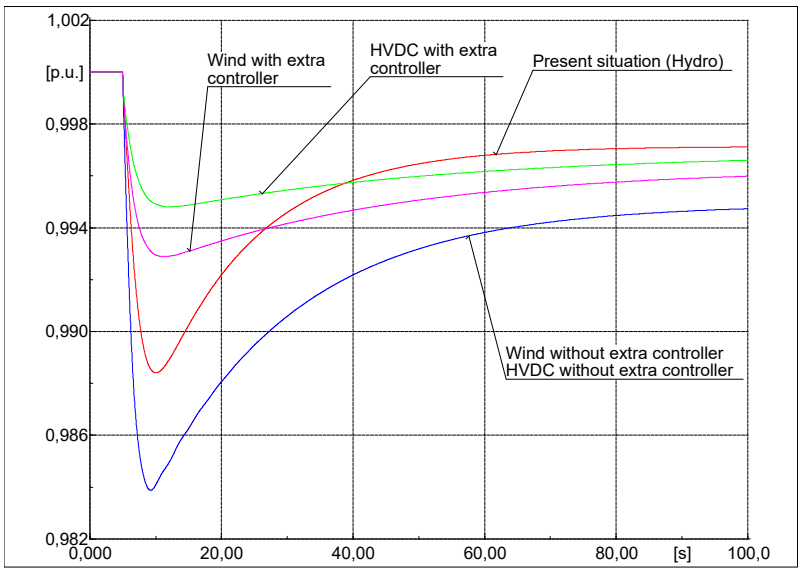

Figure 18: Frequency responses for different STN scenarios

	Nadir [p.u.]	Time of [s] nadir	ROCOF [Hz/s]	$\Delta f_{steady\ state}$ [p.u]	Frequency bias [MW/Hz]	System inertia [MWs]
A	0.989	10.10	-0.005	-0.0029	20.7	140
B	0.984	9.25	-0.009	-0.0051	11.8	70
C	0.993	11.27	-0.003	-	-	70
D	0.984	9.25	-0.009	-0.0051	11.8	70
E	0.995	12.00	-0.002	-	-	70

Table 4: STN results - Frequency quality indicators

Figure 18 shows the frequency response of the STN for the different scenarios due to the step-up load event. Table 4 gives information on system inertia and the frequency response indicators that were introduced in section 2.3.2. The values for permanent $\Delta f_{steady\ state}$ was measured at t = 200 s. Frequency bias was calculated using equation 2.2. The contribution from the generators to system inertia was calculated using equation 2.7.

Considering the nadir, one can observe how the frequency drop increased when HVDC or wind power without any additional control replaced half of the conventional production. This indicated that the system stability worsened when the new technologies were introduced without additional controllers. Adverse consequences could occur in the grid if the new nadirs represented critically low frequencies. The reason why the frequency had a more substantial drop when the conventional production was replaced can be found

by studying the swing equation (equation 2.13). The equation describes the frequency response to a load change and shows how a system with high inertia gets less frequency change than a system with low inertia. However, the frequency drop was reduced when the wind power generation and the HVDC link were equipped with suitable controllers (pink and green line respectively). Thus, the controllers succeeded at letting HVDC connections and wind power contribute to the inertial response. The simulations indicate that it is possible to get an even better response when HVDC or wind power replaces conventional production as long as they are allowed to contribute to the inertial response.

The nadirs occur at approximately the same time, and the small differences do not represent any significant changes in a vast network. It does not indicate any significant changes in stability for the STN simulations.

Investigating the ROCOF results, one observes how scenario B and D has about twice the ROCOF as the base scenario A. This means that the initial frequency change happens much faster for the scenarios with wind power and HVDC than the basic scenario - as long as no controllers are implemented. This is undesirable, as a too fast frequency change makes it more challenging to activate sufficient reserves before the frequency drops to critical levels. Once again, the swing equation, equation 2.13, gives the theoretical explanation: ROCOF is inversely proportional to the inertia constant. The system inertia in scenario A is almost twice as high as for scenario B and D. Thus, the ROCOF is expected to be about twice as high for scenario B and D than for scenario A. The practical simulation results correspond with the theoretical background knowledge.

Scenario A has the smallest steady state frequency deviation. This indicates a relatively robust system with a substantial frequency bias. Scenario B and D have a more significant steady-state frequency deviation than the base case. This was expected as neither wind power or HVDC links contribute inherently to the droop characteristics of the system. Thus, the frequency bias for the system with conventional generation was considerably higher than the systems where HVDC and wind power had replaced the hydropower. Using equation 2.4, it was calculated that the frequency bias contribution from generator West and East was 9.33 MW/Hz each (when activated). Comparing these results to the simulation results, one can estimate the contribution from the complex load to approximately 2.0-2.5 MW/Hz, summarized in table 5. This confirms that dynamic loads contribute to reducing the steady-state frequency deviation in the same way as conventional generators.

	Measured frequency bias [MW/Hz]	Calculated frequency bias from generators [MW/Hz]	Estimated frequency bias from load [MW/Hz]
A	20.7	18.7	2.0
B	11.8	9.3	2.5
D	11.8	9.3	2.5

Table 5: STN results - Frequency bias

As explained in section 3, the steady state contribution from the controllers has not been a central concern during the controller design process. Theoretical knowledge on wind turbines (inertial response cannot be permanent as turbine would stall, see section 2.4.5) suggests that permanent contribution should be zero. However, the STN simulations results (figure 18) revealed that the controllers do indeed contribute to the steady-state frequency response (mistakenly). Thus, steady-state frequency deviations and frequency biases should not be analyzed when controllers were activated. This also accounts for the simulations to be conducted in the N44.

The construction and tuning of the control systems were not optimized. They were merely examples of basic control systems illustrating how it is possible to improve the system response by contributions from HVDC and wind power solutions. Thus, exact numeral results should not be given too much attention. The main finding is how the controllers, in fact, facilitate an improved system response.

4.2.4 Conclusion

The simulation results show that the frequency response deteriorated considerably when the conventional generation was replaced by wind power and HVDC links that were unable to provide inertial support. This could be seen on the frequency response indicators nadir, ROCOF, and the steady-state frequency response. The reason for this development was the considerable reduction in system inertia when the conventional generator was replaced. The results were not unexpected and corresponded with the theory of system inertia, frequency bias, swing equation and frequency response. The contribution from the complex load enforced system stability, although to a significantly lower extent than the conventional generators. The results from scenario C and E shows that it is possible to replace traditional generation with wind power and HVDC links and simultaneously to obtain equally good - or even better - system stability. Thus, stability enhancement is possible when suitable control loops are added.

The results from the STN simulations gives several pointers for what to expect from the

N44 simulations. One expectation is that the frequency response will worsen (considering the frequency response indicators) when wind power and HVDC without extra controllers replace conventional production. Secondly, it can be expected that the frequency stability improves when the new technologies are equipped with suitable controllers. One can also expect that the dynamic loads will contribute considerably to system inertia and droop. Based on the STN simulations, one cannot know to what extent the expected trends will affect the complex N44 model (numerically). This depends on the amount of generation being replaced, what kind of production it replaces (hydro, nuclear, thermal), distribution of reserves, and more. Lastly, the STN simulations show that the controllers mistakenly contribute to the steady-state frequency deviation. Thus, steady-state deviations and frequency bias should only be investigated when the controllers are deactivated.

4.3 Large scale model (N44)

The Nordic 44 test network (N44) is a simplified network model of the actual Nordic grid. The single line diagram is found in appendix E. Modeling existing networks as smaller grids are often favorable for educational purposes. It is a convenient approach to explore different dynamic phenomena. It also demands less computer power than a more comprehensive model. The first version of the model that later evolved to N44 was created at NTNU. Over the years, the model has been modified, improved and expanded on several occasions by numerous contributors. N44 is available in PSS®E, as well as DIgSILENT PowerFactory. The N44 model is well suited for dynamic frequency analysis, which is why it was chosen as a foundation for the simulations conducted in this thesis.

The N44 model consists of 44 nodes, thereby the name. These are essential nodes and locations in the actual Nordic grid, in addition to several HVDC connections to other power systems. Denmark is left out of the N44 model. Thus, all nodes in the model network are distributed in the three countries Norway, Sweden and Finland. In addition to numerous traditional generators, there are initially three wind power plants in the system, one in each country. An overview of the generators, wind power production and loads (including passive HVDC connections) that have been active during the simulations, are found in appendix F.

All nodes and components that are referred to in the N44 model in PowerFactory will be mentioned by the name given in the simulation program. This is done to simplify further work for readers that are working on the N44 model themselves.

4.3.1 Modifications

During the work on this thesis, several modifications were performed on the N44 model. The modifications aimed to develop a more representative model of the present and the future Nordic grid. This includes, for instance, adding more wind generation and more advanced HVDC connections. The aim of the modifications was *not* to improve the N44 model in general, as this was outside the scope of the thesis. Existing weaknesses in the model might thus affect the simulation results, as explained in section 1.2.2.

The modifications that now are explained applies for all simulation scenarios, although each of them might not affect all scenarios. General changes in the amount of load, generation, etc. are specific to each scenario, and will be presented in their respective section and appendix F.

- Existing wind power generation has been erased. New wind power production was added to the following nodes: Forsmark, Malmo, Jarpstro, Trondheim, Blafalli and Oulu. The wind power models are as described in section 4.1.1. Data concerning capacity and number of turbines are given in table 6.
- HVDC links (active) (described in section 4.1.1) are added to the following nodes: Malmo (Hansa Power Bridge), NSN (North Sea Link) and Nordlink (Nordlink). These are replacing the existing (passive) HVDC links at the two latter nodes.
- The synchronous machine sym_OSCARSHA_2 at node Oscarshamn in Sweden was set to be the only reference machine.
- Several "Operation Scenarios" were created in PowerFactory, one for each simulation scenario (see section 4.3.2). The use of "Operation Scenarios" allowed several different versions of the system to be continuously operating. This allowed efficient testing of different scenarios without changing data and settings along the way. See the PowerFactory user manual[29] for more details.
- Settings for all hydropower governors (HYGOVs) were examined and modified if necessary to keep the temporary droop at $r = 0.4p.u.$ and permanent droop at $R = 0.06p.u.$ The remaining parameters were kept at standard values (appendix G). To adjust the droops was a joint decision with the supervisor, as it was regarded to be more representative of the actual system.
- All loads in the original N44 system were changed to complex loads to achieve a more realistic dynamic response. See section 4.1.1 for more details.
- The consumption and production were modified for each scenario. The values were

based on actual system data from 2017, but adjusted to fit the system concerning nodes, bidding areas, and future developments.

- Several nodes were relieved to allow active HVDC connections and wind power to be installed without violating the license restriction of 50 nodes in PowerFactory. The nodes that were erased was: "ARRIE_HV", "KARLSH_H", "LT_HVDC", "VYBORG_H", "ESTLINK_" and "DANNEBO_". See further description later in this subsection.

Removal of nodes

The license for PowerFactory provided by NTNU limited the number of active nodes in the model to 50. As the model contained 44 nodes prior to the modifications, the number of new nodes were heavily restricted. The additional wind power had to be limited to a handful new nodes (in contrast to the possibility of adding new wind power to almost all nodes) and only a few of the HVDC connections could be modeled as active.

To relieve nodes that later could be used for active HVDC links or wind power plants, some existing HVDC links were simplified (going from one additional node to none). The original HVDC links, represented by a cable, a node and a load were simply replaced by a single load, as seen on figure 19 and 20. The data for the original loads were kept unchanged. When deciding which HVDC links to simplify, the primary focus was to keep the most significant connections concerning power flow and impedance. It was also important not to simplify more nodes than considered strictly necessary.

A drawback with the simplifications was that some information was lost, as the cables contain some unique data (resistances, reactances, etc.). However, the HVDC links that were simplified were considered to have a minor impact on the entire system dynamics and only lead to a small increase in inaccuracies. As these inaccuracies are considered to be relatively small compared to the aggregated uncertainties in the system, they were not expected to reduce the validity of the results. Thus, it was considered an overall advantage to relieve the nodes.

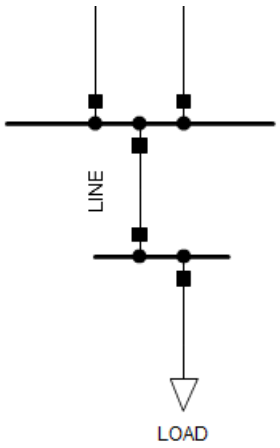

Figure 19: Original model configuration for HVDC link (passive)

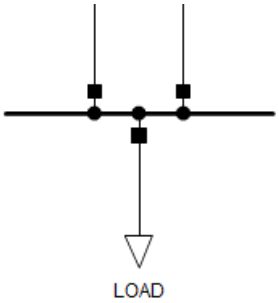

Figure 20: Simplified model configuration for HVDC link (passive)

Additional wind power capacity

Wind power production is increasing rapidly in the Nordics[2]. Turbines should be added to most of the N44 nodes to get an optimal representation of wind power in the system. However, due to the limits of 50 nodes in the grid, only a few wind production units were implemented. These were adjusted to carry the total expected wind production for the future scenarios.

Considering the current and expected production in 2030[2][40][42], the wind power production units have been distributed in the N44 model. The main price areas concerning wind power were found, and the future capacity estimated based on a comprehensive NVE report[2] and extrapolation of current capacity and capacity under construction. This is presented in table 6, below.

	Price area	Capacity [MW]	Number of 2.5 MW turbines
Blafalli	NO2	2800	1120
Trondheim	NO3	3400	1360
Jarpstro	SE2	3300	1320
Forsmark	SE3	3500	1400
Malmo	SE4	2600	1040
Oulu	FI	3000	1200

Table 6: Data for wind power generators in the N44 model

After adding the wind farms to the model, the transformers connecting the wind power to

the grid were adjusted to the bus voltage at the connection point, as well as their power transfer capacity.

4.3.2 Development of the scenarios

Future scenarios in the Nordic power system with special emphasis on HVDC connections and wind power generation were created for the simulations. The goal was to develop scenarios that would help illuminate the different implications of increased HVDC and wind capacity in the Nordic power system. Situations with system inertia were expected to be very high or very low was chosen for investigation. These extremes where convenient to examine as they represented the boundaries for system operations (concerning inertia), and most other operating points would be covered by these situations. Thus, the simulation results would also provide information on less extreme situations.

No controllers were activated for the present scenarios (1 and 2). For the future scenarios (3 and 4), controllers were implemented on all wind turbines and three HVDC interconnections (see 4.3.5 Assumptions). Simulations were conducted when all controllers were disabled, when HVDC controllers where enabled (wind controllers disabled) and when wind controllers where activated (HVDC controllers disabled). The HVDC and wind controllers were activated separately to easier explore their contribution to system stability.

Production and consumption data were extracted for representative dates from NordPool's historical database and used as the base for the distribution of power production and consumption in N44. Some pragmatic modifications were necessary to implement the real system data to the model without violating any component limits or PowerFactory constraints. See section 4.3.5 Assumptions for more information. An estimated growth in energy consumption of around 10% for Norway and Finland and 1% for Sweden towards 2030 was taken into account (see 4.3.5 Assumptions).

Wind power in the Nordic power system of 2030 was estimated based on data from NVE[2], as explained in section 2.5.2. The expected installed wind power capacity in Norway, Finland and Sweden combined will be around 18 GW by 2030, around twice as much as today. Due to the limited number of nodes, all capacity was concentrated at only six buses. The distribution within these nodes was based on current wind production and wind turbines under construction. HVDC connections were operating for all scenarios. The specific flows on each cable were based on a real operating situation, like production and consumption. The flows were adjusted to fit the data to the model without violating any constraints in the system. Wind power and HVDC flows were adjusted to give a realistic total contribution. All specific generation, import/export and consumption data are found in appendix F. Additional information is presented below.

1 - Present: Summer at night
Goal: To illuminate the present situation in the Nordic grid when the system has a very low load. Such a situation represent operating hours where the system inertia is low.

Low production and consumption characterize this case. The scenario includes significant wind power production. There is also considerable import as the prices on the continent often are low by night. This reduces the need for local production. Many generators are out of service, and the remaining are running at relatively modest loads. The distribution of loads, generation and import are based on an actual system operation situation; 18th of June 2017 at 4-5 am. This hour was chosen due to the very low load and considerable import.

2 - Present: Winter at peak hours
Goal: To study the current situation in the Nordic grid during operation hours where the load is very high. During such hours the production, and therefore system inertia, is high.

A high load and high generation characterize this case. There is significant wind power production, but almost all conventional generating units are still operational. The power flows are moderate between the Nordic grid and other power systems as the energy prices are high both in the Nordics and on the continent. The distribution of loads, generations, import and export is inspired by a real system situation on the 9th of February 2017 at 8-9 am. This hour was chosen due to the cold winter weather and therefore the significant load.

3 - Future: Summer at night
Goal: To study a future (2030) extreme where the system inertia is very low. It was assumed to be a windy night to investigate the impact of increased wind generation.

Like scenario 1, this scenario is characterized by a low load, low generation and high import. A lot of new wind power and exchange capacity are installed for this future scenario. This allows the Nordic conventional production to be considerably lower than for the similar summer scenario anno 2017. Several generating units are turned off and the system inertia is very low.

4 - Future: Winter at peak hours
Goal: To study a 2030 operational situation where the system is heavily loaded and the inertia is high.

Like scenario 2, this winter scenario was characterized by a high load and high generation. Most generating units were running. The wind conditions were assumed to be generous, allowing the wind generation to be substantial. This permits power export from the Nordics to the continent.

4.3.3 Simulation events

A number of different events that were expected to cause large disturbances in the system has been investigated. It was decided to investigate extreme events, in the same way as it was decided to consider the very highest and lowest inertia situations. Numerous simulations were run to explore the implications of the events on all the scenarios to investigate the trends and to discover the most critical situations. Most events were switch-events, meaning that the given component was disconnected from the rest of the grid. One event was a three-phase short-circuiting. All events were initiated at $t = 5s$.

Name	Component	Event data
Beta	Skagerrak HVDC cables	Switch event: 1600 MW (import) to zero.
Delta	Generator: Kvilldal	Switch event: 1240 MW to zero.
Epsilon	Generator: Oscarshamn 3	Switch event: 1450 MW to zero.
Zeta	Generator: Olkiluoto 2/3	Switch event: 890/1600 MW to zero.
Gamma	Critical line*	Switch event: From critically loaded to disconnected (no power transfer).
Eta	Critical line*	Short circuit event, all phases. Cleared after 0.1 s.

Table 7: Data for simulation events

* See table 8 for information about the lines affected.

The disconnection of Skagerrak HVDC cable was chosen as it was the largest HVDC system connecting the Nordics to other power systems, with a total capacity of more than 1600 MW. Skagerrak consists of four cables (Skagerrak 1-4). It is very unlikely that the whole system fails simultaneously. However, as this thesis investigates the very "worst-case" situations, it was chosen to have a simulation event where the entire Skagerrak system (1600 MW) is disconnected. The generator events (case Delta, Epsilon, Zeta) were chosen as they represented the largest generation units for each country in the model grid. There are two different generators to be disconnected for event Zeta. Olkiluoto 2 (890 MW) is Finland's current largest generator and was therefore disconnected in the 2017 scenarios. Olkiluoto 3 (1600 MW) is expected to commence at the end of this decade[37], and will at that point become the largest generating unit in Finland. Hence, Olkiluoto 3 was the generator to be disconnected in Finland for the 2030 scenarios. Event Gamma and Eta were unique events in the way that they differed from scenario to scenario. The lines that were disconnected were chosen based on their load flow. The most heavily loaded lines, often feeding important nodes, were chosen. This implied that both the line itself and the load flow at the point of disconnection would differ between the scenarios. Thus, event

Gamma and Eta produced results that were not directly comparable to the same extent as the other events. See details in table 8.

Scenario	Critical line	Connecting nodes	Power flow prior to event [MVA]
1	Sweden-Finland 1	Grundfors, Uolu	1676
2	Sweden-Finland 1	Grundfors, Uolu	3533
3	North Sweden	Porjus, Jarpstro	1297
4	Sweden-Finland 1	Grundfors, Uolu	2681

Table 8: Load flows on critical lines prior to event Gamma and Eta

The author is aware that several of the events are more significant than the dimensioning fault or are composites of smaller components (e.g., the Skagerrak HVDC connection consist of four cables). The author is also aware that precautions have been made to minimize the risk of significant events happening (e.g. Olkiluoto 3 will be equipped with a system protection scheme of 300 MW, reducing max disconnecting event from 1600 MW to 1300 MW) and some events are quite improbable (e.g. max generator production during low load hours). Thus, one could argue that some of the events are too unlikely or extreme. However, the strategy has been to explore the very extremes and the worst-case situations. The results and the trends that might be uncovered would also apply to less extreme events.

4.3.4 Measurement points

The simulations provided results for a range of values on different locations in the grid. A closer look was given to frequencies, voltages and load flows. The system frequency was measured on a generator at a central node named Ringhals (Sweden, close to Gothenburg). This node was chosen as a reference point for the system frequency as it is one of the most central nodes in the N44 grid, while still being some distance from the events. The voltages have been measured at nodes in each country; Node Oslo1, node Malmö and node Helsinki. These were chosen as they represented central nodes close to massive consumption points in their respective countries.

Load flows were investigated at significant lines connecting the Nordic countries: Sweden - Finland 1 (Grundfors - Oulu), Sweden - Finland 2 (Porjus - Oulu), the Hasle crossings 1 and 2 (Ringhals - Hasle), central Sweden - central Norway (Høgåsen - Trondheim), northern Sweden - northern Norway 1 (Porjus - Ofoten) and northern Sweden - Norway northern 2 (Ajaure - Røssåga). These lines were chosen to study how reserves were activated in each country as a response to disturbances. The load flow results are presented

graphically for only the first four lines, to keep the plots less messy. Tabular results are presented for all lines. When investigating the load flows, the focal point has been on flow changes, oscillations and on where reserves were activated. Specific line capacities to individual system components were not examined.

When only a few elements are examined, valuable information can be missed. If more time and resources were at hand, one should preferably investigate all components to detect possible negative implications due to disturbances in the system. This goes in particular for voltage and load flow measurements, which are recognized to be more local entities than frequency. This is recommended for further work.

4.3.5 Assumptions

Assumptions are necessary when studying simplified models and future cases. Following is a summary of the essential assumptions for the simulations:

- It is assumed that the Nordic consumption will increase 10% in Norway and Finland and 1% in Sweden, following analytical estimations by NVE[2]. The increase is distributed proportionally within the respective countries and throughout the day.
- Loads are assumed to behave similarly in 2030 as 2017, concerning dependencies. This contradicts the expectations of more loads being decoupled in the future[25]. An in-depth study of loads and their expected future dependencies were not conducted and implemented in the simulation model as it was out of scope for this thesis. However, it could be an interesting topic for further work (section 7.2). Not considering changes in load composition was convenient to hold the future variables to a minimum (keeping the focal point on contributions from wind power and HVDC connections). However, it might have given slightly better frequency responses for the 2030 scenarios than what is realistic as dependent loads contribute positively to system inertia.
- Wind power and HVDC capacities are assumed to increase in accordance with estimates by the Nordic TSOs[4] and NVE[2] respectively. These are shown in table 2 and 6.
- Controllers were implemented on all wind turbines and three of the HVDC cables. Allowing all wind turbines to provide synthetic inertia by 2030 is unlikely, but was chosen for the investigation to illuminate the full potential of wind power contribution to the initial frequency support. It was decided to only implement controllers on the the three HVDC connections that are currently under construction: Hansa

Power Bridge, North Sea Link and Nordlink. Only the most modern HVDC interconnections were given controllers to explore a more moderate synthetic inertia contribution (compared to wind power, where controllers where implemented on all turbines).

- The use of controllers assumed that there was some stored energy behind the power electronics available as reserves.

- It was assumed sufficient to model all Nordic wind power as six aggregated plants consisting of numerous turbines. This was a necessity due to the restriction of nodes (see section 4.3.1). All turbines were modeled as FRC WT (type 4), see appendix C.

- At least one conventional unit was operating in all areas at all times. Wind power and HVDC combined could *theoretically* cover most of the load for certain situations in the Nordic grid in the future, and thus relieve all generators in whole price areas or even countries. However, it was regarded very unlikely that this would happen before 2030 in a system without significant means of system stability enhancements (which is the base case for the future scenarios).

- Generators and the HVDC disconnection that were disconnected (see section 4.3.3) were assumed to be operating at rated power prior to the disturbances. This made the comparison of different scenarios and events easier. However, this resulted in some awkward production distributions where some generators were running at rated power, while some at an artificially low output. The average power output and the total numbers of units operating were still reasonable.

- It is assumed that the final distributions of production and consumption (appendix F) for all scenarios are realistic and give adequate representations of a real system. They are based on existing market data for the Nordic grid[1], production capacities and component ratings in N44. Some wiggle room has been allowed to satisfy component ratings, load flows, etc.

[1]Relevant data could be found on NordPool's web solution[27], by selecting the categories "Consumption" and "Production" in the drop-down menu and choosing appropriate hourly data for the desired countries.

5 Results

The results will be presented in this section. Brief explanations of the graphical and tabular results will be given.

5.1 Inertia calculation

Considering generator data from the N44 model and equation 2.9, the system inertia for each scenario has been calculated (see appendix J). The results are presented in table 9.

Scenario	Kinetic energy [GWs]
1	193
2	357
3	130
4	371

Table 9: Results - Inertia (calculations)

5.2 Frequency bias calculation

Considering generator data from N44 and equation 2.4, the system frequency biases, λ_R, for each scenario has been calculated. The results are presented in table 10, below. For calculation and data details, see appendix K.

Scenario	λ_R [MW/Hz]
1	8900
2	15500
3	5900
4	15500

Table 10: Results - Frequency bias factor (calculations)

5.3 Disconnections of generators and HVDC line

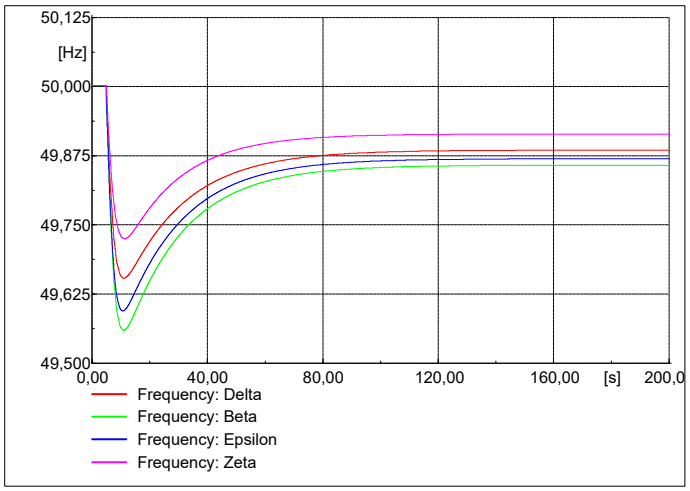

Figure 21: Results - Scenario 1: Frequency responses

The simulation events that disconnects the largest generators in Norway, Finland and Sweden, as well as the Skagerrak HVDC connection, share many characteristics. The main differences concern magnitude and location. The HVDC connection, as well as the generators, are providing a considerable amount of power before the events are triggered. Because of all their similarities, these events (Beta, Delta, Epsilon and Zeta) and their general responses tend to be quite similar, as exemplified in figure 21. Thus, a presentation of the results for one of the events will be sufficient to explain the general trends and characteristics. Results for Beta (disconnection of the Skagerrak HVDC connection) will be presented as it was one of the largest disconnections. One particular case concerning event Zeta will be presented separately. The frequency responses that are not given in this chapter are found in appendix H.

Event Beta - Disconnection of Skagerrak HVDC cables

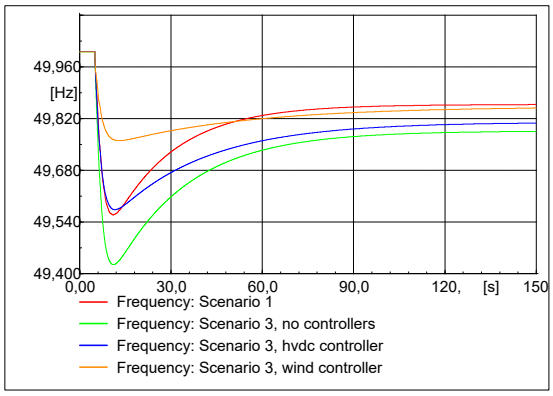

Figure 22: Results - Beta, summer scenarios: Frequency responses

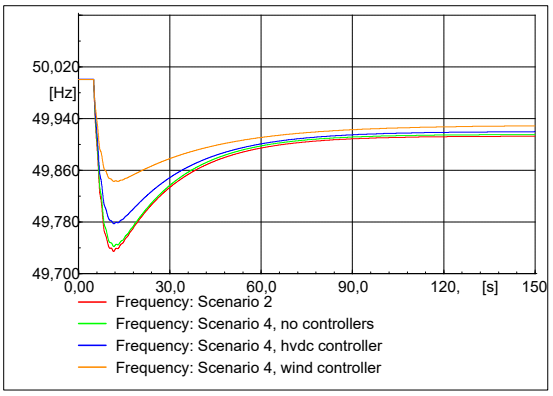

Figure 23: Results - Beta, winter scenarios: Frequency responses

Scenario	f_{nadir} [Hz]	t_{nadir} [s]	ROCOF [Hz/s]	Δf_{perm} [Hz]	λ_R [MW/Hz]
1	49.56	6	-0.15	-0.14	11400
2	49.73	7	-0.12	-0.09	17800
3 no cont	49.42	6	-0.21	-0.21	7600
3 hvdc cont	49.57	7	-0.15	-	-
3 wind cont	49.76	8	-0.06	-	-
4 no cont	49.74	7	-0.10	-0.08	20000
4 hvdc cont	49.78	7	-0.08	-	-
4 wind cont	49.84	7	-0.06	-	-

Table 11: Results - Beta: Frequency response indicators

Figure 22 and 23 and table 11 show the frequency responses for event. Several trends can be spotted, including how the winter scenarios (scenario 2 and 4) have a modest frequency response when comparing to the summer scenarios (scenario 1 and 3). One may also observe how the reactions worsen from 2017 to 2030 for the summer scenarios, but are approximately unchanged for the winter scenarios. A third trend is how the controllers support the system and improve the frequency stability. This goes for both the wind and HVDC controllers, summer and winter.

Notice that permanent frequency deviation is presented only for cases without controllers. This is because the controllers were not designed concerning permanent response, as explained in chapter 3.

Based on the results of the frequency response indicators, scenario 3 without additional

controllers are identified to be the most critical scenario for event Beta. That is why it was chosen for further investigation, to examine if it could have a negative impact on system voltages and power flows.

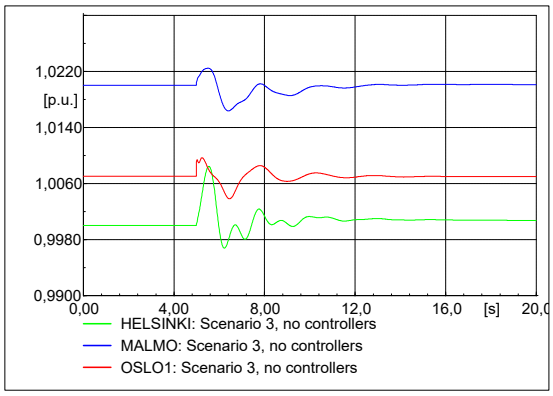

Figure 24: Results - Beta, scenario 3 (no controllers): Voltage responses

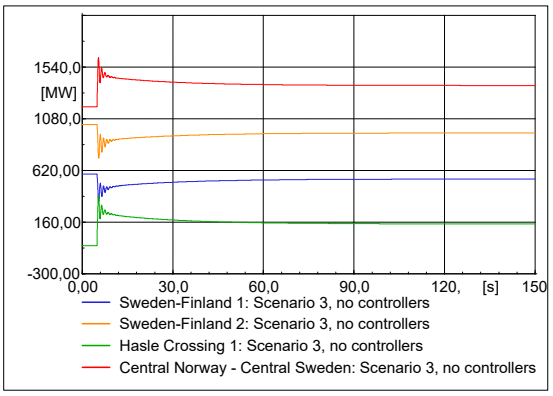

Figure 25: Results - Beta, scenario 3 (no controllers): Power flows

	Power flows [MW]		
Line	Pre event	Post event	Change
Sweden - Finland 1	597	542	-55
Sweden - Finland 2	1027	952	-72
Hasle Crossing 1 (SE-NO)	-50	143	193
Hasle Crossing 2 (SE-NO)	-50	148	198
Central Sweden - Central Norway	1185	1373	188
Northern Sweden - Northern Norway 1	597	616	19
Northern Sweden - Northern Norway 2	52	57	5

Table 12: Results - Beta, scenario 3 (no controllers): Power flows

The voltages have been measured at three central nodes in the grid. As seen in figure 24, the voltages oscillates after the disturbance, but stabilizes around 6-8 seconds after the disturbance was initiated. The oscillations are most significant at node Helsinki, where the deviation is up to 0.8% from the initial value.

Considering the load flows, one may observe substantial changes. This indicates that reserves were activated in several areas in addition to the directly affected area. After the HVDC line between Norway and Denmark (import to Norway) was disconnected, load flow from Sweden to Norway increases to support Norway. Simultaneously, Swedish export to Finland decreases slightly. This shows that some reserves were activated in Finland too. However, Norway enables most reserves themselves. The load flows oscillate after the disturbance, but the oscillations die after about 10 seconds.

Event Zeta - Largest frequency drop A closer look will be given to the summer scenarios for the disconnection of Finland's largest generator, as it induced the larges frequency drop of all simulations conducted. This was expected as the nuclear facility Olkiluoto 3 is planned to commission in 2019and has a capacity of 1600 MW[37], and thus represents the most significant system disconnection. In magnitude, it counts for the same power loss as the disconnection of the Skagerrak cables (event Beta). However, as the large Olkiluoto generators provide a considerable amount of inertia to the system, it is more critical to lose.

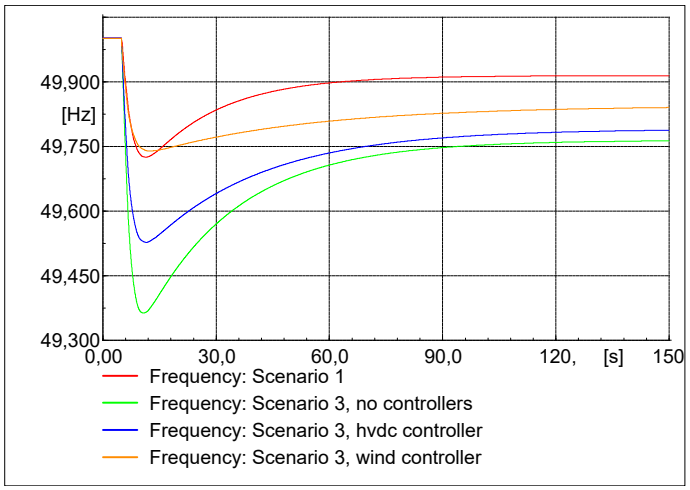

Figure 26: Results - Zeta, summer scenarios: Frequency responses

Scenario	f_{nadir} [Hz]	t_{nadir} [s]	ROCOF [Hz/s]	Δf_{perm} [Hz]	λ_R [MW/Hz]
1	49.72	6	-0.11	-0.09	10300
3 no cont	49.36	6	-0.28	-0.24	6800
3 hvdc cont	49.53	6	-0.20	-	-
3 wind cont	49.74	8	-0.11	-	-

Table 13: Results - Zeta: Frequency response indicators

From figure 26 and table 13, one may observe how the nadir drops to less than 49.4 Hz for scenario 3 (no controllers), representing a considerable drop in frequency. A second observation is that the frequency response is much more severe in 2030 than in 2017. This is partly because the largest generator in Finland today is 890 MW, while the new generator has rated power of 1600 MW. It is also observed how the controllers improve the response.

A closer look will be given to the consequences of the event for scenario 3 with no con-

trollers, as this has the most critical frequency drop.

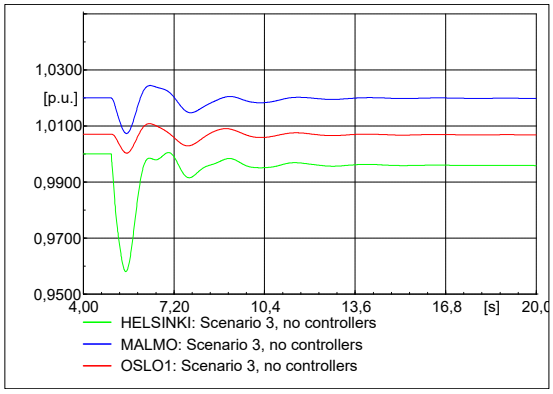

Figure 27: Results - Zeta, scenario 3 (no controllers): Voltage responses

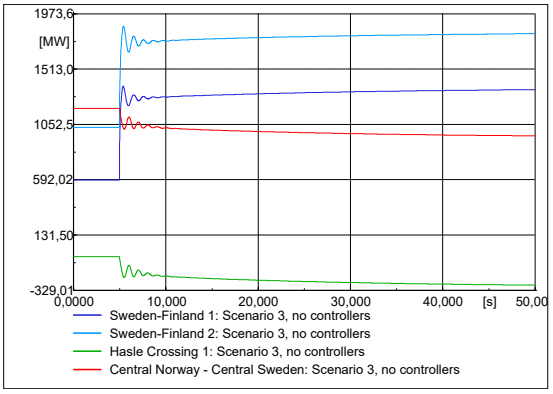

Figure 28: Results - Zeta, scenario 3 (no controllers): Power flows

	Power flows [MW]		
Line	Pre event	Post event	Change
Sweden - Finland 1	597	1355	758
Sweden - Finland 2	1027	1820	793
Hasle Crossing 1	-50	-298	-248
Hasle Crossing 2	-50	-332	-288
Central Sweden - Central Norway	1185	940	-245
Northern Sweden - Northern Norway 1	597	383	-214
Northern Sweden - Northern Norway 2	52	10	-42

Table 14: Results - Zeta, scenario 3 (no controllers): Power flows

As for event Beta, it is observed how Helsinki gets the most considerable voltage drop, around 4.1%. Voltage drop in Malmo was 1% and Oslo 0.5%. The voltage oscillations are damped to normal operation around 10 seconds after the incident.

Considering the power flows in a selection of essential lines, one may observe how the export from Sweden to Finland increases with 1550 MW - almost as much as the lost Finnish generator. This indicates that Finland provides only a tiny amount of reserves themselves. The net flow from Norway to Sweden is increased by almost 1050 MW. Thus, most reserves are activated in Norway. The power flow oscillations stabilize within 10 seconds after the disturbance.

5.4 Short-circuiting critical lines

It is more interesting to study voltage responses than system frequency when examining the implications due to a short-circuiting of a line. This is because voltage changes are expected to be more severe. It will also have more of a local impact compared to the frequency affecting the entire Nordic grid. This is why it has been chosen to focus on voltage response for this event. A presentation of the load flow will also be given. See appendix H.5 for frequency responses for this event.

Due to the low levels of inertia, scenario 3 with no controllers are expected to have the most critical responses. Thus, it was investigated further.

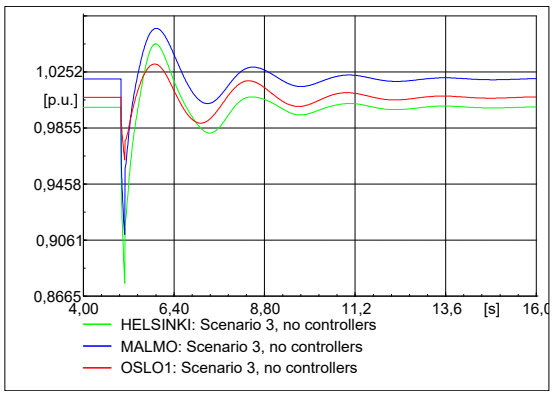

Figure 29: Results - Eta, scenario 3 (no controllers): Voltage responses

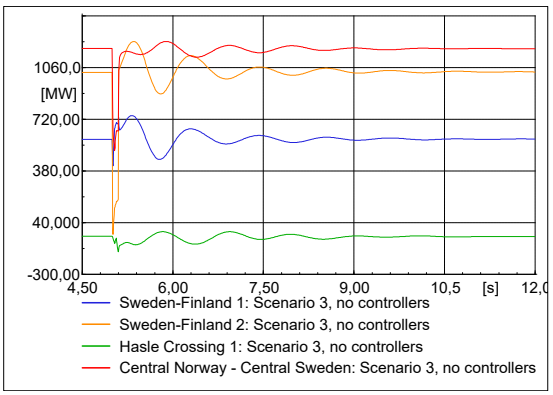

Figure 30: Results - Eta, scenario 3 (no controllers): Power flows

Scenario	u_{nadir} [p.u.]	t_{nadir} [s]
Helsinki	0.88	0.10
Malmö	0.91	0.10
Oslo1	0.96	0.10

Table 15: Results - Eta, scenario 3 (no controllers): Voltages

	Power flows [MW]	
Line	Pre event	Nadir
Sweden - Finland 1	597	412
Sweden - Finland 2	1027	-39
Hasle Crossing 1	-50	-154
Hasle Crossing 2	-50	-167
Central Sweden - Central Norway	1185	513
Northern Sweden - Northern Norway 1	597	246
Northern Sweden - Northern Norway 2	52	30

Table 16: Results - Eta, scenario 3 (no controllers): Power flows

Investigating the voltage drops, these are of much higher amplitude than for the disconnections of generators and HVDC connections. This includes both the nadirs and the oscillations. All nodes investigated have significant voltage drops, and Helsinki has a voltage drop of more than 11%. The voltage dips for Malmö and Oslo are measured to around 10% and 4.6% respectively. However, the system stabilizes and the voltage oscillations are damped 10-15 seconds after the disturbance was initiated.

Investigating the load flows on figure 30, the severity of the short circuit is easily spotted as all lines are affected. Two of the lines, Sweden-Finland 2 and Central Sweden-Central Norway, have sudden drops of around 1080 and 650 MW respectively.

5.5 Disconnection of critical lines

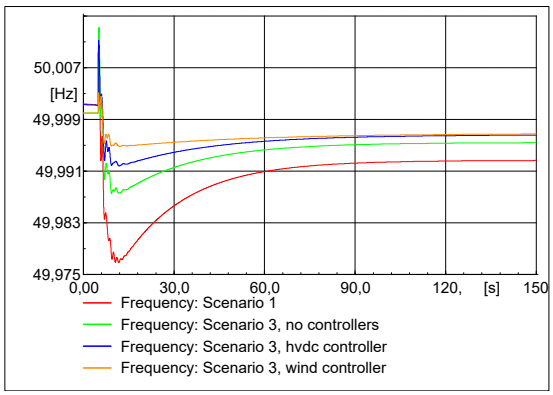

Figure 31: Results - Gamma, summer scenarios: Frequency responses

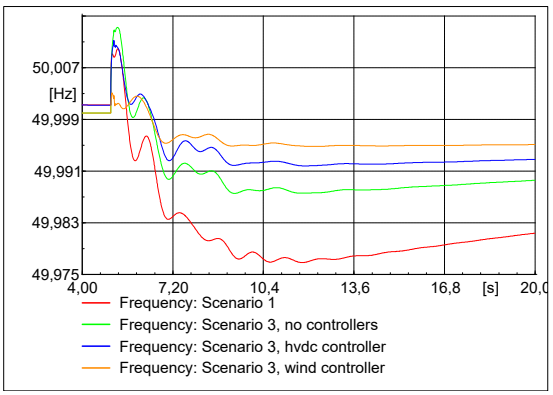

Figure 32: Results - Gamma, summer scenarios: Frequency responses (zoomed)

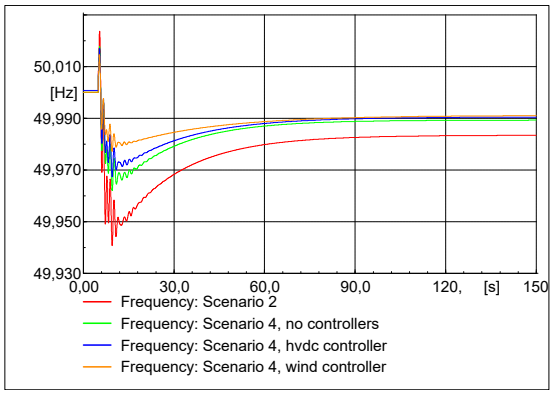

Figure 33: Results - Gamma, winter scenarios: Frequency responses

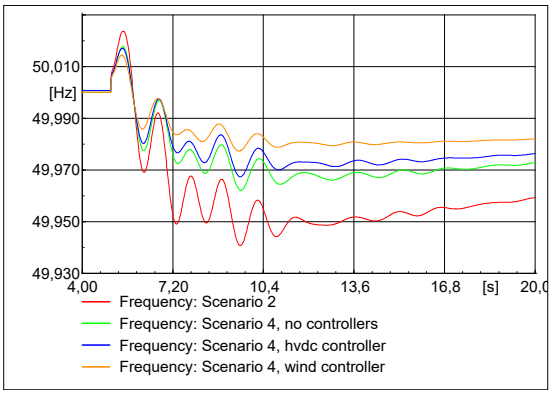

Figure 34: Results - Gamma, winter scenarios: Frequency responses (zoomed)

Scenario	f_{nadir} [HZ]
1	49.977
2	49.941
3 no cont	49.987
3 hvdc cont	49.992
3 wind cont	49.995
4 no cont	49.962
4 hvdc cont	49.967
4 wind cont	49.977

Table 17: Results - Gamma: Frequency drops

The reader should keep in mind that the critical lines that are investigated are *not* the same for all scenarios and carries a different load flow for each case (see section 4.3.3).

Large oscillations are observed, especially for the winter scenarios. However, oscillations are quickly damped. As scenario 2 was the most critical one for these simulations, it was examined further.

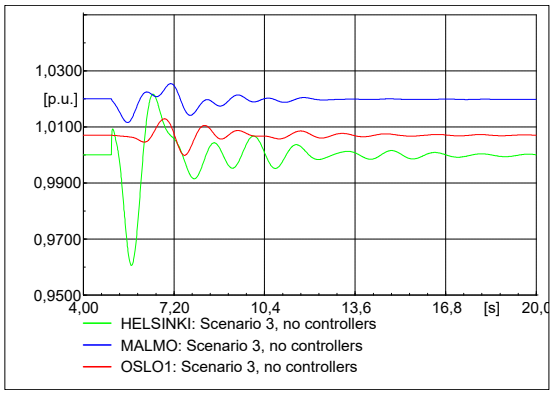

Figure 35: Results - Gamma, scenario 2: Voltage responses

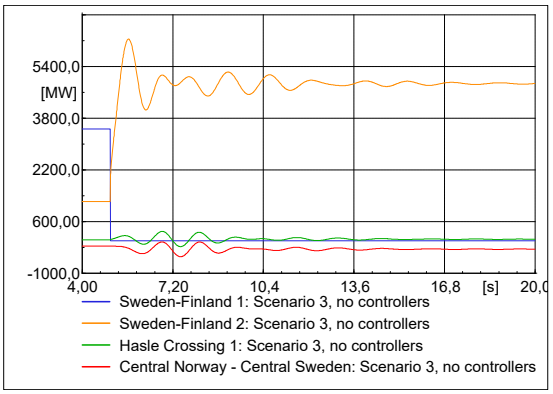

Figure 36: Results - Gamma, scenario 2: Power flows

	Power flows [MW]		
Line	Pre event	Post event	Change
Sweden - Finland 1	3460	0	-3460
Sweden - Finland 2	1216	4878	3662
Hasle Crossing 1	27	45	18
Hasle Crossing 2	-314	-295	19
Central Sweden - Central Norway	-161	-265	-104
Northern Sweden - Northern Norway 1	267	51	-216
Northern Sweden - Northern Norway 2	67	194	127

Table 18: Results - Gamma, scenario 2: Power flows

Once again, it is the Helsinki node where the most critical voltage drop is found (around 4%). However, the amplitudes of the oscillations are much smaller than for the short circuit event. For the Norwegian and Swedish nodes, the voltage deviations are comparatively low. The oscillations die within 15 seconds after disturbance.

Considering the load flow, one observes how the line Sweden-Finland 2 was disconnected. The power flow becomes redirected on the second line from Sweden to Finland (Porjus-Oulu). The power flows between Norway and Sweden are less affected, but one can observe how the flows are redirected even within Norway.

6 Discussion

Simulations in PowerFactory have been executed to study how increased wind power capacity and more HVDC interconnectors will affect the frequency stability in the Nordic grid in the future. System inertia and frequency bias have been calculated. The results are presented in the previous chapter and will now be discussed. Analyzing the frequency response indicators will be the primary approach for the discussion.

6.1 Discussion of results

6.1.1 System inertia

The fundamental development was the same for all scenarios; the Nordic grid got more HVDC and wind power capacity from 2017 to 2030. However, the inertia calculation results presented in table 9 show a significant deterioration from summer 2017 to 2030 (-33%) while the inertia levels at winter peak hours almost remained constant (+4%). These findings meet the expectations of reduced inertia in the future for the summer scenarios, while the slight increase during winter was unexpected.

System inertia is to a large extent decided by the generators in the system. The development of less inertia in summer 2030 is mainly due to wind power and HVDC replacing conventional generation. This can be seen in appendix J. Thus, the combination of low consumption and high import and variable speed production gives low levels of inertia in the system. Summer nights with high import represents operating situations where the Nordic grid already today have low system inertia, and are known to be more exposed to disturbances. The winter inertia levels are almost constant. A reason for this is that extremely high consumption calls for almost all generation to run - even expensive conventional generators that generally would be the second choice to cheaper renewable solutions. This theory is strengthened when observing which conventional generators that operate in 2030 as 2017 (appendix J). A second explanation can be the expected increase in consumption[2], calling for more production. Thus, some of the new wind power is covering the increased load, rather than replacing conventional generation. A third reason is the conservative estimation of future wind power, which could lead to a lower contribution from wind power than what might be the case (see section 6.1.8 at the end of this chapter).

The inertia calculation results are within the expected range when comparing to more comprehensive studies[4][12][13], although situations with even less inertia are also found. The kinetic energy capacity in the present Nordic power system excluding eastern Denmark

was estimated to maximum 360 GWs by the European Network of Transmission System Operators (ENTSO-E)[12]. This correlates well with the calculations results for system inertia in 2017 where the winter scenario has 357 GWs. The present low inertia scenario is estimated to 193 GWs. This is a bit higher than expected, but within the range of acceptable results. For the future scenarios, the Nordic TSOs estimated that the kinetic energy in the system would be in the range 90-310 GWs (2025)[4]. Thus, the calculated results for winter 2030 (371 GWs) is considerably higher than what is suggested in the TSO report for future high inertia situations. This might be due to an underestimation of wind power contribution in 2030, see section 6.1.8 (at the end of this chapter). The future summer scenario is estimated in this thesis to be around 130 GWs, which is a bit higher than the lowest expected values in the same report. This may indicate that the results in this thesis might be systematically too high for both low and high inertia scenarios. However, other reports estimate that the kinetic energy of the Nordic system will stay above 134 GWs 99% of the time in 2025[13]. This result is closer to the inertia estimation in this thesis, and thus indicates that the thesis results are within reasonable limits.

System inertia will span over a broader range in the future system than today. This increased range together with the more extreme low inertia situations may enhance the complexity of system operation, making it more challenging to provide satisfactory system stability at all times.

6.1.2 Controllers

As the simulation results indicated that the frequency responses might in some situations be considerably worsened approaching 2030, it may be necessary to implement measures of mitigation to ensure satisfactory stability of the grid. In section 2.4.4, several approaches to achieve better frequency responses were presented. In this thesis, it has been explored to implement controllers to wind turbines and HVDC connections to allow an inertial response. Two controllers were developed and implemented in the PowerFactory simulation model.

Many simulations have been conducted, and all of them indicates that the system responses could be improved if the controllers were implemented (e.g. event Beta and Zeta, see relevant figures and tables in section 5 "Results"). For example, the nadirs were significantly higher and the ROCOFs were lower for all disconnection events (e.g. table 11) when controllers were activated. Hence, the results suggest that HVDC links and wind turbines may be used to provide or absorb energy from the system to counteract frequency changes in the same way as conventional generators. This general finding was expected as it was the the goal for the controller designs and several other studies suggested the

same[13][17][23][44].

The improvements seen in the frequency response indicators are quite considerable, although the exact numbers are not relevant. The controllers have a simple design and are not tested outside the simulation model. Thus, they need to be tested and optimized further to confirm that the findings in this thesis are correct and to what extent the different technologies can provide support. The simulations conducted are only meant to illustrate the potential for wind power and HVDC links to contribute to frequency stability, and to explore if this could be one of the measures initiated to ensure satisfactory system stability. This has not been falsified during these studies, but must be further explored before any definite conclusions are given.

The controllers were designed to provide an inertial response, not concerning the permanent state of the system. Thus, the results with active controllers should not (and have not) been used to study frequency biases or steady-state deviations.

In short; The implemented controllers better the frequency response in all situations. The positive contribution is most present at disconnections of production units or HVDC connections. However, the controllers need to be further studied and developed to explore in detail how their contribution might be in the future grid.

6.1.3 Frequency response indicators

Investigating frequency response indicators given in the graphical and tabular results, one observes that the frequency stability deteriorates from summer 2017 to 2030. This can be seen in the increased frequency drop, ROCOFs, steady-state deviations, etc. in section 5.

Frequency drop

The change in frequency drops can be seen in particular for the events where generators and Skagerrak HVDC link were disconnected (e.g. figures 22 and 23 with their corresponding table, and figure 58 and 59 in the appendix). For these disturbances, the drops increased 30-40% from summer 2017 to 2030, representing a significant deterioration.

As explained in section 2.4.2 and seen in equation 2.13, the inertial frequency response is mainly dependent on system inertia. The inertia is significantly lower for summer 2017 than 2030, as explained earlier in this chapter. This allows a rapid and deep frequency decline before sufficient reserves are activated to stabilize the frequency. The frequency drops are increasing with approximately the same proportion as inertia is decreased. Thus, the calculated results confirm the simulation results and the theory introduced early in the thesis. The frequency drop increases even further when disconnecting the largest generator

in Finland (event Zeta). However, this is partly due to the installation of a new nuclear facility, which will replace the current largest generator in 2019. When investigating figure 26 and 63, one observe how a disconnection of the largest unit in Finland represents relatively small problems today - but a considerable challenge in the future. The frequency responses and thus frequency stability are almost unchanged for the winter scenario from 2017 to 2030 due to the stable levels of inertia (see section 6.1.1). More (dynamic) loads do also contribute directly to the system response, counteracting the negative implications of variable energy sources.

In the Nordic grid, it is stated that there should be sufficient reserves (FCR) to keep the frequency nadir above 49.50 Hz for a dimensioning incident[3]. The simulations conducted in this thesis indicates that the most significant disturbance may induce frequencies lower than this limit during the operating hours with least system inertia (indicating not sufficient amounts of appropriate reserves). Although the numerical answers cannot be directly transferred to the real Nordic grid (simulation results are *relevant*, not *equal* to the actual grid), the results show that the frequency response is considerably deteriorated and may cause undesirable low frequencies - maybe ranging below the 49.50 Hz limit. The frequency drops can be significantly reduced if the HVDC links or wind turbines provide synthetic inertia.

To ensure a safety margin before load-sheddings are initiated, the system frequency should aim to stay above 49.00 Hz at all times. No simulations induce drops that were close to this level. The most considerable disturbances cause frequencies just below 49.40 Hz. Thus, the frequency drops seen in the simulations are massive, but not by themselves be significant enough to cause load shedding. However, they leave the system in a state where it is very vulnerable to further disturbances.

The initial state of the system during simulations was stable operation at 50.00 Hz for all events. The events would have more severe consequences if they occurred at extraordinary circumstances such as during complex maintenance, long-term upgrades or during (other) disturbances. Also, the frequency under normal operation varies around 50.00 Hz, meaning that faults might be initiated at frequencies below this. Hence, the drops would be even more severe if the disturbances occurred when the grid was more exposed.

From visual inspection of the graphs and equation 2.13, one may observe how the magnitude of the disturbances correlates with the frequency drops. Thus, reducing the size of the largest potential faults could be one way to mitigate the problem of low frequencies after disturbances. If the TSO know that the system inertia will be extremely low at certain days or hours, one could demand that no generator, load or HVDC cable carried more than e.g. 800 MW. As the simulations show that the most exposed hours are during low load situations, this could be a convenient solution.

Considering the short-circuiting and disconnections of the critical lines, event Gamma and Eta, they do not give consistent results regarding development for frequency stability. This is partly because the load flows in the lines at the time of the disturbance are dissimilar, making the frequency response indicators less relevant for direct comparison. The deviations and oscillations seem to be more significant in the winter than summer scenarios. This contradicts the knowledge of system inertia and frequency response. However, the magnitudes of the incidents are the leading factor for these results. The power flows in the critical lines are higher during winter (see section 4.3.3), making the system response more severe. In general, the system components are more critically loaded during operational hours with substantial consumption, which could also affect the results.

Very modest frequency reactions are observed for the disconnections of the critical lines (comparing to the other events). Deviations within $\pm 0.05 Hz$ indicates that the system is far from its frequency stability limits. Oscillations are damped within 10 seconds for the summer scenarios and within 15 seconds for the winter scenarios. Controllers seem to improve the frequency response slightly, both concerning deviation and oscillations. Looking at the maximum frequency deviation when the critical lines where disconnected (figure 31 and 33), it was less severe than for the short-circuiting of the same lines.

The initial frequency response of the short-circuiting should not be given too much attention. The spikes that can be seen (appendix H.5) are not representing the system frequency, but generator reactions due to sudden changes in the voltage phase angle. After the transient spikes have faded, one may again study system frequency. At this point, however, the frequency deviations are small and represents no danger to the system.

Time of nadir

The time of nadir is normally not an important indicator for the frequency response, as the time for frequency minima is less critical than the magnitude of it. Also, the results show that the times of nadirs have a limited variation for the simulations conducted. Thus, it does not give much valuable information regarding changes in the grid from 2017 to 2030. No further attention will be given this indicator in the discussion.

Frequency bias

Investigating the frequency bias results (table K and plots for power disconnection events), one may observe that both the graphical and calculated results show that the frequency bias will be reduced from summer 2017 to summer 2030. The development for the winter scenarios seems rather unchanged. It is desirable to have high frequency bias in the system as this leads to reduced permanent frequency deviations after a disturbance.

The reason why the system frequency bias has been reduced for the summer scenarios are found by studying equation 2.2 along with the list of generators with droop settings

(appendix K). The equation shows that frequency bias is higher when many generators with (preferably low) droop settings are connected. Equation 2.3 shows that the steady-state frequency deviation becomes low when the frequency bias is high, which is favorable. This knowledge is confirmed by the simulation results, where low steady-state frequency deviations are found for all winter scenarios (disconnection events, see e.g. table 20). From summer 2017 to summer 2030, an adverse development is observed concerning connected generators that enhances system frequency bias. They are replaced by wind power and HVDC import, neither having droop characteristics. This is the reason why the steady state frequency deviation increases and frequency bias decreases from summer 2030 to summer 2030. A higher steady-state frequency deviation calls for more actions to bring the frequency back to nominal value.

ROCOF

ROCOF is the rate of change of frequency and is an important parameter for the very initial frequency reaction to a disturbance. Having a low ROCOF gives the primary reserves more time to be activated, preventing the frequency drop from becoming too severe.

Like several of the other indicators, ROCOF tends to be unchanged for the winter scenarios, but deteriorated for the summer scenario. E.g. for event Beta, ROCOF is considerably higher for summer 2030 (-0.21 Hz/s) than summer 2017 (-0.15 Hz/s). For the winter scenarios, the ROCOF value is marginally improving; -0.12 Hz/s in 2017 to -0.10 Hz/s in 2030 (these numbers are without activated controllers). The same tendency is found for all power disconnection events. The ROCOF is improved when controllers are implemented.

The simulation results along with the information on which generators that are running in each scenario, show that the Nordic system has less inertia during summer than winter and that there is an adverse development from 2017 to 2030 concerning situations with low inertia. As explained in section 2.3.2 and shown in equation 2.1, the ROCOF is inversely proportional to the system inertia constant. Thus, it is expected that ROCOF is increased when inertia is decreased. This is confirmed by the simulation results for all power disconnection events. The reduced ROCOF when controllers are activated confirms that the controllers can enable fast power support to the system.

6.1.4 Voltage response

Frequency stability has been the main concern in this thesis. However, a closer look has been given to voltages and load flows during the most critical disturbances. The goal of this has been to explore in more detail how the disturbances affect the system and to possibly detect severe system consequences concerning other aspects than frequency

stability. Voltage responses have been investigated for scenario 3 (no controllers) for the events where Skagerrak HVDC lines and the largest Finnish generator were disconnected, as well as the short-circuiting of a critical line event. The disconnection of a crucial line was explored for scenario 2. These situations were given a closer look as they were considered the most severe scenarios for the given events.

The results show in general moderate temporarily changes in voltages for the large switching events, with the most severe situations occurring in Finland (figure 24, 27, 29 and 35). Considering the disconnection events, the voltage deviations were within 5%. Helsinki was the most affected node, with a voltage drop of more than 4% when the largest generated unit in Finland was disconnected. 4% is significant, but within acceptable limits. Voltage dips like the one observed for the disconnections do not have severe system consequences, although it reduces the quality of supply, and may increase losses, age components, etc[8].

For the short-circuiting of a critical line, the voltage drops became more severe than for the disconnections. At nodes in Helsinki, Malmö and Oslo, the voltage dips were about 12.4%, 10.8% and 4.5% respectively for the most critical scenario (summer 2030 without additional controllers). These dips reduced voltage quality significantly. However, the system returned quickly back to the original state without becoming unstable. Oscillations died within 10 seconds after the initialization of the event. Voltage drops of large magnitude should be expected for events of such extraordinary proportions as studied in this thesis. The system remained stable even though voltage dips of more than 10% were detected. Thus, one could argue they are within acceptable limits.

One observes how voltage dips are more of a local problem than the frequency drops. While frequency affects the whole system and frequency support can be initiated within the entire frequency area are voltage stability more dependent on local reserves. Reactive power control is vital for maintaining the voltage stability, as reactive power cannot be transferred over very long distances. Thus, the need for reactive support must be considered near the affected area. Finland has more trouble than Norway and Sweden to activate sufficient reactive reserves to ensure voltage stability, which may be one of the reasons why the country seems more exposed for voltage disturbances. The load flow results when disconnecting Finland's largest unit supports this. Table 14 shows how active reserves are activated as far away as southern Norway, while figure 64 and table 19 shows that almost no reactive reserves are activated in Norway. Figure 65 displays the active and reactive power production for a generator in Helsinki, and confirms the findings: Most reactive reserves are activated locally, while active reserves are more distributed.

In general, the voltage regulation seems to work fine, especially for the less extreme events. However, it is recommended that this topic should be examined closer (see section 7.2 Recommendations for further work).

6.1.5 Load flow response

The power flows on all cross-border lines were investigated. They were chosen to allow an investigation on where reserves were activated due to disturbances, in addition to being essential lines for power flows between countries.

Larger power disconnections (magnitude) leads to larger load flow changes and oscillations (figure 25 and 28). The load flow oscillations usually stabilize within 10 seconds from the disturbances was initiated. The system responds logically, which strengthens the validity of the model. E.g., when there is an outage in Sweden, the Swedish export to other countries is reduced. The same goes for events in Norway and Finland. In general, it was observed that all countries provided support to stabilize the frequency even if the incident occurred in an area outside their borders. This makes intuitive sense as the frequency is a global parameter and all areas respond to stabilize and restore it. However, it was observed by investigating figure 25 and 28 (and corresponding tables) that Norway and Sweden were able to activate a more substantial amount of reserves than Finland. For example, Norway provided most of the reserves when the import from the Skagerrak HVDC cables was disconnected. When disconnection of similar size occurred in Finland (event Zeta), most of the reserves were activated outside the country. Finland seems to struggle to activate sufficient amounts of reserves, even for disconnections within the countries own border. One of the reasons for this comparably low amounts of hydropower, which are quickly and easily activated.

For event Gamma, disconnection of an important line, one observed large and rapid oscillations on the remaining line between Finland and Sweden (figure 36). However, the oscillations faded out within 15 seconds and the system remains stable. The line increased its power flow massively due to the incident.

Considering the short-circuiting event (figure 30 and table 16), one observe massive drops for two of the power lines. However, the system was able to bring the power flows back to initial values and dampen the oscillations within a reasonable time (5 seconds). The system remained stable. The significant load flows and load flow changes could represent challenges to the system and its components. This should be further examined to see in detail what possible implications the shift in power flow might represent (see section 7.2 Recommendations for further work).

The power flow reactions were heavily dependent on disconnection magnitude and location. Oscillations and changes in load flow were significant, but within expected limits for events of such severance. The system remained stable for all events. There must be sufficient free capacity on the affected lines when the power flows increases. This must be taken into account when planning and operating the grid. During high load scenarios, it is crucial

that the system operator allows free capacity on some of the most critical Nordic power corridors to satisfy the N-1 criteria (see appendix A).

The studies of the flows on critical lines have been brief and were only meant to detect any unstable or essential reactions that had to be handled. Violation of transmission line capacities was not considered, as the aggregated wind power plants and other pragmatic simplifications could be the cause of any artificially large power flows. The findings indicated a healthy system without any critical power flow reactions for even the most significant disturbances. Further studies should be made to explore the power flow reaction more thoroughly (see section 7.2. A different approach might be necessary as PowerFactory is not ideal for analyzing power flows.

6.1.6 Small test network

A Small Test Network (STN) was developed to facilitate simulations in a less complex environment. It was developed to study the new technologies and to get results that could be compared to the N44 results. The STN simulation results indicated that the system would get less inertia and frequency bias, as well as a worsened frequency response (considering the frequency response indicators) when HVDC or wind power replaced conventional generation without additional controllers (see table 4). The reactions would, however, improve considerably if additional controllers were implemented. The STN did not investigate events where lines where disconnected or short-circuited. All main trends and findings found by analyzing the STN grid and results were also observed for N44.

Conducting simulations and testing on two different networks reduces the chances for systematic errors and mistakes, and increases the validity of the results. Thus, the comparable results for the STN strengthen the results from the larger and more complex N44.

6.1.7 Hypotheses

The hypothesis that was presented in the introduction suggested that more HVDC interconnections and installed wind power capacity would decrease system inertia, and that the increased inertia would be associated with a deteriorated frequency response. This hypothesis proved to be partially right. Both analytical investigation of operating generators and graphical simulation results show that there is less system inertia in 2030 than 2017 - but only during operating hours where the system inertia already is low (summer scenarios). By analyzing the frequency response indicators, it showed that the reduced inertia did, in fact, lead to a deteriorated frequency response like the hypothesis suggests. This finding was further strengthened by the knowledge presented throughout the theory

chapter (inertia, swing equation, etc.). The results for the high inertia scenarios indicated that the total system inertia in 2030 would be close to present levels. During these hours, the simulations indicate that the frequency stability is *not* worsened. The STN simulations strengthen these findings concerning the results and the hypotheses.

6.1.8 Implications of assumptions

Several assumptions were necessary to make the simulation models and conduct the simulations (section 4.3.5). This may have affected the results in different ways, which will now be discussed.

The distributions of consumption and production for the different cases were based on real data for the Nordic grid, but with some pragmatic adjustments to fit the model. As all simulations ran smoothly, no components were saturated and the system remained stable, one can assume that the distribution was within the range that allowed the simulation model to run satisfactory and to give reasonable results. Thus, it is considered unlikely that the power distributions had a significant negative effect on the main trends in the results. However, numeric results might have been slightly affected. This counts especially for load flows and voltages, which are local parameters.

It was decided to let at least on conventional generator run in all price areas at all times. Theoretically, it will be possible for wind power and HVDC import to cover all loads in certain situations in the future. However, to model this without any measures to enhance system stability would be trivial as a system (almost) without inertia would be extremely exposed to any incidents, and such a case would never be facilitated by the TSO's. That is why a minimum of conventional generators was allowed to run. If this assumption proved to be too conservative, meaning more conventional generators than necessary were connected to the grid, the future inertia could be even lower than estimated in this thesis - and the system stability even more exposed to disturbances. However, this does not change the trends that are seen from 2017 to 2030, only amplifying them.

The assumption of load increase is significant for the results, and might have affected the trends detected. The increased consumption counteracts the impact of more wind power and HVDC as parts of the new generation covers the increased load. If the load increase is overestimated, the future stability situation is further deteriorated as additional conventional generation would be replaced. The results are not as sensitive for an underestimation of the load increase, as more load would be covered by wind power or import and not conventional generation. In the simulation model, HVDC and wind power contribution are not limited by their capacity, but by the assumption that one conventional generator is operating in each price area at all times. Thus, this assumption might have

affected the results to have too high inertia and system stability.

The estimates of future wind power and HVDC connections form the core of the input data to the simulation model. The 2030 HVDC capacity has relatively low uncertainty as most HVDC projects are planned years ahead and because there are in general fewer projects than e.g. new wind power plants. Wind power capacity is harder to predict as projects take less time from initiation to production, the current and expected growth is very strong, and the market and political incentives for the next decade are uncertain. An estimation from WindEurope for the Nordics (including Denmark) is in the range 20-40000 MW for 2030[41], which depicts the vast variety of possible outcomes. The results for the winter scenarios are very sensitive to the HVDC and wind power capacity as all new capacity may be used to replace conventional generation, leading to reduced system inertia. The current results display little change in inertia levels in 2030 compared to 2017. If wind power and HVDC increased their capacity more than expected, the result of "(almost) unchanged inertia levels" might change to "decreased inertia levels". However, it is not critical for system stability if the winter scenarios reduced their levels of inertia. The total system inertia would still be high and the frequency stability satisfactory. The simulations conducted may be less sensitive to wind power and HVDC capacity uncertainties than one might have expected for the low inertia scenarios. This is partly because the trend is more important than the numerical results, and more or less wind and HVDC import will most likely only adjust the strong trend of reduced system inertia in the future. Secondly, the total contribution of wind power and HVDC import is limited by the assumption of at least one generator running in all price areas. In short; the estimates of future wind power and HVDC connections are associated with significant uncertainties. These might have given too high inertia for winter scenarios. The summer scenarios seem to be less sensitive to the uncertainties, as it is mainly limited by the one node in each price area assumption.

Loads were assumed to behave similarly in 2030 as 2017, despite the expectancy of more loads being connected through power electronics in the future[25]. Thus, this assumption did probably lead to a systematic error of too favorable frequency responses in the future. The contribution from dynamic loads to system stability is much less than the contribution from conventional generators, as discussed for the STN (section 4.2.3). Thus, the results are therefore expected to systematically give slightly higher levels of inertia than what can be expected in the real grid. This shifts the numerical results, but does not affect the general trends.

Controllers were installed on different shares of their respective technologies with the primary goal to illuminate how (and if) wind power and HVDC connections could affect the system frequency response in the future. The given shares were merely examples of different degrees of implementations. Additional control systems were installed on all

wind turbines. The resulting system responses were significantly improved when the wind controllers were activated. If a different share of wind turbines were enabled to contribute with synthetic inertia, their contribution would be similar, but of less magnitude. The same applies to the HVDC connections contributing to frequency response. However, the controllers were only implemented on three HVDC links, so the total contribution from HVDC in the future might be even more substantial than the thesis results suggested. Thus, the share of units the controllers were implemented on shows the principal of how the controllers may improve system response, while the magnitude of improvement will be decided by how many units the controllers are implemented on.

Wind power generation was aggregated at six Nordic nodes and consisted only of FRC wind turbines (type 4, appendix C). The practical simplification of having only one wind turbine type is not expected to affect the results significantly. As long as the turbines are decoupled from the grid (which is a premise of this thesis) they would most likely be able to contribute to synthetic inertia in the same way as the FRC turbines, as long as suitable controllers are installed. Concerning the poor distribution of wind power plants, this is expected to affect the local properties of voltages and load flows to a larger degree than system frequencies. Thus, these assumptions are not expected to impact significantly on the system frequency response.

All disconnection event units were assumed to be operating at rated power prior to the disconnection. This is reasonable for scenarios with very high loads, such as the winter scenarios. It is more unlikely for summer scenarios, as the power demand is low. Having similar events for different scenarios was a premise for the simulations. This made comparisons between scenarios easier. However, this assumption implies an unlikely power distribution for summer scenarios, as some generators are operating at rated power while most other have lower outputs. Thus, the events are of higher magnitude than what is likely for the given scenarios. The simulation results are still correct, but one should keep in mind that the frequency response indicators for low inertia situations are a bit worse than what would be the case if the units that were disconnected ran at less than rated power (which is more likely).

Summarizing how the assumptions might have affected the results, one must first acknowledge that the simulations are built on assumptions that might have changed the results in both directions. Thus, the simulated frequency responses might both be higher and lower than what is shown in this thesis. Secondly, the assumptions seem to mostly affect the numeric results, while the trends (reduced inertia for future summer scenarios, etc.) are less sensitive. Most assumptions seem to have potentially affected the results to be too modest, meaning that the frequency stability in the system might be slightly worse than the results indicate. This means that the development of inertia reduction in the future

could be even stronger than the results suggest. For the high inertia scenarios, this should not be critical for system stability as the system inertia still would be high. For the low inertia scenarios, this could mean that even more critical frequencies may be reached and more measures of mitigation must be made.

6.2 Sources of error

- **Simplifications** - Numerous simplifications have been made during this project and in the development of the N44 grid. These were necessary to limit model complexity, making the model itself and the inputs more manageable. However, unnecessary or mistaken simplifications may lead to errors in the results.
- **Model** - An existing model, N44, was used for the major part of the simulations. This model could contain incorrect settings and faults, causing systematic errors in the results. Also, the structure, components and parameters might not be entirely up to date.
- **Controllers** - It was not within the scope to create and optimize any state of the art control systems. Basic control systems were designed and used for the simulations to illustrate the potential of synthetic inertia. If the controllers turned out to be too basic, giving unrealistic results or violating technical constraints, the results based on the control systems could have been heavily affected. As a response to this, the results have been interpreted based on trends rather than exact numeric answers.
- **Calibration** - No calibration of the modified model against real-life solutions was conducted. This could lead to systematic errors.
- **Human error** - For vast and complex models, such as N44, many parameters are decided and adjusted. This increases the chances for typos and misclicks, resulting in wrong numbers and parameters in the model or background data causing simulation errors or misleading results. However, countless reviews of data, input and output as well as reasonable and logic results indicate that human errors had a minor effect on the results. The main takeaway from the results are trends and not numbers, so most small typos would probably not inflict the main results significantly.

6.3 Validity of the results

A simulation model of a large real-world system will be associated with limitations, assumptions and inaccuracies. The author of this thesis is aware that the results may be related to errors and inaccuracies. However, the main trends found in the results are in

accordance with existing knowledge, results from the literature study and expectancies (hypothesis, etc.). Simulations in a smaller STN model confirmed the primary results from the N44 simulations. This increases the validity of the results. A peer review or a second, more extensive study, would increase the validity of results further.

The results are relevant for the actual Nordic grid and several power systems.

7 Conclusion

Concluding remarks will be presented in this chapter. Possible topics for future work will be proposed.

7.1 Summary and concluding remarks

The main objective of this master thesis was to study how increased HVDC capacity and wind power generation affects the frequency stability of the power system in the future.

Simulations of a Nordic model in DIgSILENT PowerFactory demonstrates that the frequency stability for the system does not change significantly for operating situations with very high loads (winter scenarios). This is partly because the consumption is expected to increase towards 2030, but also because the most extreme load situations call for almost all conventional generators to run. The new technologies seem to complement the existing generation and to cover the expected consumption growth, rather than replacing them. Thus, the results suggest that the very high levels of system inertia will remain close to constant under the most extreme load situations (peak hours during winter) from 2017 to 2030.

For the summer scenarios where the inertia in the present system already is low, the calculation and simulation results indicated that the new technologies would replace a substantial part of the current generation. This leads to reduced system inertia, which deteriorates the frequency response. This was in accordance with the hypothesis, stating that "reduced system inertia will deteriorate the frequency response following a power imbalance". The reduction of operating generators from 2017 to 2030 happens despite an expected increase in consumption. Thus, the future summer scenarios with high wind production and low local generation were identified as the most crucial of the scenarios investigated. Several simulations indicate that the frequency dips might increase by more than 30% by summer 2030 if no measures of mitigation are initiated. The most severe dips reach below 49.40 Hz. The disconnection events of highest magnitude proved to trigger the most critical frequency responses.

A hypothesis presented in the introduction stated that "new technologies, which is without synchronous coupling to the grid, will reduce system inertia if they are not equipped with suitable controllers". As explained above, this proved only to be right for the summer scenarios. For the operating situations with high consumption, the system inertia was almost unchanged.

As the results indicated that system stability deteriorates significantly towards 2030, it will be necessary to introduce measures of mitigation to maintain the current levels of frequency stability. Several possible measures of mitigation have been mentioned. One of them, introducing synthetic inertia to wind turbines and HVDC links, have been thoroughly explored and tested. Two general controllers have been developed to examine if wind power and HVDC connections would be able to provide frequency support to the system in 2030. Both when the HVDC controllers and the wind power controllers were connected, the frequency response indicators considerably improved. The system got an even more favorable response than in the existing grid for some indicators. The controllers were conceptual and should be tested further. However, they do indicate that the new technologies of HVDC and wind power might be a part of the solution and not just the cause of the problem.

In addition to the system frequency, some voltage and power flow responses have been examined. The voltage reactions were considerable, especially for a short circuit event where the voltage drop was more than 10% in Sweden and Finland. Voltage changes of such magnitude are critical and might inflict stress on the system and its components. Significant oscillations occurred, but where quickly damped. The system always remained stable. Finland had consistently higher voltage drops than Sweden and Norway for all disturbances. By investigating reactive power flows and reactive generation in Finland, it was evident that the country had more troubles regulating reactive reserves than its neighbors. This might be the main reason why Finland seemed to be more vulnerable to voltage drops. Cross-border lines were investigated considering the active power flows. These experienced significant and rapid changes accompanied by large oscillations at several events. Most critical was the disconnection and short-circuiting of essential lines, where large power flows were redirected. The system remained stable, but the large fluctuations could cause unnecessary stress on system components. The power flow results suggested that Sweden and Norway were able to activate much larger amounts of active reserves after a disconnection of a generator or HVDC cable than Finland.

The system has been tested for massive events under out of the ordinary circumstances with very high and very low system inertia. However, the results are relevant for smaller disturbances too, as the trends (e.g. frequency dips increases significantly for low inertia scenarios) would apply for similar events of all magnitudes. The main simulations were conducted in a Nordic model, but the general results may also apply to other power systems that are facing similar changes of increased decoupled generation.

Several assumptions were necessary to develop the model with its scenarios and events. These are associated with uncertainties and might have affected the results. Specific numeric results are especially vulnerable. Some of the assumptions might have caused

a systematic error of too high system inertia in the future, meaning that the frequency responses could be more critical than what the results suggest. However, the main findings and most important trends are expected to be less sensitive to any inaccuracies caused by the assumptions.

7.2 Recommendations for further work

A considerable amount of work has been put down to approach the objective of the thesis. Modern power systems are complex and the field investigated is enormous. Thus, several interesting topics remain to be explored to fully understand the implications on how wind power and HVDC connections affect the stability in a power system. A few suggestions include:

- **Enhance the N44 model** - Due to the 50 node restriction of the PowerFactory license that was available at NTNU, it was necessary to find pragmatic approaches where nodes were excluded. If a license without node restrictions were acquired, one could implement better HVDC link models, distribute the wind power more realistically, it would be unnecessary to remove some of the original nodes, and a general increased complexity would be allowed. This would strengthen the model and give more valid results. More nodes would also allow the model to include Denmark and other missing nodes.
- **Investigate the controller effects on components** - In this thesis, the focal point has been on the whole system and not on individual components. To better understand how the provision of synthetic inertia affects the operation of the wind turbines and HVDC connections, a detailed analysis of these components should be carried out. Further studies are necessary to confirm if the solutions investigated in this report represents viable solutions in a real grid.
- **Improve the controllers** - It could be a separate thesis to develop, test and optimize controllers that allow wind power and HVDC links to contribute to the inertial response. The controllers created for this thesis were basic and conceptual. Thus, a more extensive approach to improve the controllers is suggested.
- **Share of controllers** - It would be interesting to investigate different shares of HVDC connections and wind turbines with implemented controllers. In this thesis, only one share of both technologies were tested. However, it is recommended to further develop and test the controllers before different shares are investigated extensively.

- **Investigate the load flow and voltages** - To explore the load flow and voltage reactions have been very interesting and rewarding. However, as it was not within the scope to commence an extensive investigation on the topics, only a brief study was conducted. Thus, a thorough examination of the voltages and load flow in the system would be convenient to illuminate further system implications of the different scenarios and events.

- **Study less extreme events** - This thesis has investigated the most extreme situations and out of the ordinary events in a grid with very high and low inertia. These situations do not occur often. To better understand how the everyday operation of the grid would be affected by reduced inertia, it would be convenient to investigate less extreme situations.

- **Explore other initial conditions** - A selection of events have been tested on a stable system from an initial operating point at f = 50 Hz. To better understand the worst case scenarios, a study where simulations were conducted during less favorable conditions would be interesting.

- **Contribution from dynamic loads** - As more loads are being connected via power electronics in the future, the positive contribution from loads to system stability is expected to be reduced[25]. This has not been taken into account for the simulations conducted, but would be appropriate for further studies.

- **Comparison with other solutions** - Only synthetic inertia have been explored in this thesis as a measure to enhance system stability. To study other viable solutions, and later to compare them with each other, would be of great interest.

References

[1] Jonas Skaare Amundsen, Gudmund Bartnes, and Eirik Øyslebø. *Kraftmarkedsanalyse 2016 - 2030*. Tech. rep. NVE, Jan. 2017.

[2] Jonas Skaare Amundsen et al. *Kraftmarkedsanalyse 2016 - 2030, Underlagsrapport med detaljerte forutsetninger*. Tech. rep. NVE, Oct. 2017.

[3] *Appendix of System Operation Agreement (English 2017 update)*. Tech. rep. European Network of Transmission System Operators for Electricity, Sept. 2017.

[4] *Challenges and Opportunities for the Nordic Power System*. Tech. rep. Svenska kraftnät, Statnett, Fingrid and Energinet.dk, Aug. 2016.

[5] Stephen J Chapman. *Electric machinery fundamentals*. 5th ed. McGraw-Hill, 2012.

[6] Richard C. Dorf and Robert H. Bishop. *Modern Control Systems*. 12th ed. Pearson, 2011.

[7] Mohammad Dreidy, H. Mokhlis, and Saad Mekhilef. "Inertia response and frequency control techniques for renewable energy sources: A review". In: *Renewable and Sustainable Energy Reviews* 69 (2017).

[8] *Driften av kraftsystemet 2016*. Tech. rep. NVE, June 2017.

[9] Norges vassdrags- og energidirektorat. *Vindkraft*. `https://www.nve.no/energiforsyning-og-konsesjon/vindkraft/` (visited on 04/12/17). Feb. 2015.

[10] Robert Eriksson, Niklas Modig, and Katherine Elkington. "Synthetic inertia versus fast frequency response: a definition". In: *IET Renewable Power Generation* (Sept. 2017). DOI: 10.1049/iet-rpg.2017.0370.

[11] *Europe's onshore and offshore wind energy potential*. Tech. rep. European Environment Agency, 2009.

[12] *Future System Inertia*. Tech. rep. Available: `https://www.entsoe.eu/Documents/Publications/SOC/Nordic/Nordic_report_Future_System_Inertia.pdf`. The European Network of Transmission System Operators for Electricity, 2015.

[13] *Future System Inertia 2*. Tech. rep. Available: `http://www.statnett.no/Global/Dokumenter/Kraftsystemet/Systemansvar/Nordic20report,%20Future%20System%20Inertia2_Vfinal.pdf`. The European Network of Transmission System Operators for Electricity.

[14] Håkon Hellebust. "Balancing Power and Reserves in Norway with Increased Wind Power Production – Analysis of Imbalances". unpublished. Project report. NTNU, 2018.

[15] Hannele Holttinen. "Impact of Hourly Wind Power Variations on the System Operation in the Nordic Countries". In: (Nov. 2004). DOI: 10.1002/we.143.

[16] Jahangir Hossain and Apel Mahmud. *Large Scale Renewable Power Generation: Advances in Technologies for Generation, Transmission and Storage*. Springer Science & Business Media, 2014. ISBN: 978-981-4585-29-3.

[17] J. Huang and R. Preece. "HVDC-based fast frequency support for low inertia power systems". In: (Feb. 2017), pp. 1–6. DOI: 10.1049/cp.2017.0040.

[18] Mustafa Kayikçi and Jovica V. Milanović. "Dynamic Contribution of DFIG-Based Wind Plants to System Frequency". In: *IEEE Transactions on Power Systems* 24 (2 May 2009).

[19] *Kraftsituasjonen veke 45, 2017*. Tech. rep. Norges vassdrags- og energidirektorat, Nov. 2017.

[20] *Langsiktig markedsanalyse*. Tech. rep. STATNETT, Oct. 2016.

[21] Jim Machowski, Jim Bumby, and Janusz Bialek. *Power system dynamics: stability and control*. 2nd ed. Wiley, 2008. ISBN: 978-0-470-72558-0.

[22] E. P. McCarthy. "Phase lead compensator design". In: *Electronics Letters* 26 (Oct. 1990). DOI: 10.1049.

[23] N.W. Miller, K. Clark, and M. Shao. *Impact of frequency response wind plant controls on grid performance*. e-cigre: SESSION PAPERS & PROCEEDINGS. GE Energy. 2012.

[24] *Nordic Grid Code 2007*. Tech. rep. Nordel, Jan. 2007.

[25] S. Palm and P. Schegner. "Static and transient load models taking account voltage and frequency dependence". In: (June 2016), pp. 1–7. DOI: 10.1109/PSCC.2016.7540887.

[26] Nord Pool. *About us*. https://www.nordpoolgroup.com/About-us/ (visited on 05/12/17).

[27] Nord Pool. *Historical Market Data*. https://www.nordpoolgroup.com/historical-market-data/ (visited on 24/05/18).

[28] *PowerFactory 15, Tutorial*. DIgSILENT. Aug. 2013.

[29] *PowerFactory 2018, User Manual*. DIgSILENT. Dec. 2017.

[30] Chinthaka Seneviratne and C. Ozansoy. "Frequency response due to a large generator loss with the increasing penetration of wind/PV generation – A literature review". In: *Renewable and Sustainable Energy Reviews* 57 (Jan. 2016).

[31] *Technical Reference Documentation Complex Load*. DIgSILENT. Dec. 2017.

[32] *Technical Reference Documentation PWM Converter*. DIgSILENT. Dec. 2017.

[33] *Template documentation Fully Rated WTG Template*. DIgSILENT. Dec. 2017.

[34] Pieter Tielens and Dirk Van Hertem. "The relevance of inertia in power systems". In: *Renewable and Sustainable Energy Reviews* 55 (2016).

[35] The European Network of Transmission System Operators for Electricity. *Glossary*. `https://www.entsoe.eu/data/data-portal/glossary/Pages/home.aspx?Filtername=doc_term&FilterMultiValue=*HVDC*`. (Visited on 04/25/2018).

[36] The European Network of Transmission System Operators for Electricity. *Glossary*. URL: `%5Curl%7Bhttps://docstore.entsoe.eu/data/data-portal/glossary/Pages/home.aspx?Filtername=doc_term&FilterMultiValue=*hvdc*%7D` (visited on 02/13/2018).

[37] TVO. *OL3*. https://www.tvo.fi/OL3-. (visited on 03/05/18).

[38] Andreas Ulbig, Theodor S. Borsche, and Göran Andersson. "Analyzing Rotational Inertia, Grid Topology and their Role for Power System Stability". In: 48 (30 2015).

[39] Andreas Ulbig, Theodor S. Borsche, and Göran Andersson. "Impact of Low Rotational Inertia on Power System Stability and Operation". In: *IFAC Proceedings Volumes* (Aug. 2014).

[40] David Edward Weir and Nikolai Aksnes. *Vindkraft - produksjon i 2017*. Tech. rep. NVE, Feb. 2017.

[41] *Wind energy in Europe: Scenarios for 2030*. Tech. rep. WindEurope, Sept. 2017.

[42] *Wind in power 2017*. Tech. rep. WindEurope, Feb. 2018.

[43] M. Yu et al. "A review of control methods for providing frequency response in VSC-HVDC transmission systems". In: (Sept. 2014), pp. 1–6. DOI: `10.1109/UPEC.2014.6934693`.

[44] J. Zhu et al. "Inertia Emulation Control Strategy for VSC-HVDC Transmission Systems". In: *IEEE Transactions on Power Systems* 28.2 (May 2013), pp. 1277–1287. ISSN: 0885-8950.

A Glossary

A short selection of relevant concepts are explained in this appendix:

Ancillary services
An ancillary service may be defined as a service that is vital for the operation of a power system[36]. The content of this wide definition varies between countries and frequency areas, although frequency and voltage control are commonly included.

Automatic Generation Control (AGC)
AGC is a system where multiple generators adjust their output in response to load changes in the power system. The power output is modified by adjusting the mechanical power input to the shaft. The goal of AGC is to maintain system frequency and power exchanges at scheduled levels, as well as to allocate the power generation in a convenient manner[21].

Dimensioning fault
The fault that has the most significant impact on the given power system are usually named "the dimensioning fault"[24]. This is often the loss of the most substantial production unit in the grid[3]. The Nordic power system is designed to have, and normally operating under the condition that there are, adequate amounts of reserves to not allow a frequency drop below 49.50 Hz after a dimensioning fault[13][8]. Thus, the power grid and its subsystems should be able to handle a dimensioning fault without causing any critical reactions. The dimensioning fault in Norway is normally 1200 MW, while it is 1340 MW in the Nordic grid in general[8].

N-1 criterion
The N-1 criteria states that the relevant system should be able to withstand loss of any *one* component without failing[24]. It is a convenient way to describe system security. Considering the Nordic electrical grid that usually follows the N-1 philosophy, it means that the system should be able to work satisfactorily even if any *one* essential component such as a power line, generator, industrial load, etc., suddenly fails.

Spinning reserves
There must always be available spinning reserves that can be used for primary control to ensure satisfactory operation of the power grid. Spinning reserves are reserves that are connected to the grid and in operation without being used. For example, if a hydro plant is running at 50 % of rated power output, the remaining 50% would be considered spinning reserves. Thus, for a given synchronously connected generator, the spinning reserves are the difference between the power rating and the output. If no spinning reserves were available in the system, there would be no conventional reserves available for frequency support. This is why it is necessary for stable grid operation to have machines that are not

operating at full power output. Spinning reserves should be distributed across the grid to ensure that no transmission lines are overloaded due to the contribution from these reserves[21].

B Frequency control action overview

On figure 37, an overview is given for some frequency controlled actions in the Nordics, and when they are activated[24].

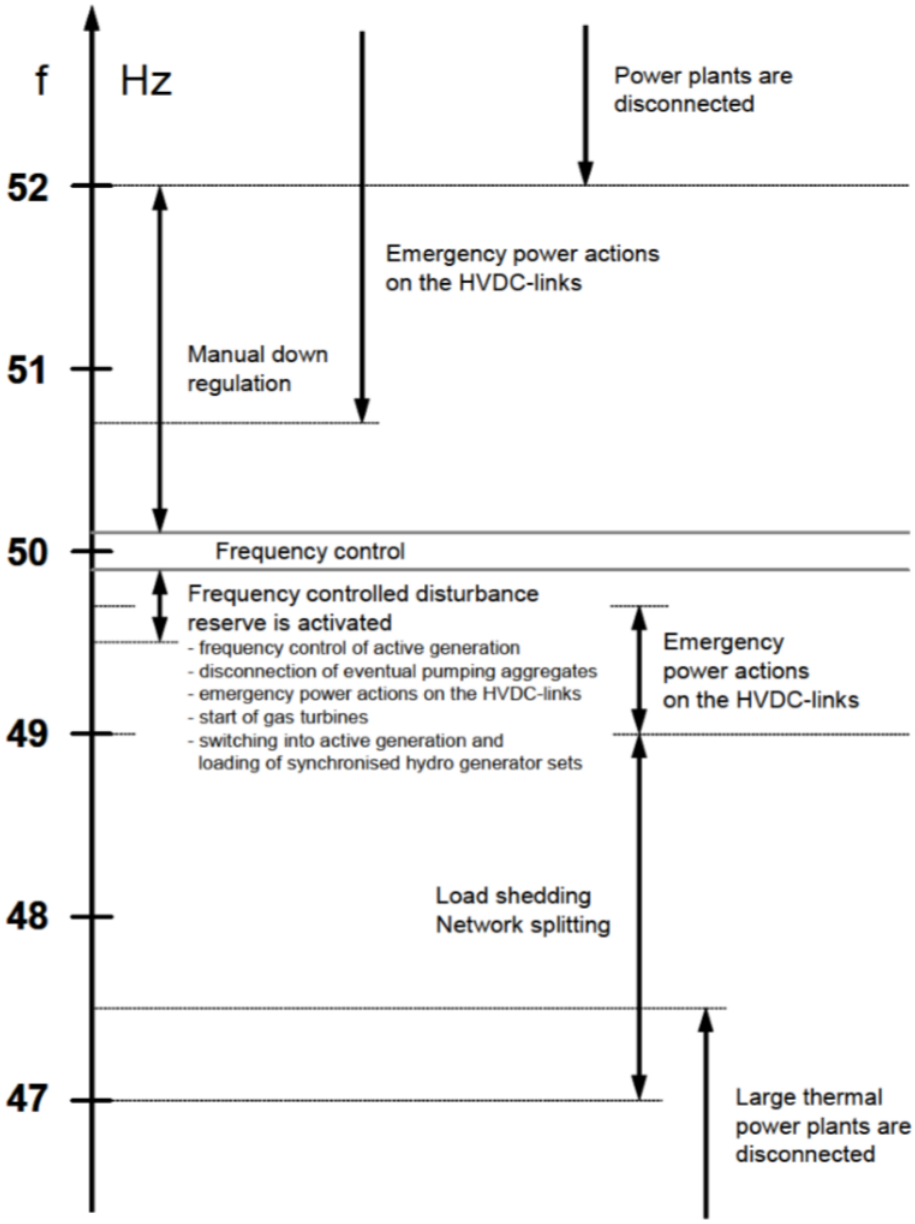

Figure 37: Frequency controlled actions in the Nordics[24]

C Modern wind turbines

There are four main types of wind turbines in the present wind power industry[30]. These are presented as single line diagrams below, figure 38 to 41. One of the most important distinctions between the designs is how they are connected to the grid. Looking at type 1, figure 38, the fixed speed induction generator is directly connected to the step-up transformer that feeds the grid. The frequency of the generator and the network are therefore coupled. When investigating the fully rated converter wind turbine in figure 41, it can be observed how the generator is connected to the grid via power electronics - in this case a back-to-back converter. Thus, the frequencies on each side of the converter are decoupled over the DC link. The book "Power system dynamics: stability and control" (2008) by Jim Machowski et al.[21] is the primary source for this section.

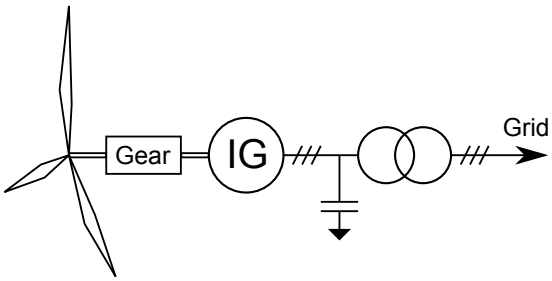

Figure 38: Wind turbine generator system - Type 1

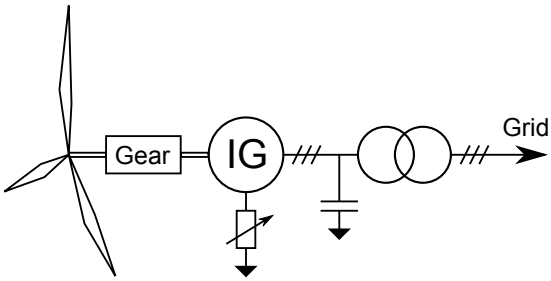

Figure 39: Wind turbine generator system - Type 2

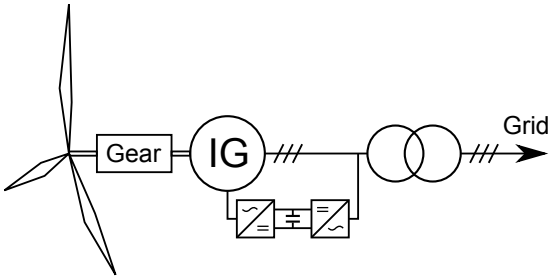

Figure 40: Wind turbine generator system - Type 3

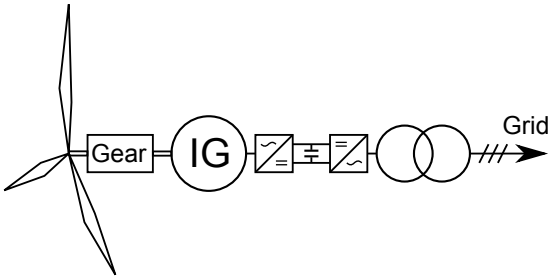

Figure 41: Wind turbine generator system - Type 4

Type 1: Fixed speed induction generator (FSIG)

This simple wind turbine design utilizes a squirrel-cage induction generator (SCIG). Looking at figure 38, it can be observed how the SCIG is directly coupled to the grid. Thus, it must run at constant speed, nearly fixed to the frequency of the grid. This leaves little room for control mechanisms, and power output and torque varies with the gust of winds. This also means that the power output will be less than for variable speed turbines, as the blade speed cannot be optimized. Power output modifications are mostly exercised by

pitch control as it has no electrical control systems. When turbine generators are directly coupled, all transient torques that appear in the shaft (due to turbulence in the wind) will produce stress on the mechanical system. All induction machines consume reactive power and need therefore reactive compensating to improve the power factor. This can be done by installing a capacitor bank.

Type 2: Wound rotor induction generators
As shown in figure 39, this design is fairly similar to type 1, but with some important modifications. The generator is a wound rotor induction generator and thyristor controlled variable resistances are used to achieve variable speed operation. This provides more compliance with the power system to which it is attached. This design requires reactive compensation, like type 1.

Type 3: Doubly-Fed Induction Generator (DFIG)
As seen in figure 40, this wind turbine design contains an induction machine with a wound rotor and a stator that is directly coupled to the grid. The rotor is fed at slip frequency through a back-to-back converter. A back-to-back converter consists of two converters that are connected via a DC link. This permits the frequency of the rotor to be electrically decoupled from the grid frequency. Variable speed is achieved by injecting an adjustable voltage into the rotor. The converter coupling allows the DFIG to both absorb and deliver power to the grid. The converter is typically rated 25-30% of generator rating and is thus cheaper than the converter used in type 4, which is fully rated.

Type 4: Fully rated converter wind turbine (FRC WT)
This generator design, figure 41, allows a high degree of flexibility and control, because of the full-scale converter. The converter fully decouples the generator from the network, enabling the variable speed operation. As the converter must be fully rated to the turbine power output, it is quite expensive. That is the reason why DFIG has been more popular than the fully rated converter wind turbine for some time. However, as the prices on power electronics decrease rapidly, the FRC WT becomes more popular. It is expected to be the preferred alternative in the future wind power plants. The type 4 turbine utilizes an induction machine, like the DFIG.

General comments to the turbine designs
Most modern turbines are type 3 or 4. The drawback with these types is that they do not provide inertia to the system as the power electronic configuration make the rotors electrically decoupled from the grid. However, by implementing additional control mechanisms, a similar response can be emulated. Type 1 and 2 are of more traditional design and may provide some inertia[30].

Type 3 and 4 utilizes power electronics to facilitate variable speed operation. By doing this,

the phase and magnitude of the rotor current can be adjusted. Variable speed operation allows the power output to be maximized while keeping the stress on the system low. Type 1 and 2 typically use capacitors to maintain the power factor and reactive power, and thus the voltage. However, without the controllability that the power electronic offer, type 1 and 2 become inferior to the other types. The power electronics and the controlling mechanisms on type 3 and 4 allow voltage control.

D Block diagram - PowerFactory PWM Current Controller

There is a built-in current controller in the PWM converter used for modelling HVDC connections in this thesis. The block diagram is displayed below.

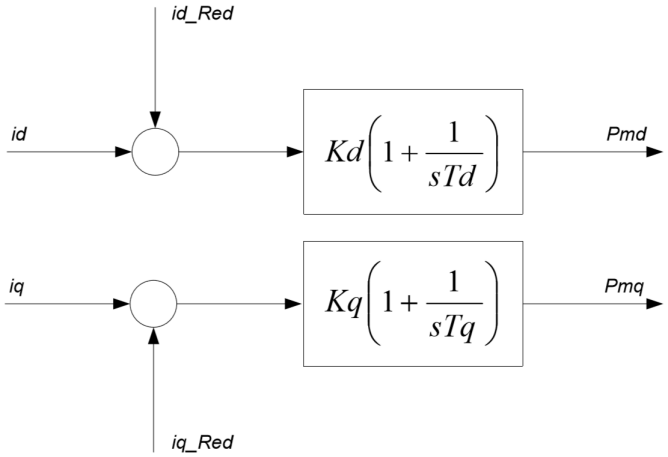

Figure 42: PWM current controller[32]

The inputs to the controller are the dq-currents on the AC side of the converter. The output signals are the pulse-width modulation indexes in the dq-frame[32].

E PowerFactory line diagrams

E.1 Main grid

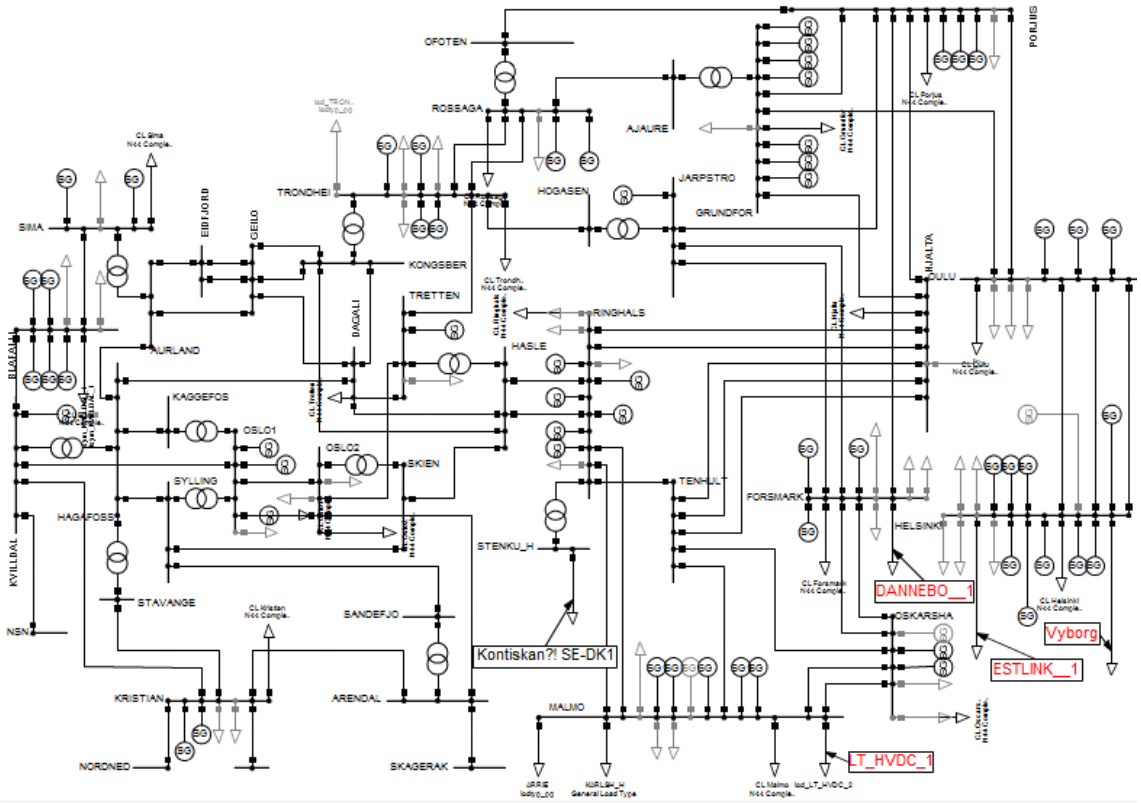

Figure 43: Single line diagram - N44 Main grid

E.2 HVDC connections sub-grid

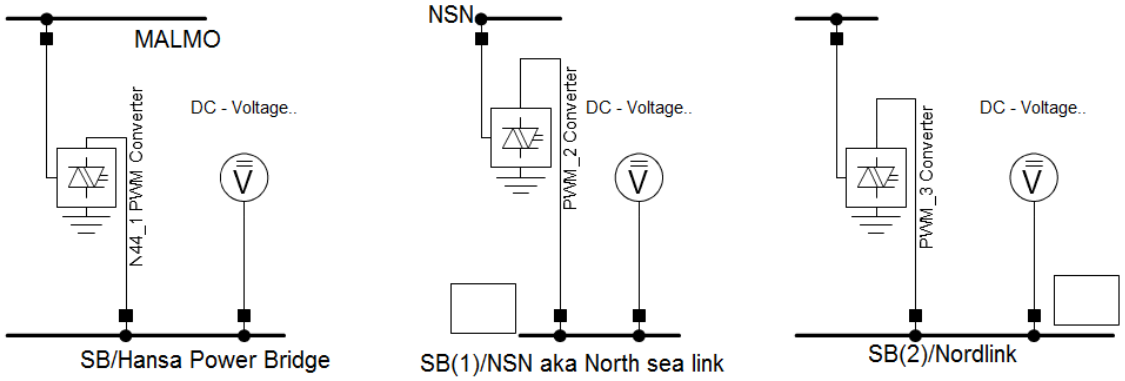

Figure 44: Single line diagram - N44 subgrid: HVDC

E.3 Wind power sub-grid

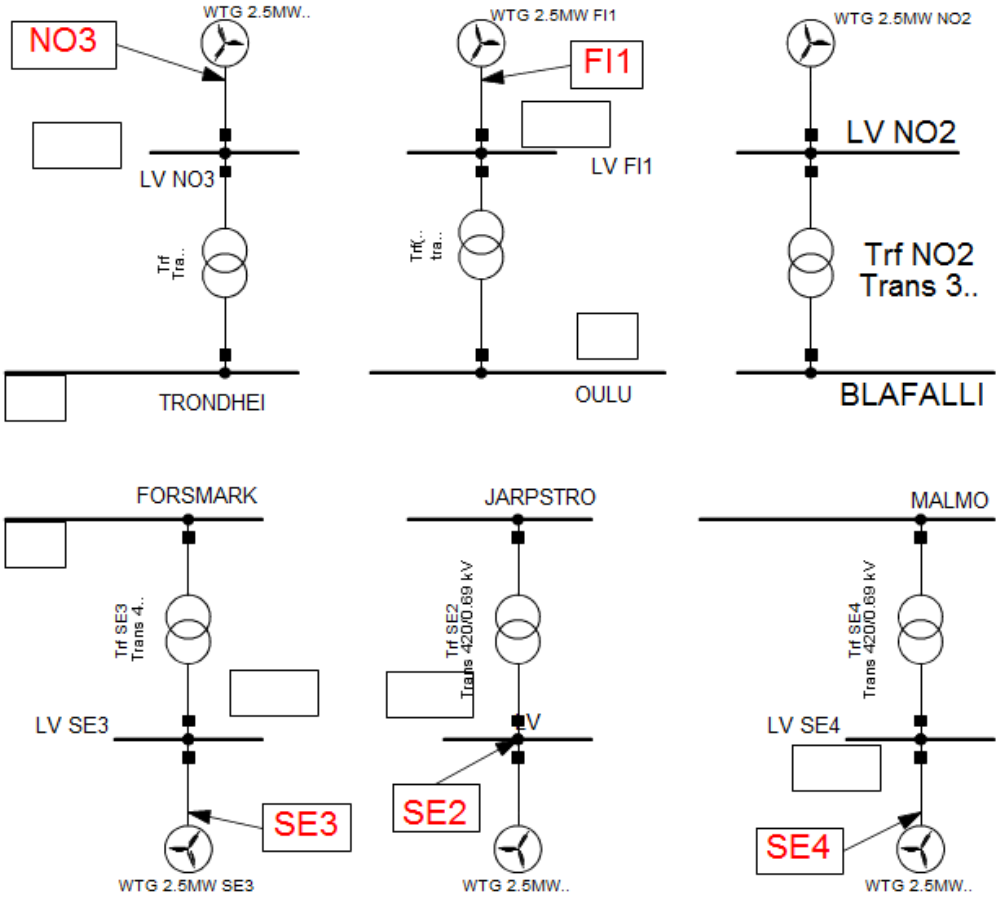

Figure 45: Single line diagram - N44 subgrid: Wind power

F Scenario data

For all scenarios, the following applies:

- The machines and loads that er not included in the tables are out of service.
- sym_OSKARSHA_2 is the reference machine.

F.1 Scenario 1

		Terminal	Active Power	Power	
	Name	Busbar	[MW]	factor	
LOADS	CL Blafalli	BLAFALLI	1420,	1	
	CL Forsmark	FORSMARK	1720,	1	
	CL Grundfor	GRUNDFOR	980,	1	
	CL Helsinki	HELSINKI	4940,	1	
	CL Hjalta	HJALTA	180,	1	
	CL Kristian	KRISTIAN	1420,	1	
	CL Malmo	MALMO	1680,	1	
	CL Oscarshamn	OSKARSHA	2280,	1	
	CL Oslo1	OSLO1	680,	1	
	CL Oslo2	OSLO2	680,	1	
	CL Oulu	OULU	2120,	1	
	CL Porjus	PORJUS	860,	1	
	CL Ringhals	RINGHALS	1720,	1	
	CL Rossaga	ROSSAGA	1620,	1	
	CL Sima	SIMA	1380,	1	
	CL Tretten	TRETTEN	680,	1	
	CL Trondheim	TRONDHEI	2320,	1	
	hvdc_ARRIE	MALMO	-300,	-1	
	hvdc_KARLSH_H	MALMO	-200,	-1	
	lod_DANNEBO__1	FORSMARK	-200,	-1	
	lod_ESTLINK__1	HELSINKI	-300,	-1	
	lod_LT_HVDC_2	MALMO	-200,	-1	
	lod_NORDNED_1	NORDNED	-200,	-1	
	lod_SKAGERAK_1	SKAGERAK	-1600,	-1	
	lod_STENKU_H_1	STENKU_H	-200,	-1	
	lod_VYBORG_H_1	HELSINKI	0,	1	

		Terminal	Active Power	Power	Voltage
	Name	Busbar	per turbine [MW]	factor	[p.u.]
WIND TURBINES	WTG 2.5MW FI1	LV FI1	0.4	1,	1,
	WTG 2.5MW NO2	LV NO2	0.4	1,	1,
	WTG 2.5MW NO3	LV NO3	0.4	1,	1,
	WTG 2.5MW SE2	LV SE2	0.4	1,	1,
	WTG 2.5MW SE3	LV SE3	0.4	1,	1,
	WTG 2.5MW SE4	LV SE4	0.4	1,	1,

Figure 46: Data - Scenario 1, part 1

		Terminal	Active Power	Power	Voltage
	Name	Busbar	[MW]	factor	[p.u.]
	sym_BLAFALLI_1	BLAFALLI	580,	0,95	1,
	sym_FORSMARK_1	FORSMARK	600,	0,95	1,
	sym_FORSMARK_2	FORSMARK	600,	0,95	1,
	sym_GRUNDFOR_1	GRUNDFOR	760,	0,95	1,
	sym_GRUNDFOR_2	GRUNDFOR	760,	0,95	1,
	sym_GRUNDFOR_3	GRUNDFOR	760,	0,95	1,
	sym_HELSINKI_1	HELSINKI	680,	0,95	1,
	sym_HELSINKI_2	HELSINKI	680,	0,95	1,
	sym_HELSINKI_3	HELSINKI	680,	0,95	1,
	sym_HELSINKI_4_OLK	HELSINKI	890,	0,95	1,
	sym_JARPSTRO_1	JARPSTRO	780,	0,95	1,
	sym_KRISTIAN_1	KRISTIAN	580,	0,95	1,01
	sym_KVILLDAL_1	KVILLDAL	1240,	1,	1,005
	sym_MALMO_1	MALMO	300,	0,95	1,02
	sym_MALMO_2	MALMO	300,	0,95	1,02
	sym_OSKARSHA_2	OSKARSHA	0,	0,95	1,
GENERATORS	sym_OSKARSHA_3	OSKARSHA	1000,	1,	1,
	sym_OSLO1_1	OSLO1	520,	0,95	1,007
	sym_OSLO2_1	OSLO2	260,	0,95	1,004
	sym_OULU_1	OULU	320,	1,	1,
	sym_OULU_2	OULU	320,	0,95	1,
	sym_PORJUS_1	PORJUS	580,	0,95	1,
	sym_PORJUS_2	PORJUS	580,	0,95	1,
	sym_RINGHALS_1	RINGHALS	520,	0,95	1,
	sym_RINGHALS_2	RINGHALS	520,	0,95	1,
	sym_RINGHALS_3	RINGHALS	520,	0,95	1,
	sym_ROSSAGA_1	ROSSAGA	780,	0,95	1,02
	sym_ROSSAGA_2	ROSSAGA	780,	0,95	1,02
	sym_SIMA_1	SIMA	720,	0,95	1,
	sym_SIMA_2	SIMA	720,	0,95	1,
	sym_TRETTEN_1	TRETTEN	260,	0,95	1,
	sym_TRONDHEI_1	TRONDHEI	500,	0,95	1,
	sym_TRONDHEI_2	TRONDHEI	500,	0,95	1,

Figure 47: Data - Scenario 1, part 2

F.2 Scenario 2

		Terminal	Active Power	Power	
	Name	Busbar	[MW]	factor	
LOADS	CL Blafalli	BLAFALLI	3000,	1,	
	CL Forsmark	FORSMARK	4450,	1,	
	CL Grundfor	GRUNDFOR	2500,	1,	
	CL Helsinki	HELSINKI	9550,	1,	
	CL Hjalta	HJALTA	450,	1,	
	CL Kristian	KRISTIAN	3000,	1,	
	CL Malmo	MALMO	4550,	1,	
	CL Oscarshamn	OSKARSHA	5950,	1,	
	CL Oslo1	OSLO1	2500,	1,	
	CL Oslo2	OSLO2	2500,	1,	
	CL Oulu	OULU	4100,	1,	
	CL Porjus	PORJUS	1500,	1,	
	CL Ringhals	RINGHALS	4450,	1,	
	CL Rossaga	ROSSAGA	3000,	1,	
	CL Sima	SIMA	2650,	1,	
	CL Tretten	TRETTEN	2500,	1,	
	CL Trondheim	TRONDHEI	4100,	1,	
	lod_DANNEBO__1	FORSMARK	750,	1,	
	lod_ESTLINK__1	HELSINKI	-200,	-1,	
	lod_LT_HVDC_2	MALMO	-200,	-1,	
	lod_NORDNED_1	NORDNED	500,	1,	
	lod_SKAGERAK_1	SKAGERAK	-1600,	-1,	
	lod_STENKU_H_1	STENKU_H	-750,	-1,	
	lod_VYBORG_H_1	HELSINKI	0,	0,	
	hvdc_ARRIE	MALMO	600,	1,	
	hvdc_KARLSH_H	MALMO	-300,	-1,	

		Terminal	Active Power	Power	Voltage
	Name	Busbar	per turbine [MW]	factor	[p.u.]
WIND TURBINES	WTG 2.5MW FI1	LV FI1	0.8	1,	1,
	WTG 2.5MW NO2	LV NO2	0.8	1,	1,
	WTG 2.5MW NO3	LV NO3	0.8	1,	1,
	WTG 2.5MW SE2	LV SE2	0.8	1,	1,
	WTG 2.5MW SE3	LV SE3	0.8	1,	1,
	WTG 2.5MW SE4	LV SE4	0.8	1,	1,

Figure 48: Data - Scenario 2, part 1

		Terminal	Active Power	Power	Voltage
	Name	Busbar	[MW]	factor	[p.u.]
	sym_BLAFALLI_1	BLAFALLI	1000,	1,	1,
	sym_BLAFALLI_2	BLAFALLI	1200,	0,9	1,
	sym_BLAFALLI_3	BLAFALLI	1200,	0,9	1,
	sym_BLAFALLI_4	BLAFALLI	1200,	0,9	1,
	sym_BLAFALLI_5	BLAFALLI	1200,	0,9	1,
	sym_FORSMARK_1	FORSMARK	500,	0,9	1,
	sym_FORSMARK_2	FORSMARK	740,	0,9	1,
	sym_FORSMARK_3	FORSMARK	740,	0,9	1,
	sym_GRUNDFOR_1	GRUNDFOR	1020,	0.7	1,
	sym_GRUNDFOR_2	GRUNDFOR	1020,	0.7	1,
	sym_GRUNDFOR_3	GRUNDFOR	1020,	0.7	1,
	sym_GRUNDFOR_4	GRUNDFOR	1020,	0.7	1,
	sym_GRUNDFOR_5	GRUNDFOR	1020,	0.7	1,
	sym_GRUNDFOR_6	GRUNDFOR	1020,	0.7	1,
	sym_GRUNDFOR_7	GRUNDFOR	1020,	0.7	1,
	sym_HELSINKI_1	HELSINKI	800,	0,9	1,
GENERATORS	sym_HELSINKI_2	HELSINKI	800,	0,9	1,
	sym_HELSINKI_3	HELSINKI	800,	0,9	1,
	sym_HELSINKI_4_OLKILU	HELSINKI	890,	0,9	1,
	sym_HELSINKI_5	HELSINKI	800,	0,9	1,
	sym_HELSINKI_6	HELSINKI	800,	0,9	1,
	sym_HELSINKI_7	HELSINKI	800,	0,9	1,
	sym_HELSINKI_8	HELSINKI	800,	0,9	1,
	sym_HELSINKI_9	HELSINKI	800,	0,9	1,
	sym_JARPSTRO_1	JARPSTRO	1080,	0,9	1,
	sym_KRISTIAN_1	KRISTIAN	1000,	1,	1,02
	sym_KRISTIAN_2	KRISTIAN	1000,	0,9	1,01
	sym_KVILLDAL_1	KVILLDAL	1240,	1,	1,005
	sym_MALMO_1	MALMO	580,	0,9	1,02
	sym_MALMO_2	MALMO	940,	0,9	1,02
	sym_MALMO_3	MALMO	940,	0,9	1,02
	sym_MALMO_4	MALMO	940,	0,9	1,02
	sym_MALMO_6	MALMO	940,	0,9	1,02

Figure 49: Data - Scenario 2, part 2

GENERATORS	sym_OSKARSHA_2	OSKARSHA	0,	0,9	1,
	sym_OSKARSHA_3	OSKARSHA	1450,	1,	1,
	sym_OSLO1_1	OSLO1	900,	0,9	1,007
	sym_OSLO1_2	OSLO1	1200,	0,9	1,007
	sym_OSLO2_1	OSLO2	900,	0,9	1,01
	sym_OULU_1	OULU	100,	0,9	1,
	sym_OULU_2	OULU	200,	0,9	1,
	sym_OULU_3	OULU	200,	0,9	1,
	sym_PORJUS_1	PORJUS	1160,	0,9	1,
	sym_PORJUS_2	PORJUS	1160,	0,9	1,
	sym_PORJUS_3	PORJUS	1160,	0,9	1,
	sym_RINGHALS_1	RINGHALS	800,	0,9	1,
	sym_RINGHALS_2	RINGHALS	800,	0,9	1,
	sym_RINGHALS_3	RINGHALS	800,	0,9	1,
	sym_RINGHALS_4	RINGHALS	800,	0,9	1,
	sym_RINGHALS_5	RINGHALS	800,	0,9	1,
	sym_RINGHALS_6	RINGHALS	800,	0,9	1,
	sym_ROSSAGA_1	ROSSAGA	700,	1,	1,02
	sym_ROSSAGA_2	ROSSAGA	1800,	0,95	1,02
	sym_SIMA_1	SIMA	1000,	0,9	1,
	sym_SIMA_2	SIMA	1000,	0,9	1,
	sym_TRETTEN_1	TRETTEN	500,	0,95	1,
	sym_TRONDHEI_1	TRONDHEI	700,	0,7	1,
	sym_TRONDHEI_2	TRONDHEI	900,	0,9	1,
	sym_TRONDHEI_3	TRONDHEI	900,	0,9	1,
	sym_TRONDHEI_4	TRONDHEI	900,	0,9	1,

Figure 50: Data - Scenario 2, part 3

F.3 Scenario 3

		Terminal	Active Power	Power	
	Name	Busbar	[MW]	factor	
LOADS	CL Blafalli	BLAFALLI	1550,	1,	
	CL Forsmark	FORSMARK	1750,	1,	
	CL Grundfor	GRUNDFOR	1150,	1,	
	CL Helsinki	HELSINKI	5450,	1,	
	CL Hjalta	HJALTA	0,	0,	
	CL Kristian	KRISTIAN	1550,	1,	
	CL Malmo	MALMO	1700,	1,	
	CL Oscarshamn	OSKARSHA	2300,	1,	
	CL Oslo1	OSLO1	750,	1,	
	CL Oslo2	OSLO2	750,	1,	
	CL Oulu	OULU	2350,	1,	
	CL Porjus	PORJUS	850,	1,	
	CL Ringhals	RINGHALS	1750,	1,	
	CL Rossaga	ROSSAGA	1750,	1,	
	CL Sima	SIMA	1500,	1,	
	CL Tretten	TRETTEN	750,	1,	
	CL Trondheim	TRONDHEI	2550,	1,	
	hvdc_ARRIE	MALMO	-200,	-1,	
	hvdc_KARLSH_H	MALMO	-200,	-1,	
	lod_DANNEBO__1	FORSMARK	-400,	-1,	
	lod_ESTLINK__1	HELSINKI	-900,	-1,	
	lod_LT_HVDC_2	MALMO	-200,	-1,	
	lod_NORDLINK_1	NORDLINK	-400,	-1,	
	lod_NORDNED_1	NORDNED	0,	0,	
	lod_SKAGERAK_1	SKAGERAK	-1600,	-1,	
	lod_STENKU_H_1	STENKU_H	-200,	-1,	
	lod_VYBORG_H_1	HELSINKI	0,	0,	

		Terminal	Active Power	Power	Voltage
	Name	Busbar	per turbine [MW]	factor	[p.u.]
WIND TURBINES	WTG 2.5MW FI1	LV FI1	1.6	1,	1,
	WTG 2.5MW NO2	LV NO2	1.6	1,	1,
	WTG 2.5MW NO3	LV NO3	1.6	1,	1,
	WTG 2.5MW SE2	LV SE2	1.6	1,	1,
	WTG 2.5MW SE3	LV SE3	1.6	1,	1,
	WTG 2.5MW SE4	LV SE4	1.6	1,	1,

Figure 51: Data - Scenario 3, part 1

		Terminal	Active Power	Power	Voltage
	Name	Busbar	[MW]	factor	[p.u.]
GENERATORS	sym_BLAFALLI_1	BLAFALLI	200,	1,	1,
	sym_FORSMARK_1	FORSMARK	400,	1,	1,
	sym_GRUNDFOR_1	GRUNDFOR	400,	1,	1,
	sym_HELSINKI_1	HELSINKI	400,	1,	1,
	sym_JARPSTRO_1	JARPSTRO	400,	1,	1,
	sym_KRISTIAN_1	KRISTIAN	400,	1,	1,
	sym_KVILLDAL_1	KVILLDAL	1240,	1,	1,
	sym_MALMO_1	MALMO	400,	1,	1,
	sym_MALMO_2	MALMO	200,	1,	1,02
	sym_OLKILUOTO_3	HELSINKI	1600,	1,	1,
	sym_OSKARSHA_2	OSKARSHA	0,	0,	1,
	sym_OSKARSHA_3	OSKARSHA	1450,	1,	1,
	sym_OSLO1_1	OSLO1	200,	1,	1,
	sym_OSLO2_1	OSLO2	200,	1,	1,
	sym_OULU_1	OULU	400,	1,	1,
	sym_OULU_2	OULU	700,	1,	1,
	sym_PORJUS_1	PORJUS	300,	1,	1,
	sym_RINGHALS_1	RINGHALS	300,	1,	1,
	sym_ROSSAGA_1	ROSSAGA	300,	1,	1,
	sym_SIMA_1	SIMA	300,	1,	1,
	sym_TRETTEN_1	TRETTEN	200,	1,	1,
	sym_TRONDHEI_1	TRONDHEI	300,	1,	1,

Figure 52: Data - Scenario 3, part 2

The power flows for the modeled HVDC lines are 550 MW (pf = 1) for North Sea Line and Nordlink, and 300 MW (pf = 1) for Hansa Power Bridge.

F.4 Scenario 4

		Terminal	Active Power	Power	
	Name	Busbar	[MW]	factor	
LOADS	CL Blafalli	BLAFALLI	3250,	1,	
	CL Forsmark	FORSMARK	4500,	1,	
	CL Grundfor	GRUNDFOR	3000,	1,	
	CL Helsinki	HELSINKI	10600,	1,	
	CL Hjalta	HJALTA	0,	0,	
	CL Kristian	KRISTIAN	3250,	1,	
	CL Malmo	MALMO	4600,	1,	
	CL Oscarshamn	OSKARSHA	6000,	1,	
	CL Oslo1	OSLO1	2750,	1,	
	CL Oslo2	OSLO2	2750,	1,	
	CL Oulu	OULU	4500,	1,	
	CL Porjus	PORJUS	1500,	1,	
	CL Ringhals	RINGHALS	4500,	1,	
	CL Rossaga	ROSSAGA	3300,	1,	
	CL Sima	SIMA	2900,	1,	
	CL Tretten	TRETTEN	2750,	1,	
	CL Trondheim	TRONDHEI	4500,	1,	
	hvdc_ARRIE	MALMO	-300,	-1,	
	hvdc_KARLSH_H	MALMO	-300,	-1,	
	lod_DANNEBO__1	FORSMARK	-400,	-1,	
	lod_ESTLINK__1	HELSINKI	-500,	-1,	
	lod_LT_HVDC_2	MALMO	-350,	-1,	
	lod_NORDNED_1	NORDNED	-350,	-1,	
	lod_SKAGERAK_1	SKAGERAK	-1600,	-1,	
	lod_STENKU_H_1	STENKU_H	-350,	-1,	
	lod_VYBORG_H_1	HELSINKI	0,	0,	

		Terminal	Active Power	Power	Voltage
	Name	Busbar	per turbine [MW]	factor	[p.u.]
WIND TURBINES	WTG 2.5MW FI1	LV FI1	1.6	1,	1,
	WTG 2.5MW NO2	LV NO2	1.6	1,	1,
	WTG 2.5MW NO3	LV NO3	1.6	1,	1,
	WTG 2.5MW SE2	LV SE2	1.6	1,	1,
	WTG 2.5MW SE3	LV SE3	1.6	1,	1,
	WTG 2.5MW SE4	LV SE4	1.6	1,	1,

Figure 53: Data - Scenario 4, part 1

		Terminal	Active Power	Power	Voltage
	Name	Busbar	[MW]	factor	[p.u.]
	sym_BLAFALLI_1	BLAFALLI	900,	0,95	1,
	sym_BLAFALLI_2	BLAFALLI	900,	0,95	1,
	sym_BLAFALLI_3	BLAFALLI	900,	0,95	1,
	sym_BLAFALLI_4	BLAFALLI	900,	0,95	1,
	sym_BLAFALLI_5	BLAFALLI	900,	0,95	1,
	sym_FORSMARK_1	FORSMARK	200,	0,95	1,
	sym_FORSMARK_2	FORSMARK	200,	0,95	1,
	sym_FORSMARK_3	FORSMARK	200,	0,95	1,
	sym_GRUNDFOR_1	GRUNDFOR	800,	0,95	1,
	sym_GRUNDFOR_2	GRUNDFOR	800,	0,95	1,
	sym_GRUNDFOR_3	GRUNDFOR	800,	0,95	1,
	sym_GRUNDFOR_4	GRUNDFOR	800,	0,95	1,
	sym_GRUNDFOR_5	GRUNDFOR	800,	0,95	1,
	sym_GRUNDFOR_6	GRUNDFOR	800,	0,95	1,
	sym_GRUNDFOR_7	GRUNDFOR	800,	0,95	1,
	sym_HELSINKI_1	HELSINKI	700,	0,95	1,
GENERATORS	sym_HELSINKI_2	HELSINKI	700,	0,95	1,
	sym_HELSINKI_3	HELSINKI	700,	0,95	1,
	sym_HELSINKI_5	HELSINKI	700,	0,95	1,
	sym_HELSINKI_6	HELSINKI	700,	0,95	1,
	sym_HELSINKI_7	HELSINKI	700,	0,95	1,
	sym_HELSINKI_8	HELSINKI	700,	0,95	1,
	sym_HELSINKI_9	HELSINKI	700,	0,95	1,
	sym_JARPSTRO_1	JARPSTRO	850,	0,95	1,
	sym_KRISTIAN_1	KRISTIAN	900,	0,95	1,01
	sym_KRISTIAN_2	KRISTIAN	900,	0,95	1,01
	sym_KVILLDAL_1	KVILLDAL	1240,	0,95	1,005
	sym_MALMO_1	MALMO	500,	0,95	1,02
	sym_MALMO_2	MALMO	700,	0,95	1,02
	sym_MALMO_3	MALMO	700,	0,95	1,02
	sym_MALMO_4	MALMO	700,	0,95	1,02
	sym_MALMO_5	MALMO	700,	0,95	1,02
	sym_MALMO_6	MALMO	700,	0,95	1,02

Figure 54: Data - Scenario 4, part 2

	sym_OLKILUOTO_3	HELSINKI	1600,	0,95	1,
	sym_OSKARSHA_2	OSKARSHA	0,	0,95	1,
	sym_OSKARSHA_3	OSKARSHA	1450,	0,95	1,
	sym_OSLO1_1	OSLO1	900,	0,95	1,007
	sym_OSLO1_2	OSLO1	900,	0,95	1,007
	sym_OSLO2_1	OSLO2	850,	0,95	1,004
	sym_OULU_1	OULU	300,	0,95	1,
	sym_OULU_2	OULU	500,	0,95	1,
	sym_OULU_3	OULU	500,	0,95	1,
	sym_PORJUS_1	PORJUS	900,	0,95	1,
	sym_PORJUS_2	PORJUS	900,	0,95	1,
	sym_PORJUS_3	PORJUS	900,	0,95	1,
	sym_RINGHALS_1	RINGHALS	800,	0,95	1,
GENERATORS	sym_RINGHALS_2	RINGHALS	600,	0,95	1,
	sym_RINGHALS_3	RINGHALS	800,	0,95	1,
	sym_RINGHALS_4	RINGHALS	800,	0,95	1,
	sym_RINGHALS_5	RINGHALS	800,	0,95	1,
	sym_RINGHALS_6	RINGHALS	800,	0,95	1,
	sym_ROSSAGA_1	ROSSAGA	700,	0,95	1,02
	sym_ROSSAGA_2	ROSSAGA	900,	0,95	1,02
	sym_SIMA_1	SIMA	900,	0,98	1,
	sym_SIMA_2	SIMA	900,	1,	1,
	sym_TRETTEN_1	TRETTEN	700,	1,	1,
	sym_TRONDHEI_1	TRONDHEI	600,	1,	1,
	sym_TRONDHEI_2	TRONDHEI	600,	1,	1,
	sym_TRONDHEI_3	TRONDHEI	600,	1,	1,
	sym_TRONDHEI_4	TRONDHEI	600,	1,	1,

Figure 55: Data - Scenario 4, part 3

The power flows for the modeled HVDC lines are 500 MW (pf = 1) for North Sea Line and Nordlink, and 300 MW (pf = 1) for Hansa Power Bridge.

G Component data

G.1 Governor - HYGOV

Name: HYGOV(1)

Model Definition: User Defined Models\gov_HYGOV

☐ Out of Service ☐ A-stable integration algorithm

	Parameter
r Temporary Droop [pu]	0,4
Tr Governor Time Constant [s]	10,
Tf Filter Time Constant [s]	0,1
Tg Servo Time Constant [s]	0,5
Tw Water Starting Time [s]	1,
At Turbine Gain [pu]	1,
Dturb frictional losses factor pu [pu]	0,01
qnl No Load Flow [pu]	0,01
R Permanent Droop [pu]	0,06
PN Turbine Rated Power(=0->PN=Pgnn) [Mw]	0,
Gmin Minimum Gate Limit [pu]	0,
Velm Gate Velocity Limit [pu]	0,15
Gmax Maximum Gate Limit [pu]	1,

Figure 56: Data - Governor HYGOV

G.2 AVR - SEXS

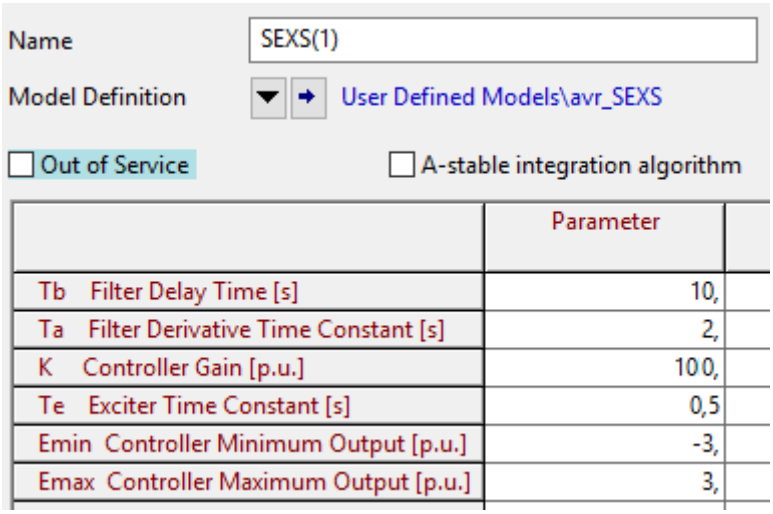

Figure 57: Data - AVR SEXS

H Simulation results

H.1 Delta - Frequency responses

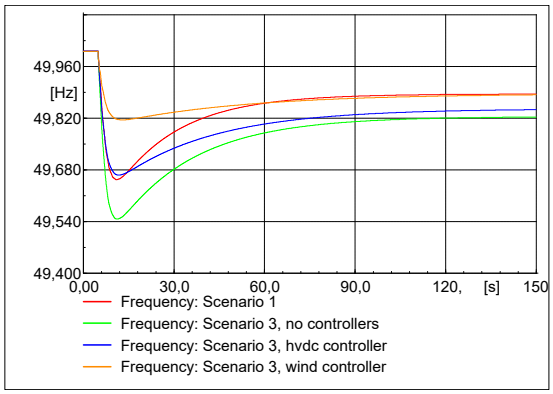

Figure 58: Results - Delta, summer scenarios: Frequency responses

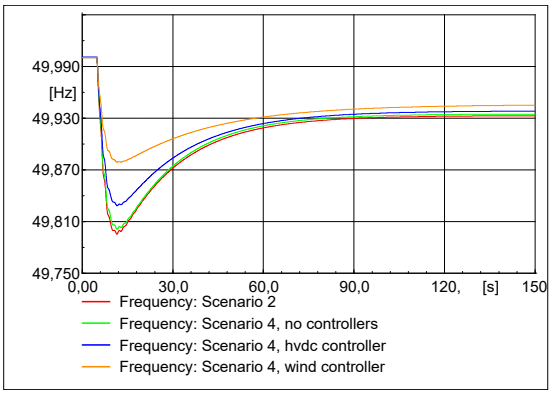

Figure 59: Results - Delta, winter scenarios: Frequency responses

H.2 Epsilon - Frequency responses

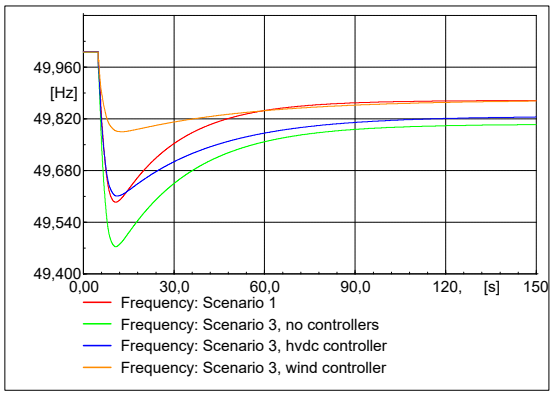

Figure 60: Results - Epsilon, summer scenarios: Frequency responses

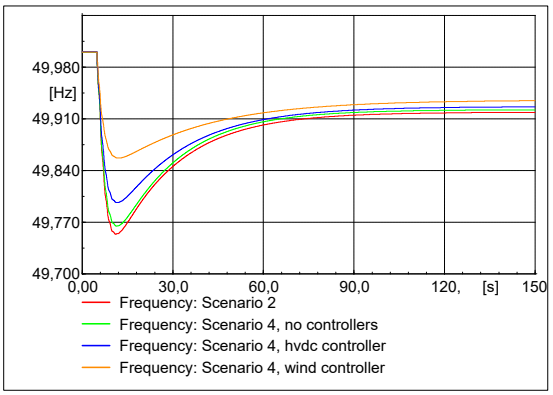

Figure 61: Results - Epsilon, winter scenarios: Frequency responses

H.3 Zeta - Frequency responses

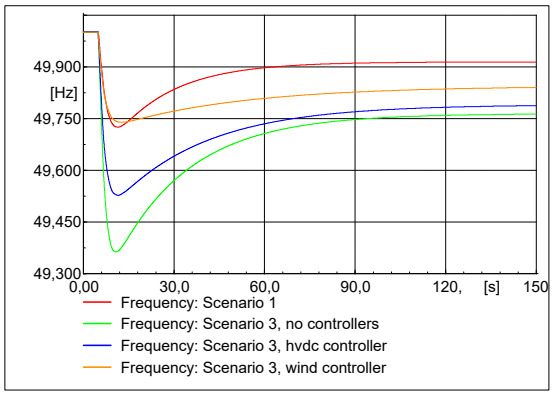

Figure 62: Results - Zeta, summer scenarios: Frequency responses

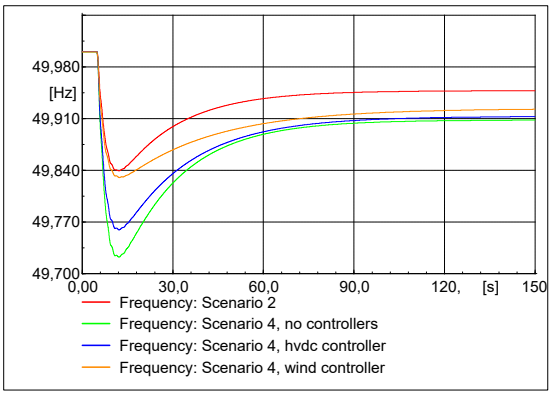

Figure 63: Results - Zeta, winter scenarios: Frequency responses

H.4 Zeta - Reactive response in Finland

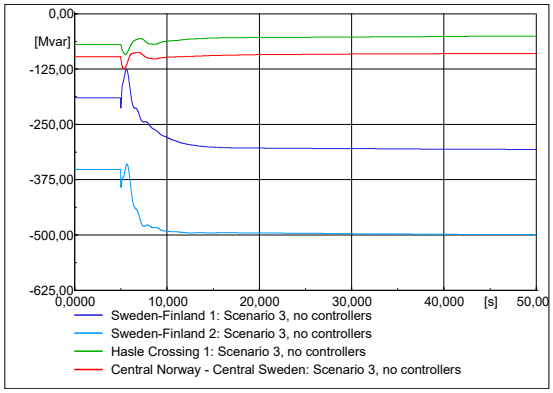

Figure 64: Reactive power flows from Sweden to Finland (event Zeta)

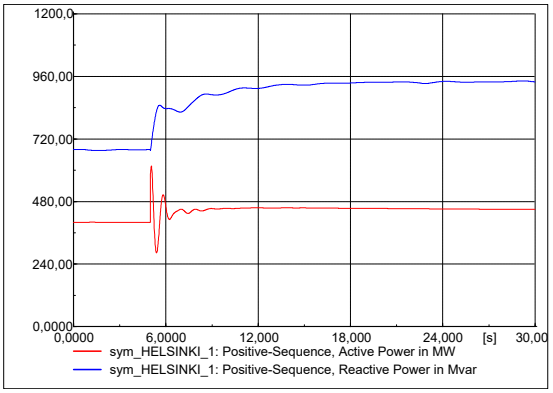

Figure 65: Response for a generator at node Helsinki (event Zeta)

	Reactive power flows [MVar]		
Line	Pre event	Post event	Change
Sweden - Finland 1	-190	-307	-117
Sweden - Finland 2	-352	-500	-148
Hasle Crossing 1	-70	-51	19
Hasle Crossing 2	-57	-31	16
Central Sweden - Central Norway	-97	-90	7
Northern Sweden - Northern Norway 1	-142	-137	5
Northern Sweden - Northern Norway 2	-30	-27	3

Table 19: Results - Zeta, scenario 3 (no controllers): Reactive power flows

Figure 65 shows how the active and reactive power output changes a response to an outage in Finland (also at node Helsinki). One observes how the generator activates large amounts of reactive power and modest amounts of active power. When studied together with figure 28, one can observe how reactive compensation is mainly activated in the area that is affected by the disturbance, while active power can be activated outside the area. This corresponds to the knowledge on voltage being mainly a local parameter where appropriate reserves must me activated close to the imbalance while frequency is a global parameter where reserves can be activated nearly anywhere within the frequency area.

H.5 Eta - Frequency responses

The sudden frequency changes that can be seen on figure 66 happen because of rapid changes in the voltage phase angle, and are local information for the generator at where the frequency is measured. Thus, for the first seconds of this simulation, one can not let the measured frequency at one node represent the whole system. As it is more relevant to study the voltage response than the frequency response for this short-circuit event, the voltage response has been presented in chapter 5 Results.

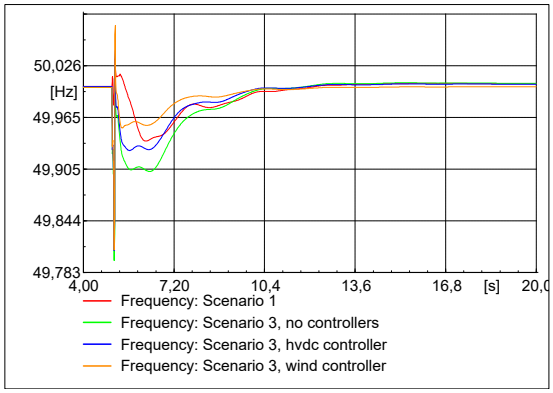

Figure 66: Results - Eta, summer scenarios: Frequency responses

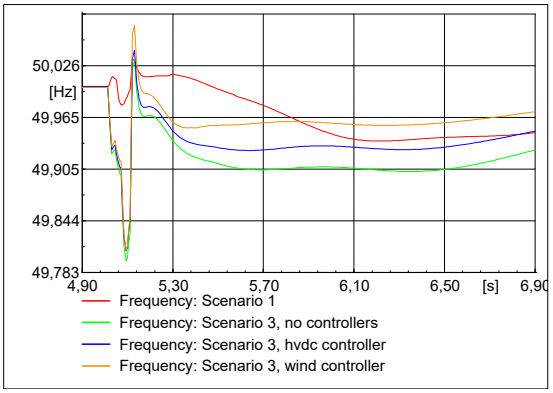

Figure 67: Results - Eta, summer scenarios (zoomed): Frequency responses

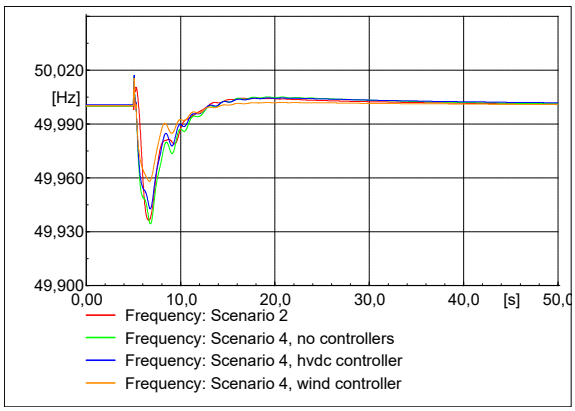

Figure 68: Results - Eta, winter scenarios: Frequency responses

Scenario	f_{nadir} [HZ]
1	49.94
2	49.94
3 no cont	49.80
3 hvdc cont	49.81
3 wind cont	49.81
4 no cont	49.93
4 hvdc cont	49.94
4 wind cont	49.96

Table 20: Results - Eta: Frequency drops

After the first few seconds, when the rapid frequency spikes have faded, one can once more study the frequency as a representation of the whole system. At this point, however, the frequency deviations are relatively low and significantly less critical than for the other events. The frequency converges back to original values 10-15 seconds after the short-circuiting.

It should be noted that the critical lines that are investigated are *not* the same for all scenarios and carries a different load flow for each case (see section 4.3.3). The individual responses must be examined keeping that in mind.

I Swing equation and inertial response - An example

Understanding the swing equation is vital when investigating the need for inertia in a power system. The term $\frac{d\omega_e}{dt}$ in equation 2.10 gives the acceleration/deceleration of the rotor. As system frequency is related to the frequency of the connected generators, the term $\frac{d\omega_e}{dt}$ provides information about the dynamics of the power system where the generator is connected.

Considering a system in balance and under stable operation, the production meets consumption, $P_m = P_e$, and $\Delta P_e = 0$. In this situation, the frequency change of the system must equal zero (see equation 2.10 and 2.13). This makes intuitive sense, as a system in balance maintains a constant speed.

However, if the load suddenly is reduced, e.g. as a result of a fault in the system, then $P_m > P_e$. Now, the frequency change becomes positive and the system accelerates. Considering equation 2.8, it can be observed that the kinetic energy stored in the rotational body (the rotor) is increasing as it picks up speed. In short, the inertial response of the rotor when the load is suddenly reduced is to store some of the energy as kinetic energy. This counteracts the system frequency from rising even faster. Considering when some generation is lost in the system, $P_m < P_e$, the opposite reaction happens. Some of the kinetic energy of the rotor is fed to the system as rotational speed and frequency is reduced. This reduces the deceleration.

To summarize: Inertia opposes changes in the frequency instantaneously after a disturbance. The result is that the frequency changes slower in a high inertia network than a low inertia system. This allows power reserves and other measures time to be activated to contain and restore the frequency to its nominal value.

J Spreadsheets - Inertia calculation

			Activation/Scenarios				Inertia/Scenario			
	S_n	H	1	2	3	4	1	2	3	4
sym_BLAFALLI_1	1295	3	1	1	1	1	3885	3885	3885	3885
sym_BLAFALLI_2	1635	3	0	1	0	1	0	4905	0	4905
sym_BLAFALLI_3	1635	3	0	1	0	1	0	4905	0	4905
sym_BLAFALLI_4	1635	3	0	1	0	1	0	4905	0	4905
sym_BLAFALLI_5	1635	3	0	1	0	1	0	4905	0	4905
sym_FORSMARK_1	988	5,97	1	1	1	1	5896	5896	5896	5896
sym_FORSMARK_2	1300	5,97	1	1	0	1	7761	7761	0	7761
sym_FORSMARK_3	1300	5,97	0	1	0	1	0	7761	0	7761
sym_GRUNDFOR_1	1357	4,54	1	1	1	1	6161	6161	6161	6161
sym_GRUNDFOR_2	1357	4,54	1	1	0	1	6161	6161	0	6161
sym_GRUNDFOR_3	1357	4,54	1	1	0	1	6161	6161	0	6161
sym_GRUNDFOR_4	1357	4,54	0	1	0	1	0	6161	0	6161
sym_GRUNDFOR_5	1357	4,54	0	1	0	1	0	6161	0	6161
sym_GRUNDFOR_6	1357	4,54	0	1	0	1	0	6161	0	6161
sym_GRUNDFOR_7	1357	4,54	0	1	0	1	0	6161	0	6161
sym_HELSINKI_1	1086	5,5	1	1	1	1	5975	5975	5975	5975
sym_HELSINKI_2	1086	5,5	1	1	0	1	5975	5975	0	5975
sym_HELSINKI_3	1086	5,5	1	1	0	1	5975	5975	0	5975
sym_HELSINKI_4_OLKILUOTO_2	1000	5,5	1	1	0	0	5500	5500	0	0
sym_HELSINKI_5	1278	5,5	0	1	0	1	0	7029	0	7029
sym_HELSINKI_6	1278	5,5	0	1	0	1	0	7029	0	7029
sym_HELSINKI_7	1278	5,5	0	1	0	1	0	7029	0	7029
sym_HELSINKI_8	1278	5,5	0	1	0	1	0	7029	0	7029
sym_HELSINKI_9	1278	5,5	0	1	0	1	0	7029	0	7029
sym_JARPSTRO_1	1444	3,3	1	1	1	1	4767	4767	4767	4767
sym_KRISTIAN_1	1538	3,5	1	1	1	1	5384	5384	5384	5384
sym_KRISTIAN_2	1538	3,5	0	1	0	1	0	5384	0	5384
sym_KVILLDAL_1	1400	3,5	1	1	1	1	4900	4900	4900	4900
sym_MALMO_1	778	7	1	1	1	1	5444	5444	5444	5444
sym_MALMO_2	1300	7	1	1	1	1	9100	9100	9100	9100
sym_MALMO_3	1300	7	0	1	0	1	0	9100	0	9100
sym_MALMO_4	1300	7	0	1	0	1	0	9100	0	9100
sym_MALMO_5	1300	7	0	0	0	1	0	0	0	9100
sym_MALMO_6	1300	7	0	1	0	1	0	9100	0	9100
sym_OLKILUOTO_3	1600	6	0	0	1	1	0	0	9600	9600
sym_OSKARSHA_2	2000	6	1	1	1	1	12000	12000	12000	12000
sym_OSKARSHA_3	1600	6	1	1	1	1	9600	9600	9600	9600
sym_OSLO1_1	1420	4,1	1	1	1	1	5821	5821	5821	5821
sym_OSLO1_2	1612	4,1	0	1	0	1	0	6607	0	6607
sym_OSLO2_1	1450	4	1	1	1	1	5800	5800	5800	5800

Figure 69: Inertia calculations, part 1

sym_OSLO1_1	1420	4,1	1	1	1	1	5821	5821	5821	5821
sym_OSLO1_2	1612	4,1	0	1	0	1	0	6607	0	6607
sym_OSLO2_1	1450	4	1	1	1	1	5800	5800	5800	5800
sym_OULU_1	452	3,2	1	1	1	1	1447	1447	1447	1447
sym_OULU_2	1000	3,2	1	1	1	1	3200	3200	3200	3200
sym_OULU_3	1000	3,2	0	1	0	1	0	3200	0	3200
sym_PORJUS_1	1527	4,74	1	1	1	1	7238	7238	7238	7238
sym_PORJUS_2	1527	4,74	1	1	0	1	7238	7238	0	7238
sym_PORJUS_3	1527	4,74	0	1	0	1	0	7238	0	7238
sym_RINGHALS_1	1350	4,82	1	1	1	1	6507	6507	6507	6507
sym_RINGHALS_2	938	4,82	1	1	0	1	4522	4522	0	4522
sym_RINGHALS_3	1350	4,82	1	1	0	1	6507	6507	0	6507
sym_RINGHALS_4	1350	4,82	0	1	0	1	0	6507	0	6507
sym_RINGHALS_5	1350	4,82	0	1	0	1	0	6507	0	6507
sym_RINGHALS_6	1350	4,82	0	1	0	1	0	6507	0	6507
sym_ROSSAGA_1	988	3,59	1	1	1	1	3546	3546	3546	3546
sym_ROSSAGA_2	2144	3,59	1	1	0	1	7699	7699	0	7699
sym_SIMA_1	1575	3,5	1	1	1	1	5512	5512	5512	5512
sym_SIMA_2	1575	3,5	1	1	0	1	5512	5512	0	5512
sym_TRETTEN_1	1200	3,99	1	1	1	1	4788	4788	4788	4788
sym_TRONDHEI_1	915	3,56	1	1	1	1	3258	3258	3258	3258
sym_TRONDHEI_2	1100	3,56	1	1	0	1	3916	3916	0	3916
sym_TRONDHEI_3	1100	3,56	0	1	0	1	0	3916	0	3916
sym_TRONDHEI_4	1100	3,56	0	1	0	1	0	3916	0	3916
	TOTAL INERTIA:						193156	357407	129829	370607

Figure 70: Inertia calculations, part 2

Explanation of the spread sheet (figure 69 and 70)

Relevant data are presented in the three first columns. In the four next columns, which are marked green and red, it is stated if the generator is activated for the given scenarios. "1" means activated and "0" means out of service. In the four last columns, the inertia for each generator for each scenario are calculated (utilizing equation 2.7) based on the generator's ratings and inertia constants - and if they are activated or not. On the very last row, the inertias are summarized to calculate the total system inertia (from the generators) for each scenario.

K Spreadsheets - Frequency bias calculation

			Frequency bias per								
		DROOP	generator	Activation/Scenarios				Frequency bias/Scenario			
	P_n	R		1	2	3	4	1	2	3	4
sym_BLAFALLI_1	1295,06	**0,06**	432	1	1	1	1	432	432	432	432
sym_BLAFALLI_2	1634,96	**0,06**	545	0	1	0	1	0	545	0	545
sym_BLAFALLI_3	1634,96	**0,06**	545	0	1	0	1	0	545	0	545
sym_BLAFALLI_4	1634,96	**0,06**	545	0	1	0	1	0	545	0	545
sym_BLAFALLI_5	1634,96	**0,06**	545	0	1	0	1	0	545	0	545
sym_FORSMARK_1	987,654		0	1	1	1	1	0	0	0	0
sym_FORSMARK_2	1300		0	1	1	0	1	0	0	0	0
sym_FORSMARK_3	1300		0	0	1	0	1	0	0	0	0
sym_GRUNDFOR_1	1357	**0,06**	452	1	1	1	1	452	452	452	452
sym_GRUNDFOR_2	1357	**0,06**	452	1	1	0	1	452	452	0	452
sym_GRUNDFOR_3	1357	**0,06**	452	1	1	0	1	452	452	0	452
sym_GRUNDFOR_4	1357	**0,06**	452	0	1	0	1	0	452	0	452
sym_GRUNDFOR_5	1357	**0,06**	452	0	1	0	1	0	452	0	452
sym_GRUNDFOR_6	1357	**0,06**	452	0	1	0	1	0	452	0	452
sym_GRUNDFOR_7	1357	**0,06**	452	0	1	0	1	0	452	0	452
sym_HELSINKI_1	1086,42		0	1	1	1	1	0	0	0	0
sym_HELSINKI_2	1086,42		0	1	1	0	1	0	0	0	0
sym_HELSINKI_3	1086,42		0	1	1	0	1	0	0	0	0
sym_HELSINKI_4_OLKILUOTO_2	1000		0	1	1	0	0	0	0	0	0
sym_HELSINKI_5	1278		0	0	1	0	1	0	0	0	0
sym_HELSINKI_6	1278		0	0	1	0	1	0	0	0	0
sym_HELSINKI_7	1278		0	0	1	0	1	0	0	0	0
sym_HELSINKI_8	1278		0	0	1	0	1	0	0	0	0
sym_HELSINKI_9	1278		0	0	1	0	1	0	0	0	0
sym_JARPSTRO_1	1444,44	**0,06**	481	1	1	1	1	481	481	481	481
sym_KRISTIAN_1	1538,27	**0,06**	513	1	1	1	1	513	513	513	513
sym_KRISTIAN_2	1538,27	**0,06**	513	0	1	0	1	0	513	0	513
sym_KVILLDAL_1	1400	**0,06**	467	1	1	1	1	467	467	467	467
sym_MALMO_1	777,778		0	1	1	1	1	0	0	0	0
sym_MALMO_2	1300		0	1	1	1	1	0	0	0	0
sym_MALMO_3	1300		0	0	1	0	1	0	0	0	0
sym_MALMO_4	1300		0	0	1	0	1	0	0	0	0
sym_MALMO_5	1300		0	0	0	0	1	0	0	0	0
sym_MALMO_6	1300		0	0	1	0	1	0	0	0	0
sym_OLKILUOTO_3	1600		0	0	0	1	1	0	0	0	0
sym_OSKARSHA_2	2000		0	1	1	1	1	0	0	0	0
sym_OSKARSHA_3	1600		0	1	1	1	1	0	0	0	0
sym_OSLO1_1	1419,75	**0,06**	473	1	1	1	1	473	473	473	473
sym_OSLO1_2	1611,52	**0,06**	537	0	1	0	1	0	537	0	537

Figure 71: Frequency bias calculations, part 1

sym_OSLO1_1	1419,75	0,06	473	1	1	1	1	473	473	473	473
sym_OSLO1_2	1611,52	0,06	537	0	1	0	1	0	537	0	537
sym_OSLO2_1	1450	0,06	483	1	1	1	1	483	483	483	483
sym_OULU_1	452,288	0,06	151	1	1	1	1	151	151	151	151
sym_OULU_2	1000	0,06	333	1	1	1	1	333	333	333	333
sym_OULU_3	1000	0,06	333	0	1	0	1	0	333	0	333
sym_PORJUS_1	1526,96	0,06	509	1	1	1	1	509	509	509	509
sym_PORJUS_2	1526,96	0,06	509	1	1	0	1	509	509	0	509
sym_PORJUS_3	1526,96	0,06	509	0	1	0	1	0	509	0	509
sym_RINGHALS_1	1350		0	1	1	1	1	0	0	0	0
sym_RINGHALS_2	938,272		0	1	1	0	1	0	0	0	0
sym_RINGHALS_3	1350		0	1	1	0	1	0	0	0	0
sym_RINGHALS_4	1350		0	0	1	0	1	0	0	0	0
sym_RINGHALS_5	1350		0	0	1	0	1	0	0	0	0
sym_RINGHALS_6	1350		0	0	1	0	1	0	0	0	0
sym_ROSSAGA_1	987,654	0,06	329	1	1	1	1	329	329	329	329
sym_ROSSAGA_2	2144,44	0,06	715	1	1	0	1	715	715	0	715
sym_SIMA_1	1574,89	0,06	525	1	1	1	1	525	525	525	525
sym_SIMA_2	1574,89	0,06	525	1	1	0	1	525	525	0	525
sym_TRETTEN_1	1200	0,06	400	1	1	1	1	400	400	400	400
sym_TRONDHEI_1	915,033	0,06	305	1	1	1	1	305	305	305	305
sym_TRONDHEI_2	1100	0,06	367	1	1	0	1	367	367	0	367
sym_TRONDHEI_3	1100	0,06	367	0	1	0	1	0	367	0	367
sym_TRONDHEI_4	1100	0,06	367	0	1	0	1	0	367	0	367
TOTAL FREQUENCY BIAS PER SCENARIO								**8874**	**15489**	**5854**	**15489**

Figure 72: Frequency bias calculations, part 2

Explanation of the spread sheet (figure 71 and 72)

Relevant data are presented in the three first columns. Then, the frequency biases for the individual generators are calculated in the fourth column by using equation 2.4. In the four next columns, which are marked green and red, it is stated if the generator is activated for the given scenarios. "1" means activated and "0" means out of service. In the four last columns, the frequency bias for each generator for each scenario are listed based on the generator's frequency bias values and if they are activated or not. On the very last row, the frequency biases are summarized to calculate the total frequency bias factor (from the generators) for each scenario.

L Lead compensator

Phase lead compensators are commonly used for compensating feedback control loops. The compensator has the potential to improve the dynamic performance of a closed loop system. This includes increasing the stability margins[22].

An example of a lead compensating block is the one that has been used for the controllers in this thesis, see figure 73 below. Note that $Tb > Ta$ (if vice versa, it would be a lag block).

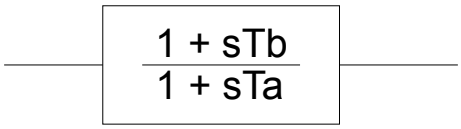

Figure 73: Block diagram - Lead compensator

The transfer function of a phase lead compensator is:

$$G(s) = \frac{1 + s \cdot Tb}{1 + s \cdot Ta} \tag{L.1}$$

Considering equation L.1 and the bode plot below, one can explore the positive aspects associated with the lead compensator. The bode plots show how the magnitude at high frequencies is increased. Comparing to a derivative controller, the increase is limited at the highest frequencies. That is seen on the bode plots, as the total contribution (magnitude) does not increase after $1/Ta$. A disadvantage of increasing gain is that it also increases noise. However, by limiting the gain for the highest frequencies, the noise will be considerably lower than for a derivative controller. One does also observe how the phase is lifted to increase the stability margins. This contributes positively to the network, but is (as seen on the bode plot) limited to a set range of frequencies[22].

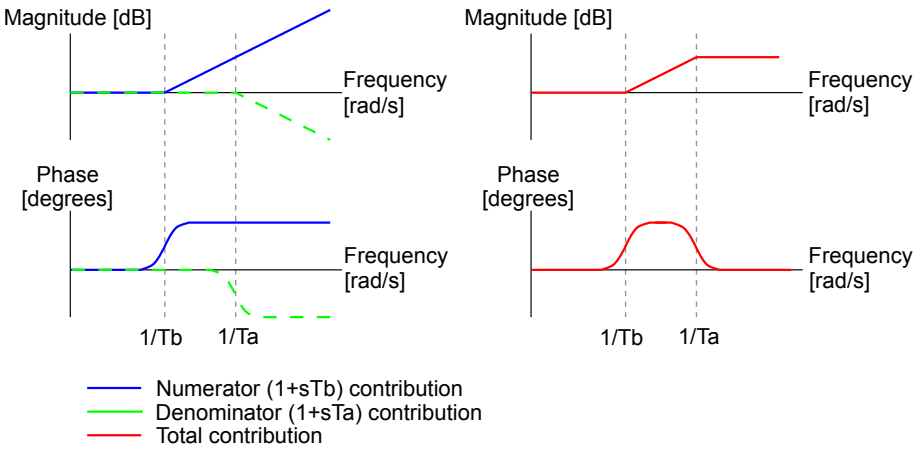

Figure 74: General bode plots for the lead compensator